

# **Dissertation**

**submitted to the**

**Combined faculties of Natural Sciences and Mathematics of the**

**Rupertus-Carolus-University Heidelberg**

**for the degree of Doctor in Natural Sciences**

**presented by**

**Branislava Ranković, M.Sc. in Biology**

**born in Belgrade, Serbia**

**Oral examination date:**

**13<sup>th</sup> of December 2019**



**The role of *oskar* mRNA in P-body formation during  
*Drosophila* oogenesis**

**Examiners:**

**Dr. Alexander Aulehla**

**Prof. Dr. rer. nat. Michael Knop**



# Acknowledgments

To make analogy with the mRNA world: as RNA molecules that travel together with their chaperones, proteins, people are always accompanied by others throughout their lives. Everything we do is interconnected with every single person we met in our world. Therefore, first I would like to thank Anne, my supervisor, for giving me the opportunity to work in her lab. Science I did here in the past four years was the great experience. I grew not only professionally but also as a person. This PhD would not be possible without the help, scientific discussion and collaboration with many people. Thus, I would like to thank my thesis advisory committee, Alexander Aulehla, Matthias Hentze and Michael Knop for guidance and fruitful scientific discussions throughout my PhD.

Thanks to the core facilities in EMBL allowing us to do great science, to the Advanced Light Microscopy Facility, to the Proteomics Core Facility (Mandy R. and Frank S.). Thanks to the Darwin Trust of Edinburgh for the funding.

Many, many thanks to the Ephrussi lab! To all the former and current members! Special thanks to Imre G. for helping me with the project setup, introducing me to the experimental tools and all the feedback in the beginning of my PhD work. Enormous gratitude to Željko Đ. and also to Dylan M. for being patient enough to help me with the thesis writing and have enough time to advise me and give valuable scientific feedback. To all the help and interesting talks (especially about P-bodies ☺) to Frank W. and Mainak B. To Anna C. and Ale R. for making life in the lab a bit easier to all of us. To my PhD fellows in the lab, for sharing their time with me, Lucia, Jane, Matteo, Masroor, Vasilij... Thanks to Lucy for being a great moral support.

I am extremely thankful to my friends, my PhD fighters, with whom I shared all the good and not that great moments, for all the support, tears and joy, to Christine, Anna and Elisa! Thanks to my mindful buddies, always being there for me, to Carina and Silvija! To my roommate, my lab mate but before everything else my friend Vaishali, for bringing a bit of light in my life, for her optimism and understanding. To my bro from Serbia, Milena, for being there when needed the most. To Ivana, my long-life friend for always being there to remind me of myself, to listen, encourage and support! Gracias a Emiliano, por su amistad y tanta inspiración. For all those lovely little chats and coffees thanks to: Chiara M., Marija P., Marija S., Tibor, Ivica, Ana K., Allyson, Anthi, Juan, Huiting, Daja, Medeleine, Dimitris, Elisabeth... Thanks to my Darwin Trust fellows and to all people I got to know in EMBL.

Most importantly I want to thank to my family! I would not be who I am without them. For unconditional love I am grateful to my sister, my greatest support, to my mother and father. Од срца најтоплије хвала!



## Summary

To maintain homeostasis, organisms have developed different mechanisms to cope with stress. One of the quickest responses to stress is the global attenuation of protein synthesis. This can be achieved by controlling the availability of transcripts by packaging them into higher order cytoplasmic ribonucleoprotein (RNP) granules. Among the best studied examples are processing bodies (P-bodies), which are known to harbour silenced mRNAs, and are implied to have a role in protecting maternal mRNAs during animal development. During *Drosophila* oogenesis, P-bodies form upon nutritional stress. It has been shown that RNP granule assembly is dependent on protein-protein interactions. In addition, it has been suggested that RNAs could play an important role in this process, providing a scaffold for RNA binding proteins (RBPs), thus promoting RNP granule formation. How RNA contributes to RNP granule assembly *in vivo* is not well explored. In *Drosophila*, *oskar* mRNA is one example of an mRNA with distinct coding and noncoding functions during animal development. Besides coding for Oskar protein, *oskar* mRNA is necessary for proper oogenesis progression and completion, karyosome formation and distribution of germline specific proteins. Furthermore, the 3'UTR of *oskar* has been shown to be important for *oskar* recruitment into transport particles during *Drosophila* oogenesis. The ability of *oskar* mRNA to oligomerize, thus concentrate P-body components, raised the question whether this molecule could play a role in the formation of P-bodies.

In this work I showed that *oskar* mRNA is an integral part of *Drosophila* P-bodies and that the 3'UTR of *oskar* is sufficient to drive P-body formation. In addition, in *oskar* mRNA non-dimerizing mutants P-body assembly was impaired. Furthermore, I observed that introducing mutations in the *oskar* 3'UTR affected recruitment of *oskar* interactors such as the translational repressor, Bruno, also shown to be involved in the oligomerization of *oskar* mRNPs. The exact mechanism how *oskar* contributes to P-body formation is at the moment still an open question. However, here I propose a hypothetical model of how this mRNA could drive P-body assembly. This process would be driven by *oskar* mRNA dimer formation followed by the recruitment of specific RBPs in order to stabilize the dimer and further promote granule maturation. Coordinated and stepwise interactions between RNA molecules and RBPs could be crucial for proper P-body formation. To summarize, in this work I showed that in the *in vivo* setting of the *Drosophila* oocyte, RNA molecules have an important function in driving RNP granule biogenesis.





# Zusammenfassung

Organismen haben verschiedene Mechanismen entwickelt mit Stress umzugehen, um die Homöostase aufrechtzuerhalten. Eine der schnellsten Antworten auf Stress ist eine globale Verringerung der Proteinsynthese. Dies kann zum Beispiel erreicht werden, indem die Verfügbarkeit von Transkripten durch Kompartimentierung in zytoplasmatische Ribonukleoprotein (RNP) Granules kontrolliert wird. Zu den am besten untersuchten Beispielen zählen Processing Bodies (P-bodies), von denen bekannt ist, dass sie transnational inaktive mRNAs enthalten, und von denen angenommen wird, dass sie eine Rolle beim Schutz von maternalen mRNAs während der tierischen Entwicklung spielen. Während der Oogenese von *Drosophila* bilden sich bei ernährungsbedingtem Stress P-bodies. Es wurde gezeigt, dass der Aufbau von RNP-Granules von Protein-Protein-Interaktionen abhängt. Darüber hinaus wird vermutet, dass RNAs eine wichtige Rolle in diesem Prozess spielen könnten, indem sie ein Gerüst für RNA-Bindeproteine (RBPs) bilden und so die Entstehung von RNP-Granules fördern. Wie genau RNA zum Aufbau von RNP-Granules *in vivo* beiträgt, ist allerdings nicht hinreichend gut erforscht. In *Drosophila* ist die *oskar*-mRNA beispielhaft für eine mRNA mit unterschiedlichen kodierenden und nicht-kodierenden Funktionen während der Entwicklung. Neben der Kodierung des Oskar-Proteins ist die *oskar*-mRNA für den ordnungsgemäßen Fortgang und die Vervollständigung der Oogenese, die Karyosomenbildung und die Verteilung keimbahnspezifischer Proteine erforderlich. Darüber hinaus wurde gezeigt, dass die 3'UTR von *oskar* mRNA für die Rekrutierung in Transportpartikeln während der *Drosophila* Oogenese wichtig ist. Die Fähigkeit der *oskar*-mRNA, P-body-Komponenten zu oligomerisieren und somit zu konzentrieren, warf die Frage auf, ob dieses Molekül eine Rolle bei der Bildung von P-bodies spielen könnte.

In dieser Arbeit zeigte ich, dass die *oskar* mRNA ein integraler Bestandteil von P-bodies in *Drosophila* ist und dass die 3'UTR von *oskar* ausreicht, um die Bildung von P-bodies voranzutreiben. Darüber hinaus ist in *oskar* mRNA Mutanten, die nicht dimerisieren können, die Bildung von P-bodies beeinträchtigt. Des Weiteren beobachtete ich, dass die Einführung von Mutationen in der *oskar* 3'UTR die Rekrutierung von Proteinen die mit *oskar* interagieren beeinflusst. Ein Beispiel dafür ist der Translationsrepressor Bruno, von dem auch gezeigt wurde, dass er an der Oligomerisierung von *oskar* mRNPs beteiligt ist. Der genaue Mechanismus, wie *oskar* mRNA zur Bildung von P-bodies beiträgt, ist derzeit jedoch ungewiss. Hier schlage ich jedoch ein hypothetisches Modell vor, wie diese mRNA den Aufbau von P-bodies vorantreiben könnte. Demnach würde dieser Prozess durch die Bildung von *oskar* mRNA Dimeren angetrieben und von der Rekrutierung spezifischer RBPs stabilisiert, was die Bildung von P-Bodies weiter fördert. Koordinierte und schrittweise Wechselwirkungen zwischen RNA-

Molekülen und RNA Bindeproteinen könnten für die ordnungsgemäße Bildung von P-bodies von entscheidender Bedeutung sein. Zusammenfassend konnte ich in dieser Arbeit zeigen, dass RNA-Moleküle in ihrer natürlichen Umgebung, der *Drosophila*-Oozyte, eine wichtige Funktion bei der Bildung von RNP-Granules haben.

## Abbreviations

**ARS:** adenine rich sequence

**BRE:** Bruno response elements

**BSF:** bicoid stability factor

**CDS:** coding sequence

**DD:** dimerization domain

**dILP:** *Drosophila* insulin-like peptide

**DDR:** DNA damage response

**fc:** follicle cells

**grPB:** P-granule related P-bodies

**eIF:** eukaryotic initiation factor

**ER:** endoplasmic reticulum

**lncRNA:** long noncoding RNA

**mRNA:** messenger RNA

**Me31B:** maternally expressed at 31B

**miRNA:** microRNA

**nc:** nurse cells

**oo:** oocyte

**OES:** oocyte entry signal

**P-bodies:** Processing bodies

**RBP:** RNA binding proteins

**RCD:** regulated cell death

**RNA:** ribonucleic acid

**RNP:** ribonucleoprotein

**SG:** stress granule

**SOLE:** spliced localization element

**UPR:** unfolded protein response

**UTR:** untranslated region

**YPS:** Ypsilon Schachtel



# Content

<b>Acknowledgments</b> .....	<i>i</i>
<b>Summary</b> .....	<i>iii</i>
<b>Zusammenfassung</b> .....	<i>v</i>
<b>Abbreviations</b> .....	<i>vii</i>
<b>1 Introduction</b> .....	<b>3</b>
1.1 Stress response in eukaryotic organisms .....	3
1.1.1 Cellular stress response .....	3
1.2 RNP granules –properties and assembly .....	5
1.2.1 Properties of RNP granules .....	5
1.2.2 Mechanisms of RNP granule formation: the role of protein components .....	7
1.2.3 Mechanisms of RNP granule formation: the role of RNA molecules.....	8
1.3 P-bodies in the <i>Drosophila</i> female germline.....	10
1.3.1 <i>Drosophila</i> oogenesis and nutritional stress.....	10
1.4 <i>oskar</i> mRNA – an essential germline determinant in <i>Drosophila</i> .....	14
1.4.1 Localization of <i>oskar</i> mRNPs .....	15
1.4.2 <i>oskar</i> mRNA translational control.....	17
1.5 <i>oskar</i> mRNA noncoding functions.....	18
<b>Aim</b> .....	<b>21</b>
<b>2 Materials and Methods</b> .....	<b>23</b>
2.1 Materials .....	23
2.1.1 Equipment.....	23
2.1.2 Consumables.....	24
2.1.3 Reagents and chemicals.....	24
2.1.4 Buffers and solutions .....	26
2.1.5 Antibodies .....	27
2.1.6 Plasmids .....	28

2.1.7 Primers .....	28
2.1.8 Oligonucleotides for smFISH probe synthesis.....	28
2.1.9 Fly lines.....	32
2.1.10 Software.....	32
2.1.11 Online sources.....	32
2.2 Methods.....	33
2.2.1 Fly husbandry.....	33
2.2.2 Fly nutrient-deprivation: conditioning flies for promoting P-body formation in the <i>Drosophila</i> germline.....	33
2.2.3 Generation of transgenic fly lines.....	34
2.2.4 Genetic crosses.....	36
2.2.5 Ovary dissection and fixation.....	37
2.2.6 Single molecule fluorescent <i>in situ</i> hybridization (smFISH).....	38
2.2.7 smFISH: probe design and labeling.....	38
2.2.8 Immunofluorescence technique.....	38
2.2.9 Ovary mounting and preparation for microscopy.....	39
2.2.10 Microscopy.....	39
2.2.11 Image processing and analysis.....	39
2.2.12 Cloning and bacterial transformation.....	40
2.2.13 DNA plasmid isolation and purification.....	40
2.2.14 RNA extraction.....	41
2.2.15 cDNA synthesis.....	41
2.2.17 qPCR.....	42
2.2.18 DNA gel electrophoresis.....	42
2.2.19 RNA <i>in vitro</i> transcription.....	42
2.2.20 RNA gel electrophoresis.....	42
2.2.21 <i>in vitro</i> dimerization assay.....	42
2.2.22 RNA affinity <i>in vitro</i> pull-down assay.....	43
2.2.23 Western blot.....	45
2.2.24 Protein PAGE.....	45
2.2.25 Sample preparation for mass spectrometry (MS) and TMT labeling.....	45
2.2.26 Mass spectrometry (MS) data acquisition.....	46
2.2.27 Mass spectrometry (MS) data analysis.....	47
2.2.28 DATA analysis.....	48

<b>3 Results</b> .....	51
3.1 <i>oskar</i> mRNA is the part of P-body granules in <i>Drosophila</i> female germline .....	51
3.1.1 P-body distribution in the <i>Drosophila</i> germline.....	51
3.1.2 <i>oskar</i> mRNA localizes in P-bodies upon nutritional stress in the <i>Drosophila</i> germline .....	52
3.1.3 <i>oskar</i> mRNA levels are not affected upon nutritional stress .....	52
3.2 An intact <i>oskar</i> 3'UTR is required for P-body formation and growth.....	54
3.2.1 A mutation in dimerizing domain of the <i>oskar</i> 3'UTR impairs P-body formation .....	54
3.2.2 A mutation in the <i>oskar</i> 3'UTR dimerizing domain affects recruitment of other components into P-bodies .....	56
3.2.3 <i>bicoid</i> and <i>gurken</i> do not localize in P-bodies upon nutritional stress in the <i>Drosophila</i> germline .....	58
3.2.4 A mutation in the <i>oskar</i> 3'UTR dimerizing domain hinders P-body growth.....	60
3.3 The effect of <i>oskar</i> mRNA dimerization on P-body formation .....	62
3.4 Defective repression of mutant non-dimerizing <i>oskar</i> mRNAs does not impair P-body formation .....	64
3.5 <i>oskar</i> 3'UTR is sufficient to support P-body formation .....	69
3.5.1 Flies expressing a <i>oskar</i> 3'UTR rescue fragment form P-bodies upon nutrient deprivation .....	69
3.6 Introducing mutations in the <i>oskar</i> 3'UTR affects RBP recruitment .....	72
3.6.1 Introducing a mutation in the DD loop of <i>oskar</i> 3'UTR affects recruitment of Bruno .....	72
3.6.2 The <i>oskar</i> 3'UTRWT vs. <i>oskar</i> 3'UTRUU proteome .....	76
<b>4 Discussion</b> .....	81
4.1 <i>oskar</i> mRNA is a component of P-bodies in the <i>Drosophila</i> germline.....	81
4.2 <i>oskar</i> mRNA drives P-body assembly in the <i>Drosophila</i> germline .....	82
4.3 P-bodies: a protective harbors of maternal mRNAs .....	87
4.4 RNA as a scaffold in RNP granule formation.....	88
4.5 Importance of RNP granule formation in response to stress .....	89
<b>Bibliography</b> .....	91
<b>List of figures</b> .....	107
<b>Appendix</b> .....	109

Appendix I .....	109
Appendix II .....	109
Appendix III .....	110
Appendix IV .....	110
Appendix V .....	111
Appendix VI .....	112
Appendix VII .....	112
Appendix VIII .....	113
Appendix IX .....	113
Appendix X .....	116
Appendix XI .....	119
Appendix XII .....	122
Appendix XIII .....	123







“The known is finite, the unknown infinite; intellectually we stand on an islet in the midst of an illimitable ocean of inexplicability. Our business in every generation is to reclaim a little more land, to add something to the extent and the solidity of our possessions.”

–Thomas Henry Huxley, *On the Reception of The Origin of Species* (1887)



# 1 Introduction

## 1.1 Stress response in eukaryotic organisms

“An organism is involved with the environment to which it is not only adapted but which is adapted to it as well.”

- Vladimir Ivanovich Vernadsky, 1980.

Every living organism senses environmental changes and responds to them in order to maintain homeostasis during development and adulthood. In order to survive, organisms developed multiple strategies to sense, respond and cope with internal and external stressors. As main building blocks of each organism, cells developed a number of mechanisms to respond to diverse fluctuations in the environment including many types of stressors (mechanical, chemical, temperature perturbations, oxygen shock, nutrient deprivation or excess, radiation etc.) (Majmundar et al., 2010; Richter et al., 2010; Sengupta et al., 2010; Wellen and Thompson, 2010). These mechanisms are commonly referred to as stress response (Mager and Ferreira, 1993).

### 1.1.1 Cellular stress response

The greatest challenge for cells is to quickly respond and adapt to changes in their surroundings. To deal with different types of stressors, cells developed a number of response mechanisms. Those include the DNA damage response (DDR) (Ciccia and Elledge, 2010) usually triggered by DNA breaks, caused for example by ionizing radiation, the unfolded protein response (UPR) in ER and mitochondria (Buchberger et al., 2010; Hetz and Papa, 2018; Shpilka and Haynes, 2017) mostly induced by heat shock or chemical toxins and autophagy which could be triggered by many external cues including nutrient deprivation (Galluzzi et al., 2018a; Kroemer et al., 2010). All these stress response mechanisms are defined as “adaptive stress response”, with ultimate role to ensure cell survival. However, if one of the mechanisms fail, stressed cells ultimately undergo regulated cell death (RCD) (Galluzzi et al., 2018a, 2018b; Neves et al., 2015). Different stressors activate different stress response mechanisms and each starts with the cell sensing the cues from the environment, transducing the signal and selecting appropriate pathways to finally regulate the gene expression machinery (Figure 1.1). Cellular stress responses can be regulated at many levels, from the transcriptional, post-transcriptional, to the translational and post-translational levels (Chen et al., 2010; Spriggs et al., 2010).

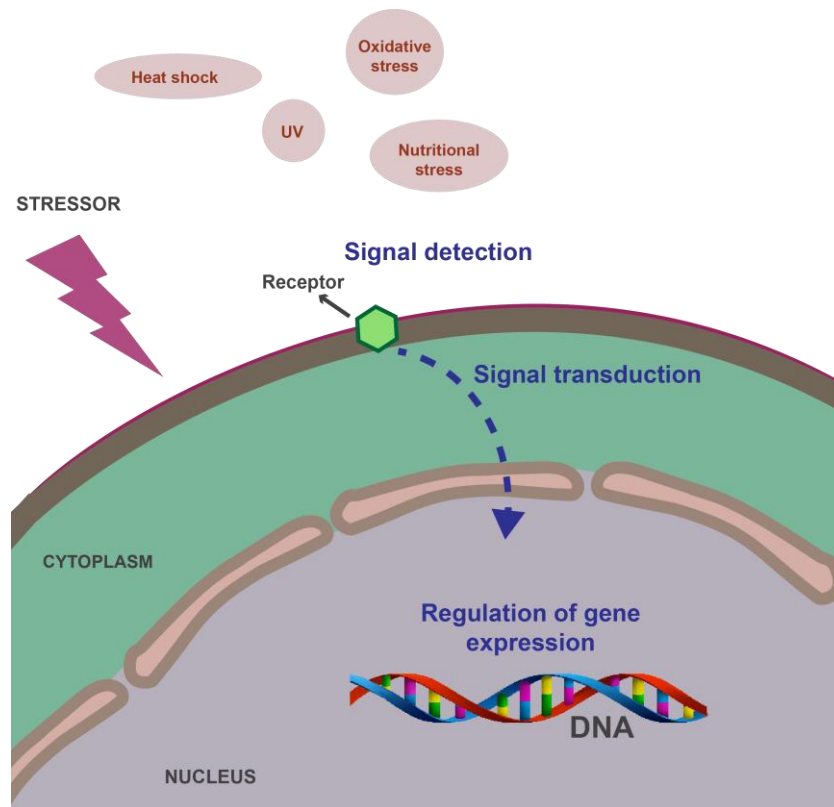


**Figure 1.1 Cellular response to stress:** Schematic representation of a eukaryotic cell exposed to different types of stressors. A general mechanism in response to external stimuli is depicted here. In order to respond to external cues (e.g. different stressors: heat shock, UV, oxidative stress, nutritional stress) cell first detects the signal from the environment via specific receptors, then transmits the signal choosing appropriate signaling pathway to finally regulate gene expression machinery.

### 1.1.2 Stress induced translational control

One of the first and most efficient stress-induced mechanisms to regulate gene expression is the control of protein synthesis by global attenuation of translation and/or local synthesis of stress response proteins (Ashe et al., 2000; Spriggs et al., 2010). Translation can be regulated at different steps including initiation, elongation and termination (Gebauer and Hentze, 2004; Hershey et al., 2012). Mostly, translational control is effected at the initiation step. There are many mechanisms that coordinate translational initiation (Hinnebusch and Lorsch, 2012; Pestova et al., 2001; Preiss and W. Hentze, 2003) and these can be broadly divided in two groups: a) global control, usually exerted by controlling phosphorylation and availability of eukaryotic initiation factors (eIFs) and b) mRNA specific control, dependent on sequences positioned in mRNA untranslated regions (5'UTRs or 3'UTRs) which are recognized by sets of regulatory factors, consisting of proteins and/or micro (mi)RNAs (Gebauer and Hentze, 2004). In addition, translational regulation can be achieved by controlling the availability of transcripts through their packaging into higher order cytoplasmic ribonucleoprotein particles (RNPs) (Besse and Ephrussi, 2008; Chekulaeva et al., 2006; Kato and Nakamura, 2012).

## 1.2 RNP granules –properties and assembly

Eukaryotic cells contain non-membranous organelles with specific functions in cellular metabolism (Stroberg and Schnell, 2017). Such organelles include large cytoplasmic assemblies of proteins and RNAs referred to as ribonucleoprotein (RNP) granules. RNP granules include the germ granules found in oocytes and embryos, neuronal granules, stress granules and P-bodies, which are present in the cytoplasm, Cajal bodies, nucleolus and paraspeckles characteristic of the nucleus (Fox et al., 2002; Gall, 2000; Kiebler and Bassell, 2006; Protter and Parker, 2016; Voronina et al., 2011, 2012). Among eukaryotes, RNP granules share common structural and functional characteristics. (A. Schisa, 2012; Decker and Parker, 2012; Kedersha et al., 2005; Voronina et al., 2012).

### 1.2.1 Properties of RNP granules

The most studied RNP granules are those found in the cytoplasmic compartment of yeast and mammalian cells - stress granules (SG) and processing (P)-bodies. SG and P-bodies have been described as subcellular non-membranous compartments harbouring repressed mRNAs destined to undergo decay, re-enter the translation or even be targeted for autophagy (Bregues et al., 2005; Buchan et al., 2013; Decker and Parker, 2012; Frankel et al., 2017; Hubstenberger et al., 2017; Liu et al., 2005; Wang et al., 2018). SG form in response to different stresses that usually lead to inhibition of translational initiation (Anderson and Kedersha, 2006; Jain et al., 2016; Kedersha et al., 1999). Besides containing silenced mRNAs, SG contain translational initiation factors (eIF4E, eIF4G, eIF4A, eIF4B, eIF3), the 40S ribosomal subunit and many RNA binding proteins (PABP, G3BP, TIA-1, TIA-R etc.) (Buchan and Parker, 2009; Decker and Parker, 2012; Parker and Sheth, 2007). Thus, these cytoplasmic foci are sometimes referred to as sites of stalled translational initiation complexes. P-bodies assemble from microsome mRNP precursors in response to different stresses that lead to global inhibition of translation (Kedersha et al., 2005; Teixeira et al., 2005). P-bodies are in general devoid of translational initiation factors and ribosomes (Andrei et al., 2005; Bregues et al., 2005; Teixeira et al., 2005) and contain degradation machinery components (Dcp1p/Dcp2p, Dhh1p/RCK/p54, Pat1p, Eds3p, Lsm1p-7p), the CCR4/POP2/NOT complex, the exonuclease Xrn1p and a number of translational repressors (e.g. Ge-1, Maternally expressed at 31B (Me31B/Dhh1), eIF4E-T) (Andrei et al., 2005; Cougot et al., 2004; Eulalio et al., 2007a; Sheth and Parker, 2003; Yu et al., 2005). Even though the decapping machinery components are the so-called core of P-bodies, these granules are not thought to be sites of RNA degradation (reviewed in Voronina *et al.*, 2011, Hubstenberger *et al.*, 2017). The biological function of SG and P-bodies is poorly understood. Several models suggest a role of these cytoplasmic foci in maintaining mRNA metabolism. As described in the model of the “mRNA cycle” (Figure 1.2) by

Decker and Parker (2012), mRNA molecules undergo constant exchange between the cytosol, SG and P-bodies. According to this model, mRNAs in polysomes go through rounds of translation initiation, elongation and termination. Once this process is perturbed by external cues, usually different types of stressors, mRNA translation is inhibited. After ribosome run off, populations of mRNAs are sequestered into P-bodies from where they can later re-enter translation or undergo degradation. On the other hand, subsets of mRNAs that do not enter P-bodies, or whose translation is initiated but does not progress further, coalesce into SG.

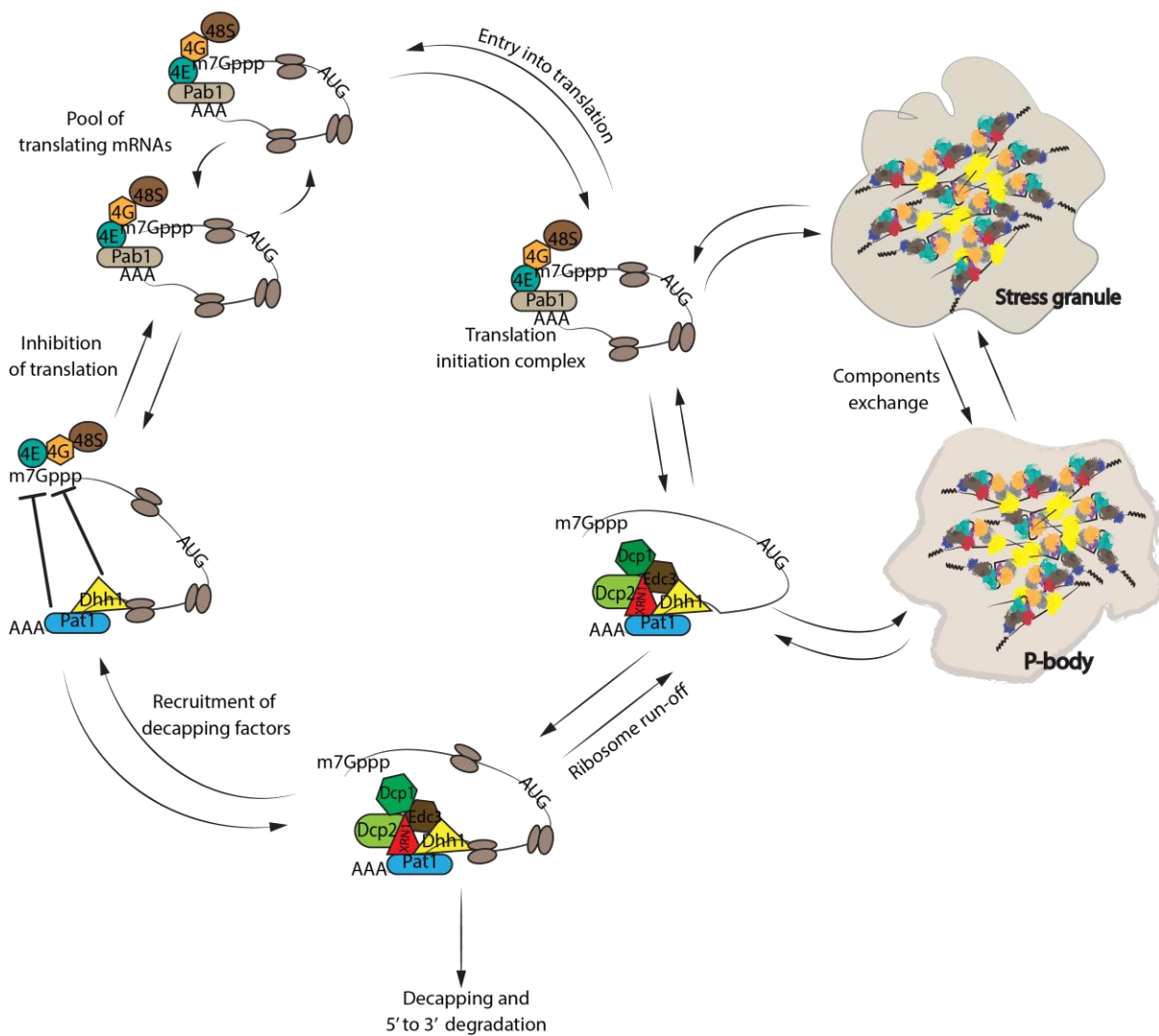


**Figure 1.2 Model of the “mRNA cycle”:** This model describes mRNA fate and dynamic movement of mRNA molecules between the translationally active mRNA pool and stress granules and P-bodies. Possible mRNP transitions between different mRNA states are also depicted. At each state, mRNPs are defined by the specific mRNA interactors. Recruitment of specific factors to mRNA decides mRNA’s fate. This figure was made according to the “mRNA cycle” model presented by Decker and Parker, 2012.



Other RNP granules, such as neuronal granules and germ granules, have been shown to have an effect on synaptic plasticity and sequester maternal mRNAs or proteins during oogenesis or development, respectively (A. Schisa, 2012; McCann et al., 2011). Unlike cytoplasmic and germ granules, the biological function of nuclear RNP granules is better understood. For example, Cajal bodies are known to be involved in mRNA processing, and the nucleolus is the compartment where rRNAs are transcribed, pre-rRNAs processed and ribosome subunits assembled (Mao et al., 2011b, 2011a). Summed up, different types of eukaryotic RNP granules display various and complex functions in the cell. The efficient control of many processes in the cells is achieved by subcellular compartmentalization. Spatially restricting cellular processes such as transcription, translational control, RNA processing, localization etc., within RNP compartments could allow local, thus quick and economic gene expression regulation in a response to environmental changes. The ability to quickly respond to external and internal cues and regulate gene expression, allows the organism to achieve and maintain its homeostatic state.

### 1.2.2 Mechanisms of RNP granule formation: the role of protein components

Many studies to date have explored the roles of RNAs and proteins in RNP granule assembly. However, the molecular basis of the mechanisms involved in RNP granule formation are poorly understood. It was shown that P-body formation is dependent on a number of its components such as the DEAD box helicase Me31B in *Drosophila* or its mammalian homologue RCK/p54. Depletion of Me31B/RCK/p54, but also other P-body components such as GW182, RAP55, LSM4, 4E-T in mammalian cells and Droscha, Pasha, Dicer-1, AGO1, GW182, HPat, LSM1, or Ge-1 in *Drosophila* S2 cells, inhibits P-body assembly (Andrei et al., 2005; Eulalio et al., 2007a; Ferraiuolo et al., 2005; Jakymiw et al., 2005; Pauley et al., 2006). Protein-protein interactions including interactions between structured domains or between intrinsically disordered regions all contribute to RNP granule formation (Figure 1.3) (Decker et al., 2007; Gilks et al., 2004; Hebert and Matera, 2000; Ling et al., 2008; Mittag and Parker, 2018; Protter et al., 2018; Tourrière et al., 2003). For example, formation of G3BP dimers is necessary for SG assembly in mammalian cells (Kedersha et al., 2016; Tourrière et al., 2003) and oligomerization of coilin promotes Cajal body formation (Hebert and Matera, 2000). In yeast Edc3 protein enhances P-body formation (Decker et al., 2007; Ling et al., 2008), and in *C. elegans* MEG1 and MEG3 were shown to be required for P-granule assembly (Wang et al., 2014). In addition, protein components of RNP granules maintain RNP granule dynamics and contribute to granule reorganization. Such example is CGH-1 in *Caenorhabditis elegans*, (orthologue of yeast ste13, mammalian RCK/p54 and *Drosophila* Me31B) which was shown to be necessary for maintaining the dynamics of grPBs in the worm's

oocytes, by preventing the transition of other grPBs components to nondynamic solid RNP aggregates (Hubstenberger et al., 2013).

### 1.2.3 Mechanisms of RNP granule formation: the role of RNA molecules

Along with proteins, RNA molecules are importantly involved in RNP granule formation. It is well known that SG and P-body assembly requires the pools of non-translating mRNAs (Liu et al., 2005; Pillai et al., 2005; Sheth and Parker, 2003; Teixeira et al., 2005). Both protein-protein and RNA-RNA interactions promote assembly of various types of RNPs, starting from relatively simple transport particles to complex RNP granules (Figure 1.3). Many localizing mRNAs in order to be transported to their final destination are packaged into specific RNPs that include transport machinery components (Hughes and Simmonds, 2019; Martin and Ephrussi, 2009; Parton et al., 2014). For such mRNAs, including *oskar* and *bicoid* mRNAs, specific *in trans* interactions between mRNA molecules are important for their recruitment into localizing mRNPs during oocyte development in *Drosophila* (Ferrandon et al., 1997; Jambor et al., 2011). Not only the messenger RNAs, but also other types of RNA molecules such as long noncoding (lnc)RNAs can be involved in RNP granule formation. One of the examples is the lncRNA NEAT1, required for paraspeckle formation in the nucleus of mammalian cells (Clemson et al., 2009; Mao et al., 2011a; Yamazaki et al., 2018). Interestingly studies showed that some RNA molecules can self-assemble *in vitro* (Van Treeck et al., 2018) and some when injected in the cytosol trigger SG formation (Mahadevan et al., 2013). In addition, it has been shown that certain features of RNA structure provide the specificity for mRNAs to be targeted into RNP granules (Langdon et al., 2018). These findings indicate the importance of RNAs in RNP granule biogenesis (reviewed in Van Treeck and Parker, 2018). Van Treeck and Parker (2018) suggested that RNA molecules could have the role of a scaffold in RNP granule formation. They proposed the model where RNA-RNA interactions are an important step in driving RNP granule assembly. Both inter- and intramolecular RNA-RNA interactions could enhance assembly of RNA binding proteins by providing an interaction surface for proteins to bind or/and by promoting conformational changes of the proteins which could further drive formation/maturation of higher order RNP complexes (Figure 1.3), (Van Treeck and Parker, 2018). Recent study by Garcia-Jove Navarro et al., showed that RNA molecules seed the nucleation centres and regulate the size of RNA-protein condensates in living cells (Garcia-Jove Navarro et al., 2019).

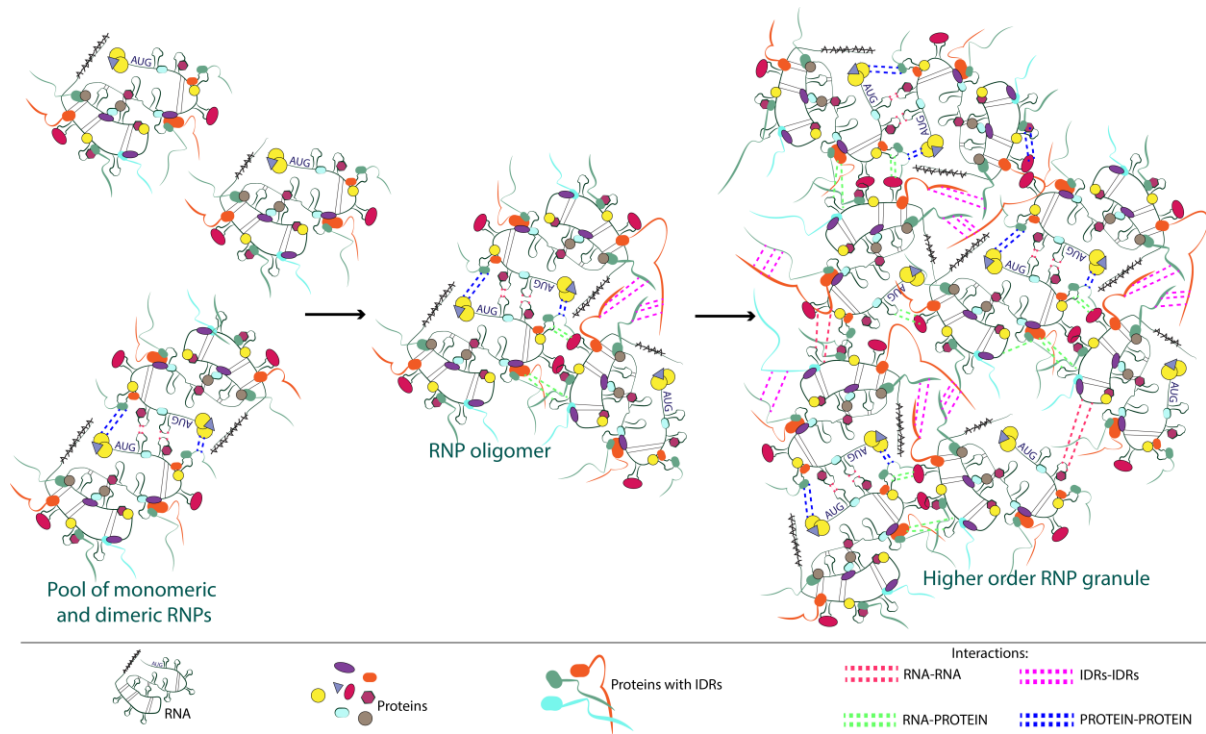


**Figure 1.3 RNP granule assembly:** RNP granules assembly is assumed to be a multistep process dependent on RNA and protein *in cis* and *in trans* interactions. RNP granule assembly is believed to start from the pools of monomeric and dimeric RNPs. Establishing inter- and intramolecular RNA interactions together with protein-protein and RNA-protein interactions leads to RNP oligomerization and growth. Proteins can interact both via well-folded domains or intrinsically disorder regions (IDRs) providing interface for new intermolecular contacts. Further growth of oligomers into a mature higher order RNP granule is promoted with coordinated interplay among specific components of RNPs. This figure is inspired by the work of Jain et al., 2016 and Van Treeck and Parker, 2018.

### 1.3 P-bodies in the *Drosophila* female germline

Processing (P-)bodies in *Drosophila* together with other RNP granules to which they are functionally and biochemically related, including Balbiani body, polar granules, perinuclear nuage, are cytoplasmic aggregates present in the insects' germ cells (reviewed in A. Schisa, 2012). Two main building blocks of P-bodies in *Drosophila* are mRNA molecules and RBPs. In *Drosophila* these cytoplasmic foci are exclusive to the germline, the oocyte and the nurse cells, and have not been detected in the soma.

#### 1.3.1 *Drosophila* oogenesis and nutritional stress

The *Drosophila* ovary is composed of 16-20 ovarioles, each of which contains a germarium and a vitellarium (Figure 1.4 A and B). Oogenesis starts within the germarium where a germline stem cell divides into a daughter stem cell and a cytoblast. The cytoblast undergoes four rounds of mitosis with incomplete cytokinesis giving rise to one oocyte and 15 nurse cells, all interconnected by cytoplasmic bridges called ring canals (Brown E.H., 1964; King, 1957; Koch and King, 1969; Koch et al., 1967; Yamashita, 2018). When follicle cells surround the syncytium, a stage 1 egg-chamber is formed. The egg-chamber exits the germarium and continues to grow and develop in the vitellarium, which is composed of egg-chambers at different developmental stages (reviewed in Yamashita, 2018) (Figure 1.4 B). *Drosophila* oogenesis is nutrient dependent and requires a significant amount of energy in order to produce a mature egg, which can be fertilized and developed into an embryo. When exposed to nutritional stress, *Drosophila* females halt egg production. This can occur through the triggering of apoptotic events in the immature germline cells either at the beginning of oogenesis, in the germarium, or at the onset of vitellogenesis (Drummond-Barbosa and Spradling, 2001; Mazzalupo and Cooley, 2006; Pritchett et al., 2009). Alternatively, this can occur by the slowing down of oocyte growth, and preserving mainly previtellogenic egg-chambers and early vitellogenic ones in order to allow them to continue development once the stressful condition has passed (Drummond-Barbosa and Spradling, 2001; Shimada et al., 2011). While the mechanism and the exact biological function of P-bodies in the *Drosophila* germline is not yet fully understood, their formation in the nurse cells and the oocyte may also contribute to the cellular response to nutrient deprivation that affects egg-chambers growth. Additionally, P-body formation may be a mechanism that evolved to protect maternal determinants essential for development during stress conditions.

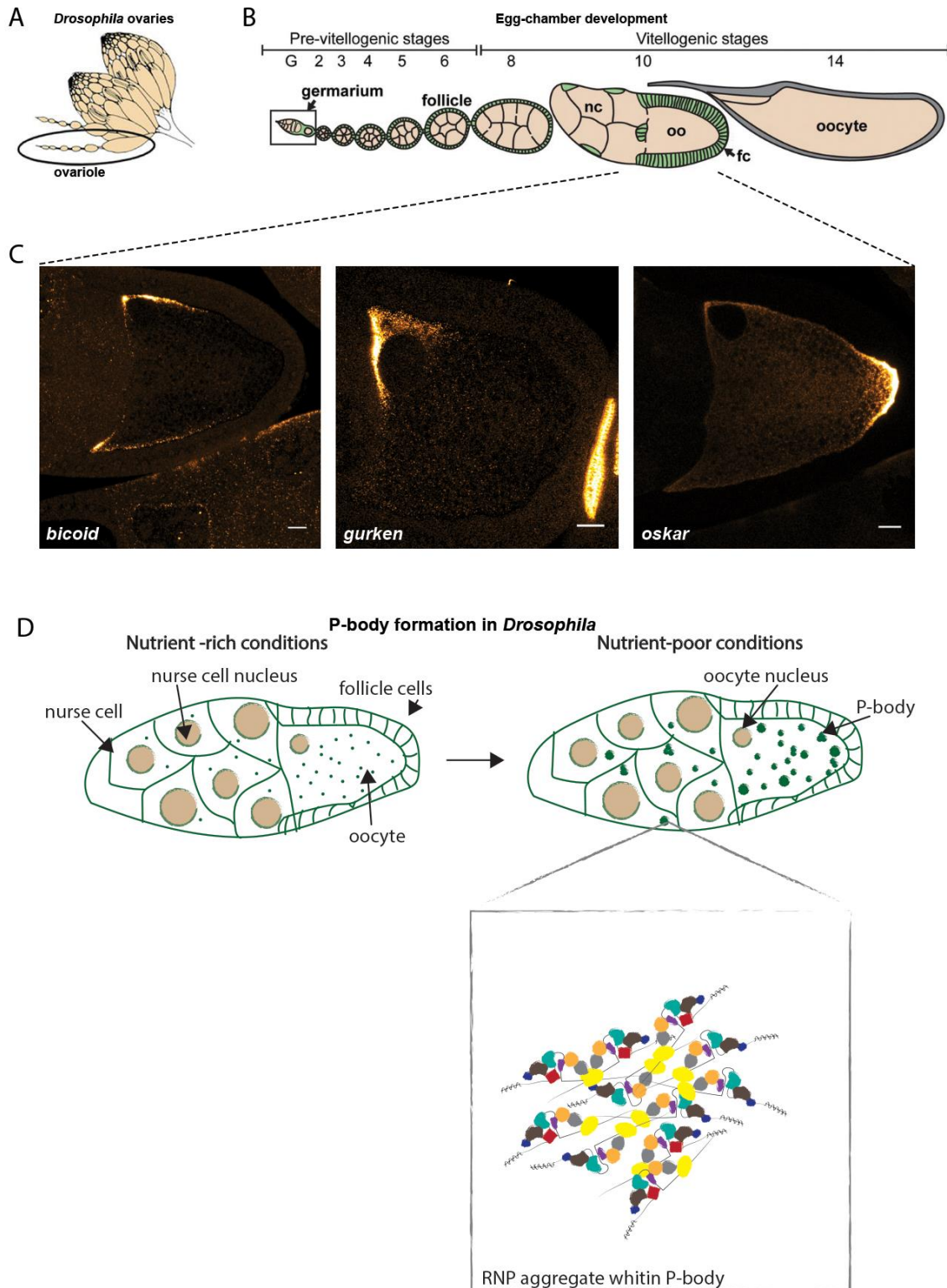


**Figure 1.4 *Drosophila* oogenesis and nutrient stress induced P-body formation:** **A** *Drosophila* pair of ovaries. Single ovariole is highlighted with the black ellipse, (adapted from Huang et al., 2014). **B** *Drosophila* egg-chamber development. *Drosophila* ovary is composed of 14-16 egg-chambers. In germarium, germline stem cells divide to form daughter cells (cystoblasts), which further undergo four additional divisions to form 16-cell germline cysts (in beige), composed of nurse cells (nc) and an oocyte (oo). Follicle cells (fc, in green) surround 16-cell germline cyst, (adapted from Ables et al., 2016). **C** smFISH of *Drosophila* mRNAs, *bicoid* (left), *gurken* (middle) and *oskar* (right) in a stage 10A oocyte. Scale bars: 10 $\mu$ m. **D** P-body formation in the *Drosophila* germline. Stage 9 egg-chambers are presented under nutrient-rich and nutrient-poor conditions. Under nutrient-rich conditions dispersed state of P-body precursors is depicted while P-bodies are depicted under nutrient-poor conditions. P-body building blocks, mRNA-protein aggregates, are highlighted in the box.

### 1.3.2 P-bodies in *Drosophila*: properties and biological function

P-bodies were first described in *Drosophila* in the late 90's (Wilsch-Bräuninger et al., 1997). Due to their sponge like appearance in electron micrographs they were first named "sponge bodies". These RNP granules were described as cytoplasmic structures devoid of ribosomes and lacking a surrounding membrane. Since they contain multiple copies of RNAs, it was initially thought that their role is to assemble RNP transport particles for localization of specific mRNAs. A number of maternal mRNAs (e.g. *bicoid*, *gurken* and *oskar*) are reported to be the part of these cytoplasmic foci (Burn et al., 2015; Weil et al., 2012). Many protein components of *Drosophila* sponge bodies are orthologs of proteins described in mammalian and yeast P-bodies (e.g. Dcp1p/DCAP-1, Dcp2p/DCAP-2, Patp, Edc3p, Ge-1, RCK/p54) (Eulalio et al., 2007b; Parker and Sheth, 2007). In *Drosophila*, two types of P-bodies have been described: dispersed or reticulated bodies. Dispersed bodies are observed in females fed with food medium supplemented with nutrients, whereas reticulated bodies are observed when females are grown on medium with no additional nutrients included or are kept as virgin females regardless, of the diet conditions (Snee and Macdonald, 2009). Since dispersed P-bodies are likely the precursors of the larger reticulated ones, in this study I will refer to reticulated P-body granules observed upon nutritional stress as P-bodies. RNP particles observed prior to nutritional stress will not be referred to as P-bodies. The mechanisms that underlie P-body formation in *Drosophila* female germline are not fully understood. As previously mentioned, this process is triggered upon nutrient deprivation (Burn et al., 2015; Snee and Macdonald, 2009) and is dependent on the insulin/target of rapamycin (TOR) signaling pathway (Burn et al., 2015). *Drosophila* insulin-like peptides (dILPs) secreted from the brain control P-body formation in the germline. Follicle cells, which first sense the signal from the environment, mediate the dILP dependent starvation response and consequently P-body assembly in the nurse cells and the oocyte (Burn et al., 2015) (Figure 1.4 D). The assembly of these cytoplasmic foci is also dependent on the organization of MT cytoskeleton and indirectly on kinesin and dynein motor activity (Shimada et al., 2011).

The biological function of *Drosophila* P-bodies is not fully known. Since a number of the components of these RNP complexes, such as Me13B, Bruno and Hrp48 are translational repressors (Huynh et al., 2004; Kim-Ha et al., 1995; Nakamura et al., 2001; Webster et al., 1997; Yano et al., 2004), it is fair to assume that one of the main functions could be inhibition of translation in the germline. Additionally, a number of components (e.g. Exu, Yps, Staufen, Tral, BSF etc.) (Berleth et al., 1988; Eulalio et al., 2007b; Martin et al., 2003; Snee and Macdonald, 2009; Wilhelm et al., 2000a) present in the transport RNPs of localizing mRNAs such as *oskar*, *gurken*, *bicoid*, *nanos* are also found in the P-bodies. Transport RNPs could be the precursors of higher order RNP aggregates such as P-bodies. Once exposed to stress

## *1 Introduction*

(e.g. nutrient-poor conditions), transport of localizing mRNAs to their destinations could be stalled by coalescing the individual mRNPs into P-body aggregates. This mechanism could protect mRNAs from degradation or inhibit unnecessary protein synthesis, which could be detrimental for the cells during conditions of stress. In addition, it has been suggested that P-bodies protect a subset of maternal mRNAs during the stress response in order to allow proper development to proceed once the stress is overcome (Boag et al., 2008).

## 1.4 *oskar* mRNA – an essential germline determinant in *Drosophila*

In *Drosophila*, establishment of the embryonic body axis is accomplished mainly by the activity of the three maternally deposited mRNAs: *gurken*, *bicoid* and *oskar* (Figure 1.4 C). While *gurken* is required for the establishment of dorsoventral axis, *bicoid* and *oskar* are essential for the establishment of anterior-posterior (AP) polarity (Riechmann and Ephrussi, 2001). Together with other maternally deposited mRNAs during *Drosophila* oogenesis, *oskar* mRNA is synthesized in the nurse cells and transported to the oocyte via the ring canals. Once in the oocyte, *oskar* mRNA localizes at the posterior pole (Figure 1.4 C) where it is translated from oogenic stage 9 onwards (Figure 1.6 A and B) (Ephrussi et al., 1991; Kim-Ha et al., 1991). In order to be translated, silent *oskar* mRNPs must be derepressed and translation initiation activated. Two isoforms of Oskar protein are synthesized, short and long Oskar. Short Oskar is essential for primordial germ cell formation and embryonic patterning (Markussen et al., 1995; Rongo et al., 1995). The protein is an integral part of the polar granules and is required for germ plasm assembly (Tanaka and Nakamura, 2008; Vanzo et al., 2007). If ectopically expressed Oskar protein is sufficient to lead to germ plasm formation (Ephrussi and Lehmann, 1992).

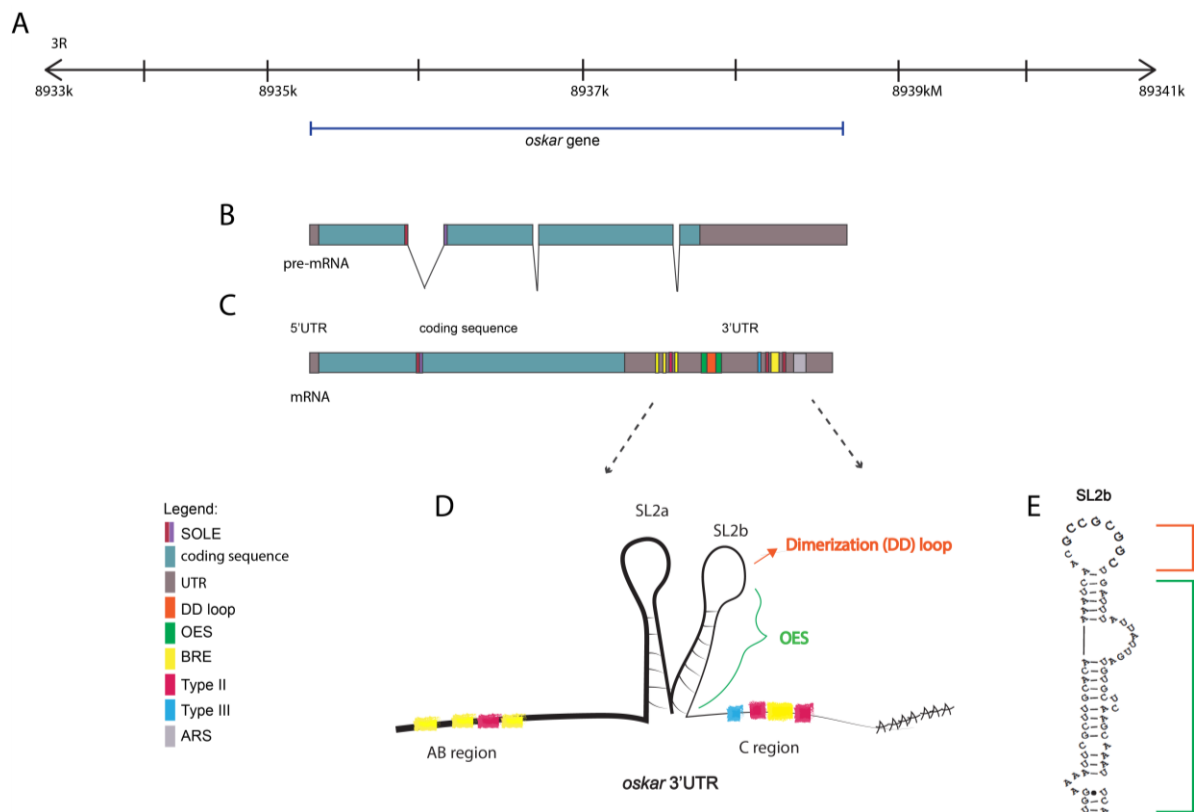


**Figure 1.5** *oskar* mRNA: **A** Scheme of *Drosophila* third chromosome right arm (3R) fragment, containing *oskar* gene coordinates (highlighted with dark blue line), (adapted from FlyBase). **B** Nascent *oskar* RNA (pre-mRNA) with four exons and three introns depicted. Coding sequence is presented in teal and untranslated regions (UTRs) in gray. **C** Mature *oskar* mRNA transcript (length: 3058 nucleotides). **D** Schematic representation of *oskar* 3'UTR fragment containing AB and C region with Bruno binding sites (BREs, Type II and Type III) and stem-loops, SL2a and SL2b. SL2b harbours oocyte entry signal (OES) (in green) and dimerization domain (DD) loop (in orange). **E** Stem-loop 2b (SL2b; adapted from Jambor et al., 2011) contains six nucleotide palindromic sequence (CCGCGG) which mediates the “kissing-loop” interaction between two *oskar* molecules.



### 1.4.1 Localization of *oskar* mRNPs

During *Drosophila* oogenesis the vast majority of mRNAs including *oskar* are transcribed in the nurse cells (Becalska and Gavis, 2009; Weil, 2014). Along with other molecules necessary for oocyte growth and development, *oskar* mRNA is transported into the oocyte compartment. When transported into the oocyte *oskar* is being localized to its final destination, the oocyte posterior pole (Ephrussi et al., 1991; Kim-Ha et al., 1991). Localizing *oskar* mRNAs travel in the form of translationally silent RNP complexes. Besides *oskar*, these RNP complexes include the protein interactors involved in *oskar* localization, as well as in *oskar* translational regulation (e.g. Staufen, Hrp48, Glo, Otu, dDcp1, Cup, Exu, Yps) (Broyer et al., 2017; Huynh et al., 2004; Kalifa et al., 2009; Lin et al., 2006; Mansfield et al., 2002; Micklem et al., 2000; Nakamura et al., 2004; St Johnston et al., 1991; Tian and Mathews, 2003; Yano et al., 2004). *oskar* mRNAs start the journey in the nurse cells in the form of 2-copy particles, which later in the oocyte assemble into oligomeric and multimeric higher order RNPs (Glotzer et al., 1997; Little et al., 2015). Transport into the oocyte is microtubule-dependent and mediated by the microtubule minus-end directed transport machinery. This includes the dynein motor protein and the cargo adapters, dynactin, Bicaudal-D and Egalitarian, each of which is required for minus end directed motion of mRNAs (Bullock and Ish-Horowicz, 2001; Dienstbier et al., 2009; McClintock et al., 2018; Navarro et al., 2004). Transport of *oskar* mRNA requires a specific *cis*-acting element in the *oskar* 3'UTR, a 67nt stem-loop termed oocyte entry signal (OES) (Jambor et al., 2014) (Figure 1.5 D and E). The *oskar* OES is functionally similar to the transport localization signal (TLS) of *k10* mRNA (Jambor et al., 2014; Serano and Cohen, 1995). Transport of *oskar* and *K10* mRNAs, but also other mRNAs comprising a similar localization signal, is in direct association with Egalitarian, an RNA binding protein that mediates the interaction between the dynein motor and the mRNA (Dienstbier et al., 2009; McClintock et al., 2018). Localization of *oskar* mRNAs to the posterior pole of the oocyte is dependent on the microtubule plus-end directed motor, kinesin which is recruited to *oskar* mRNAs by *Drosophila* atypical RNA binding Tropomyosin-1 I/C. (Brendza et al., 2000; Zimyanin et al., 2008; Simon et al., 2015; Gaspar et al., 2017b). In addition, essential step for *oskar* localization to the posterior pole is the splicing of the first intron in the *oskar* pre-mRNA, (Hachet and Ephrussi, 2004) which results in assembly of the spliced localization element (SOLE) (Figure 1.5 C) and deposition of the exon junction complex (EJC) on the mRNA (Ghosh et al., 2012). At mid-oogenic stage 9, *oskar* begins to accumulate at the posterior pole, where the mRNA is anchored by a mechanism involving the F-actin cytoskeleton, F-actin associated proteins (Babu et al., 2004) and long Oskar protein (Vanzo and Ephrussi, 2002). After oogenic stage 10B, when microtubule network is reorganized, ooplasmic streaming promotes RNP movement and further recruitment and accumulation of *oskar* mRNA molecules to the oocyte pole (Dahlgaard et al., 2007; Lu et al., 2018; Serbus et al., 2005).

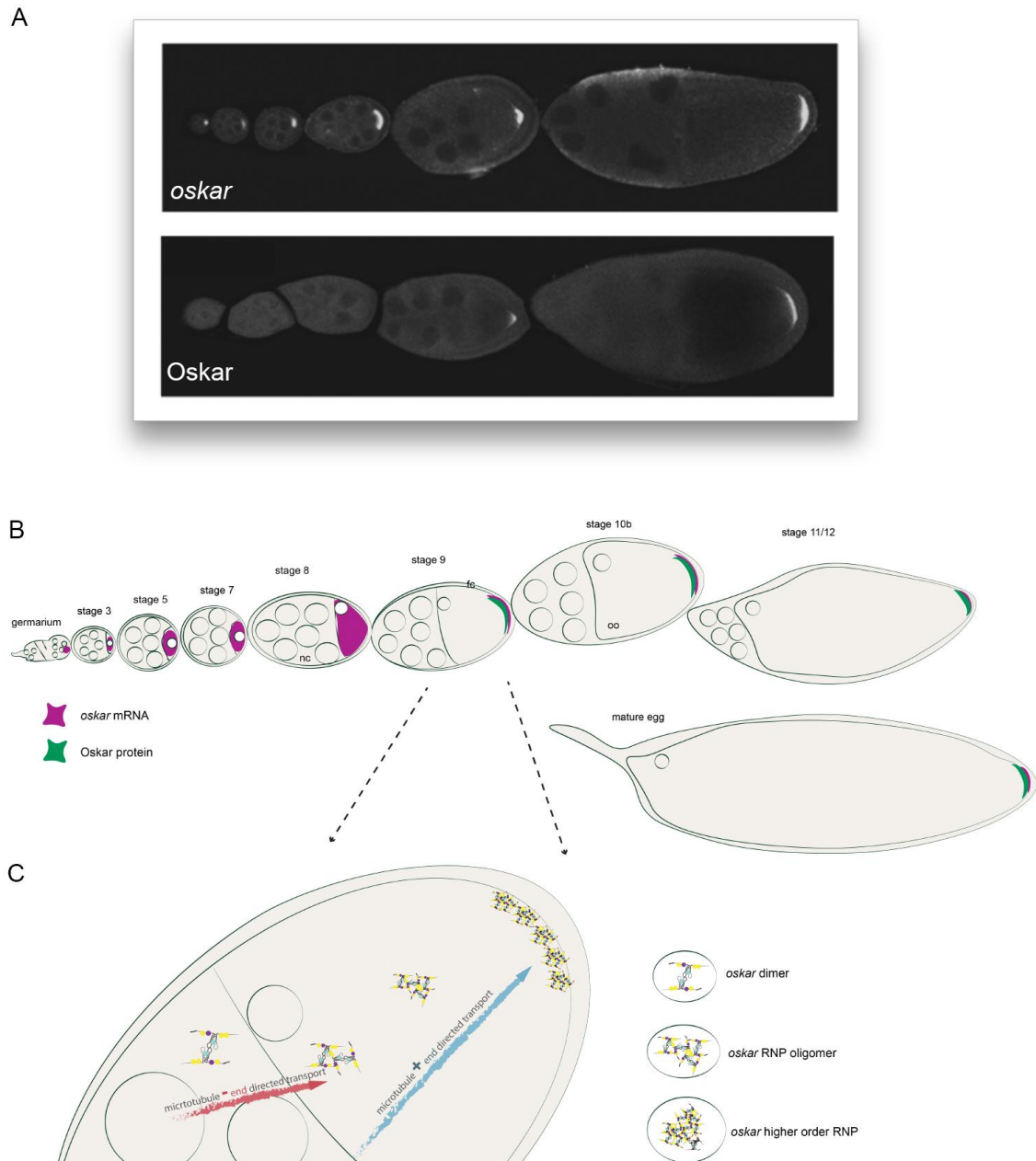


**Figure 1.6 *oskar* localization and translation:** **A** *oskar* mRNA localization during *Drosophila* oogenesis (top) and Oskar protein synthesis (bottom). *oskar* mRNA is detected with FISH and Oskar protein with immunostaining (adapted from Vanzo and Ephrussi, 2002). **B** Schematic representation of *Drosophila* oogenesis with depicted distribution of *oskar* mRNA and Oskar protein in the oocyte (oo). During oogenesis, *oskar* mRNA is transcribed in the nurse cells (nc), after which it is transported to the oocyte. Only when *oskar* mRNA reaches posterior pole of the oocyte it will be translated into Oskar protein, from the oogenic stage 9 onwards. **C** *oskar* mRNAs start the journey in the nurse cells in the form of 2-copy particles, which later in the oocyte assemble into oligomeric and multimeric higher order RNPs. Transport to the oocyte is microtubule-dependent and mediated by the microtubule minus-end directed transport machinery. Localization of *oskar* mRNAs to the posterior pole of the oocyte is dependent on the microtubule plus-end directed transport machinery.

### 1.4.2 *oskar* mRNA translational control

Regulation of translation is particularly important when gene expression has to respond rapidly to internal or external signals. During mRNA localization, translational control is essential in order to restrict protein expression spatially and temporally. This allows many copies of protein to be produced locally by transporting only a subset of mRNA molecules creating a gradient of function. In addition, restricted translation protects the cell from possible cytotoxic effects of the ectopically synthesized protein products. Examples of translational repression of localizing mRNAs have been described in different organisms (Liao et al., 2015; Martin and Ephrussi, 2009; Wilhelm et al., 2000b) and one of the best studied examples is *oskar* mRNA in *Drosophila*. *oskar* mRNA is translated after reaching the posterior pole of *Drosophila* oocyte at the mid of oogenesis (Ephrussi et al., 1991; Kim-Ha et al., 1991). Prior to its localization at the posterior of the oocyte *oskar* is translationally repressed. Once it reaches its final destination *oskar* translation is initiated. This complex translational control depends on many *oskar* mRNA *trans*-acting factors that are components of *oskar* RNPs. Those include translational repressors such as Bruno, PTB, dGe-1, Yps, Exu, Me31B, and activators such as Orb (Besse et al., 2009; Chang et al., 1999; Fan et al., 2011; Mansfield et al., 2002; Micklem et al., 2000; Nakamura et al., 2004; St Johnston et al., 1991; Tian and Mathews, 2003).

Bruno is an RNA recognition motif (RRM) containing protein that binds multiple sites in the *oskar* 3'UTR, termed Bruno response elements (BRE), and also recently identified type II and type III binding sites (Kim-Ha et al., 1995; Micklem et al., 2000; Reveal et al., 2010; St Johnston et al., 1991; Tian and Mathews, 2003) (Figure 1.5 C and D). Bruno inhibits *oskar* mRNA translation in a Cup-dependent and Cup-independent (also cap-independent) manner (Chekulaeva et al., 2006; Nakamura et al., 2004; Wilhelm et al., 2003). Cup-dependent inhibition is achieved by Bruno recruiting Cup protein which binds eIF4E and blocks eIF4E-eIF4G interaction, thus preventing recruitment of the 43S preinitiation complex and initiation of translation. On the other hand, Bruno-dependent *oskar* repression in the absence of Cup-eIF4E interaction occurs by promoting *oskar* mRNA oligomerization and co-packaging into higher order silent mRNP particles (Chekulaeva et al., 2006). Apart from its main role in translational repression, Bruno has also been implicated in *oskar* translational activation (Kim et al., 2015; Micklem et al., 2000). Interestingly many *oskar* translational regulators are components of *Drosophila* P-bodies (Besse et al., 2009; Fan et al., 2011; Nakamura et al., 2001; Snee and Macdonald, 2009). Besides Bruno, another *oskar* translational repressor, the Polypyrimidine tract binding protein (PTB), which binds along the *oskar* 3' UTR, has been demonstrated to facilitate oligomerization of *oskar* mRNA molecules (Besse et al., 2009). In mammalian models, PTB was reported to regulate the translation of so-called 5' terminal oligopyrimidine tract (TOP) mRNAs, that are sequestered into SGs

upon amino acid starvation (Damgaard and Lykke-Andersen, 2011; Tang et al., 2001). Other repressors of *oskar* translation, dGe-1 and the putative DEAD box helicase, Me31B, have been shown to be necessary for formation of, or components of *Drosophila* P-bodies (Fan et al., 2011; Nakamura et al., 2001). In addition, the Me31B ortholog in *C. elegans* (CGH-1) has been shown to be involved in P-body remodelling (Hubstenberger et al., 2013) and its homologue in mammalian cells (DDX6) was reported to be necessary for P-body formation (Ayache et al., 2015; Kamenska et al., 2016).

### 1.5 *oskar* mRNA noncoding functions

The main role of mRNAs is to serve as the template for protein synthesis. However, it has been shown that RNA molecules, lncRNAs and mRNAs, can have a dual function (Nam et al., 2016). The dual function of lncRNAs is highlighted by their regulatory and scaffolding functions and less often they contain a number of ORFs with the potential to be translated (Anderson et al., 2015; Olexiouk et al., 2016; Ruiz-Orera et al., 2014). Bifunctionality of mRNAs lies in their separate coding and noncoding functions. Besides their protein-coding function, mRNAs usually contain *cis*-acting elements within the 3'UTR by which they regulate their own stability, localization and translational control (Doi et al., 2019; Gebauer et al., 2012; Karapetyan et al., 2013; Kumari and Sampath, 2015; Martin and Ephrussi, 2009). *cis*-elements regulating different steps of mRNA life cycle do not act alone but together with *trans*-acting factors, both RBPs and other RNA molecules such as miRNAs (Gebauer et al., 2012; Hentze et al., 2018). Among many examples of mRNAs with dual function (reviewed in Hubé and Francastel, 2018) a few are known to have roles during the animal development. Those include *Xenopus laevis* VegT mRNA involved in cytoskeletal organization of the vegetal cortex of the oocyte (Kloc et al., 2005) and *oskar* mRNA (Figure 1.5) (Jenny et al., 2006).

The features responsible for noncoding functions of *oskar* mRNA lie within its around thousand nucleotides long 3'UTR (Figure 1.5 C and D) (Ephrussi et al., 1991). It has been shown that introducing mutations within the distal part of 3'UTR of *oskar* has a significant effect on the egg-laying rate of *Drosophila* (Kanke et al., 2015). In addition, in the absence of *oskar* mRNA oogenesis is arrested. Oocyte development does not progress past the oogenic stage 7 (Jenny et al., 2006) and mitotic divisions of the nurse cells are irregularly increased (Kanke et al., 2015). This phenotype is rescued by introducing transgenic *oskar* 3'UTR, which shows the essential role of the 3'UTR for oogenesis (Jenny et al., 2006). It has been shown that *oskar* mRNA is important for proper formation of the karyosome, a compact chromosomal structure within the oocyte nucleus (Kanke et al., 2015). In *oskar* mRNA null mutants, the karyosome fails to form properly and chromosomes appear fragmented (Jenny et al., 2006; Kanke et al., 2015). The same phenotype is observed in *oskar* transgenes carrying various

mutations within a distal region of 3'UTR (Kanke et al., 2015). A distal region of the *oskar* 3'UTR also has the role of sequestering *trans*-acting factors important for *oskar* mRNA translational regulation such as Bruno (Kanke et al., 2015). Furthermore, specific *cis*-acting elements within 3'UTR have been reported to be important for *oskar* mRNA transport. OES, also referred to as stem-loop 2b (SL2b), as previously mentioned, is necessary for *oskar* transport from the nurse cells to the oocyte (Jambor et al., 2014). Furthermore, this element mediates *oskar* mRNA dimerization *in vitro* (Jambor et al., 2011). The dimerization process occurs via kissing-loop mechanism between two *oskar* molecules and its mediated by a palindromic GC rich sequence in the loop of the SL2b (also referred to as dimerization domain, DD) (Jambor et al., 2011) (Figure 1.5 E). Once the mutations in the loop are introduced the dimerization process is abolished. In addition, *oskar* mRNA dimerization allows non-localizing *oskar* mRNAs to “hitchhike” with normally localizing *oskar* mRNAs and be transported together with them to the posterior of the oocyte (Jambor et al., 2011). *oskar* mRNA has the ability to dimerize and the ability to oligomerize into transport and higher order RNP particles (Glotzer et al., 1997; Jambor et al., 2011; Little et al., 2015). Thus, these observations together with the assumption that RNA molecules could not only have regulatory but also scaffolding roles (Van Treeck and Parker, 2018), and that RNA self-assembly can contribute to SG assembly (Mahadevan et al., 2013), open an intriguing question whether *oskar* mRNA could have a role in or contribute to RNP granule formation, specifically to P-body assembly.



## Aim

To understand biological function of RNP granules, it is important to get better insight into their structure and mechanism of assembly. Besides the findings that proteins are necessary and crucial for RNP granule formation (reviewed in Mittag and Parker, 2018) possible function and importance of RNAs in the assembly of the higher order RNP particles is indicated in few studies (reviewed in Van Treeck and Parker, 2018; Garcia-Jove Navarro *et al.*, 2019). One of the peculiar mRNAs with additional noncoding functions is the *oskar* mRNA, a key germline determinant in *Drosophila*. The abundance of *oskar* mRNA – around a million copies in a single mid-oogenetic oocyte and its ability to oligomerize in higher order RNP particles (Gaspar *et al.*, 2018; Glotzer *et al.*, 1997; Little *et al.*, 2015) such as P-body aggregates raises the possibility that this molecule plays an essential role in the formation of the P-bodies upon nutritional stress in *Drosophila* germline by acting as an RNA scaffold. The aim of this PhD thesis was to explore the role of RNAs in high order RNP granules formation using *oskar* mRNA as a model system. Thus, I investigated the importance of *oskar* mRNA in P-body assembly in *Drosophila* germline. *oskar* mRNA is previously shown to have the ability to dimerize and form complex RNP oligomers. Therefore, I tested whether the dimerization of *oskar* mRNA molecules could be important for P-body assembly and could it be an important step in recruiting specific RBPs which would stabilize dimeric complex and subsequently promote RNP granule growth. Coordinated interaction between RNA dimers and RBPs could be crucial for P-body assembly. Therefore, it would be interesting to investigate whether manipulation of *oskar* 3'UTR *cis*-elements could affect binding of *trans*-factors, mainly RBPs and subsequently affect P-body assembly in *Drosophila* female germline.





## 2 Materials and Methods

### 2.1 Materials

#### 2.1.1 Equipment

Agarose gel electrophoresis tank

Analytical scale (KERN PLJ)

Confocal Microscope: SP8 TCS X, DMI8 (Leica)

HC PL APO 20x/0.75 CS2 objective; Immersion: dry

HC PL APO 63x/1.40 Oil CS2 objective; Immersion: oil

Incubator (Heraeus Instruments)

Microcentrifuge 5415D (Eppendorf)

Microcentrifuge 5424R (Eppendorf)

Magnetic Mixer (Heidolph)

Magnet-stands for 15-50ml tubes (New England BioLabs)

Magnet-stands for 1.5-2ml tubes

Megafuge 40R table centrifuge (Heraeus, Thermo Fisher Scientific)

Nanodrop Spectrophotometer (Thermo Fisher Scientific)

Nutator (Labnet)

Pipettes (Gilson)

Power Supply (Sigma and Bio-Rad)

Tank for vertical gel electrophoresis (XCell SureLock Mini-Cell Electrophoresis System, Thermo Fisher Scientific)

Semi-dry transfer apparatus (Bio-Rad)

Thermocycler-PCR machine (Bio-Rad)

Thermomixer C (Eppendorf)

Tungsten needles

Tweezers (Dumont 5.5)

Tweezers (Dumont 5)

Vortex mixer (Heidolph)

Water bath container (Julabo)

Wide-field stereomicroscope (ZEISS)

### 2.1.2 Consumables

Agar plates

Cover glass 22x22mm or 24x32mm (Precision cover glasses thickness No. 1.5H (tol.  $\pm$  5  $\mu$ m) Marienfield-superior)

Falcon 15mL Conical Centrifuge Tubes (Thermo Fisher Scientific)

Falcon 50mL Conical Centrifuge Tubes (Thermo Fisher Scientific)

Filter paper (Whatman)

Glass beads

Glass Microscope slides (76x26 mm; cut edges, frosted end; by Menzel-Gläser, Thermo Scientific)

Nitrocellulose membrane (pure, 0.45micron, Protran™, PerkinElmer)

PCR reaction tubes 0.2ml (Bio-Rad)

Protein gels NuPAGE™ 4-12% Bis-Tris, 1.0 mm (Invitrogen™)

Reaction tubes 1.5ml (Eppendorf)

Reaction tubes 2ml (Eppendorf)

Reaction tubes 1.5ml DNA-lo binding (Eppendorf)

Reaction tubes 1.5ml protein-lo binding (Eppendorf)

Serological pipettes 5ml, 10ml, 25ml (Falcon)

TBE-Urea gels 6%, 10% (Novex™, Invitrogen™)

Pipette tips

Pipette filter-tips (Thermo Fisher Scientific)

### 2.1.3 Reagents and chemicals

100 v/v% ethanol

1,4-Dithiothreitol (DTT) (Sigma Aldrich)

2,2'-thiodiethanol (TDE) ( $\geq$ 99%, Sigma Aldrich, 166782-100G, #STBH31999)

Avidin-agarose (Thermo Fisher Scientific, #2029)

Agarose (Sigma Aldrich)

Antibiotics: Ampicillin (), Kanamycin (Sigma Aldrich)

Anhydrous DMSO ( $\geq$ 99.9%, Sigma Aldrich, #276855)

Biotin-16-UTP (Biotin-16-(5-aminoallyl)-UTP, Jena Bioscience, NU-821-BIO16)

cOmplete™, EDTA-free Protease Inhibitor Cocktail (Merck)

DAPI (5 mg/ml Molecular Probes D1306)

Diethyl pyrocarbonate (DEPC) (Sigma Aldrich)

Dye-NHS esters (ATTO)

## 2 Materials and Methods

Dynabeads™, MyOne™, Streptavidin C1 (Invitrogen™, 65001)  
GeneRuler 1kb DNA ladder (Thermo Fisher Scientific)  
HDGreenPlus DNA stain (INTAS)  
Heparin Sodium Salt (Sigma Aldrich, H3393)  
Immersion oil type F (Leica)  
Linear acrylamide (Thermo Fisher AM9520)  
MEGAscript™ T7 Transcription Kit (Invitrogen™, AM1354)  
Milk powder  
Mounting glue (e.g. CoverGrip™ Coverslip sealant)  
NH<sub>2</sub>-ddUTP (e.g. Lumiprobe A5040)  
Nonidet P-40 Substitute (Igepal CA-630, USB Corporation)  
Ethylene carbonate (Sigma Aldrich, #STBH5673)  
Phusion Flash High-Fidelity PCR Master Mix (Thermo Fisher Scientific, F548S)  
Pierce™ BCA Protein Assay Kit (Thermo Fisher Scientific, #23225)  
Protein ladder Precision Plus Protein™ Dual Color Standards (Bio-Rad)  
Restriction enzymes: FspAI, KpnI, NdeI, NotI (FastDigest, Thermo Fisher Scientific)  
RiboLock (Thermo Fisher Scientific)  
RiboRuler High range RNA ladder (Thermo Fisher Scientific)  
RiboRuler Low range RNA ladder (Thermo Fisher Scientific)  
Salmon sperm DNA (Sigma Aldrich, #SLBX8964)  
Sodium cacodylate trihydrate (Sigma Aldrich)  
SuperScript™ III First-Strand Synthesis SuperMix (Invitrogen™, #18080400)  
SYBR™ Green master mix for quantitative real-time PCR (Applied Biosystems™)  
T4 DNA ligase (Thermo Fisher Scientific, #EL0014)  
Terminal deoxynucleotidyl transferase (TdT, Thermo Fisher Scientific EP0161)  
Triton X-100 (Sigma Aldrich, #STBG0272V)  
QIAquick Gel Extraction Kit (Qiagen)  
QIAquick PCR Purification Kit (Qiagen)  
QIAprep Spin Miniprep Kit (Qiagen)  
QIAfilterPlasmid Midi Kit (Qiagen)  
Zero Blunt™ TOPO™ PCR Cloning Kit (Invitrogen™, 450245)

### 2.1.4 Buffers and solutions

#### Stock buffers and Solutions:

1M KCl

1M MgCl<sub>2</sub>

1M NaCl

1M EDTA

1M HEPES-NaOH pH 7.5

1M Sodium cacodylate pH 7.5

100mM Sucrose

1M NaHCO<sub>3</sub>, pH 8.4

1M Tris-HCl pH 8

1M Tris-HCl pH 7.5-7.7

10 w/v % sodium dodecyl sulphate (SDS, Sigma Aldrich, 822050)

1x Phosphate saline buffer (PBS)

2xRNA loading buffer (95% formamide, 0.025% SDS, 0.025% bromophenol blue, 0.025% xylene cyanol FF, 0.025% ethidium bromide, 0.5mM EDTA) (Thermo Fisher Scientific)

4xLDS PAGE loading buffer (Invitrogen™)

6xDNA loading buffer (10 mM Tris-HCl (pH 7.6), 0.03% bromophenol blue, 0.03% xylene cyanol FF, 0.15% orange G, 60% glycerol and 60mM EDTA) (Thermo Fisher Scientific)

10x β-casein blocking buffer solution (for northern and Southern blotting, Sigma Aldrich, B6429)

10x Transfer buffer V=1000 ml (30.3 g Tris Base, 144 g Glycine, 1% SDS)

20x MES Running buffer (50mM MES, 50mM Tris Base, 0.1% SDS, 1mM EDTA, pH 7.3) (Invitrogen™)

20x SSC (3 M NaCl, 300 mM Sodium Citrate, pH 7.0)

5x TBE (Novex™ TBE Running Buffer, Thermo Fisher Scientific)

16 w/v % paraformaldehyde (PFA) EM grade (Electron Microscopy Sciences, 15710), (Note 1)

TBST (10mM Tris-HCl pH=8, 150mM NaCl, 0.05% Tween)

TE (10mM Tris-HCl, pH 8.0, 1mM EDTA)

P2 (200mM NaOH, 1 w/v % SDS)

P3 (3M KAc, pH 5.5)

#### Working buffers and solutions:

1x LDS + 10mM DTT

1x Transfer buffer + 20% methanol

1x TBE

## 2 Materials and Methods

Fixative: 2 w/v% PFA and 0.05% Triton-X in PBS.

*In vitro* dimerization assay M1 buffer: 50mM sodium cacodylate pH 7.5, 50mM KCl, 0.1mM MgCl<sub>2</sub>

*In vitro* dimerization assay D1 buffer: 50mM sodium cacodylate pH 7.5, 300mM KCl, 5mM MgCl<sub>2</sub>

*In vitro* pull-down Lysis buffer: 25 mM Hepes-NaOH pH 7.5, 1 mM MgCl<sub>2</sub>, 150 mM KCl, 25 mM sucrose, 0.5% NP-40

*In vitro* pull-down Lysis buffer-complete (LBC): Lysis buffer + Triton-x+ 2xprotease inhibitor +10mM DTT+ Ribolock 75U)

*In vitro* pull-down Washing buffer: 25 mM Hepes-NaOH pH 7.5, 1mM MgCl<sub>2</sub>, 150mM KCl, 25mM sucrose, 0.5% NP-40

IF Blocking buffer: 1x  $\beta$ -casein blocking buffer in PBT.

Mounting (embedding) medium: 80% TDE in PBS

PBT 0.1% Triton-X in PBS

smFISH Hybridization buffer (HyB): Make 100 ml working stock of HyB (2x SSC, 1mM EDTA, 1 v/v % Triton X-100, 15 v/v % ethylene carbonate, 50  $\mu$ g/ml heparin, 100  $\mu$ g/ml salmon sperm DNA)

smFISH Washing buffer: 0.1 % Triton X-100 in PBS (PBT).

Western Blot Blocking buffer: 5% milk in TBST

Western Blot Washing buffer: 5% milk in TBST or TBST

### 2.1.5 Antibodies

Name:	Type:	Raised in:	Dilution in use:	Used for:	Provider:
$\alpha$ Me31B	primary	mouse	1:200	IF	Gift from Nakamura, 2011
$\alpha$ Oskar	primary	rabbit	1:2000 (1:300 preabsorbed)	IF	Ephrussi lab
$\alpha$ Bruno	primary	rabbit	1:1000	WB	Ephrussi lab
$\alpha$ H3	primary	rabbit	1:2500	WB	Abcam
$\alpha$ Rabbit-HRP conjugated	secondary	goat	1:10000	WB	GE Healthcare
$\alpha$ GFP-A488 conjugated	Monoclonal IgG	mouse	1:200	IF	Sigma Aldrich
$\alpha$ Rabbit IgG (H+L) Highly Cross-Adsorbed, Alexa Fluor 647	secondary	goat	1:750	IF	Invitrogen™
$\alpha$ Mouse IgG (H+L) Highly Cross-Adsorbed, Alexa Fluor 568	secondary	goat	1:750	IF	Invitrogen™
$\alpha$ Mouse IgG (H+L) Highly Cross-Adsorbed, Alexa Fluor 633	secondary	goat	1:750	IF	Invitrogen™

## 2.1.6 Plasmids

Name:	Length:	Source:
pUASP-attB-ΔK10-egfp-oskar-WT	~10240bp	Helena Jambor
pUASP-attB-ΔK10-egfp-oskar-UU	~10240bp	Helena Jambor
pUASP-attB-ΔK10-egfp-oskar-AA	~10240bp	Helena Jambor
pUASp-nc_osk-166	8916bp	Roland Gstir
pBS (K+)-oskar3'UTRWT	n.a.	n.a.
pUASP-ΔK10-attB-oskar3'UTRWT	10246bp	This study.
pUASP-ΔK10-attB-oskar3'UTRUU	10246bp	This study.
pUASP-ΔK10-attB-oskar3'UTRAA	10246bp	This study.
pUASP-ΔK10-attB	~9200bp	n.a.

## 2.1.7 Primers

Name:	Sequence:	Used for:
[BR1] T7_OES_FWD	TAATACGACTCACTATAGGGTGGAAAATTCGCTTGCACAA	<i>in vitro</i> pull-down assay
[BR2] OES_REV_359	CATTTTTTTTTTGGATTTTACATTGCAG	<i>in vitro</i> pull-down assay
[BR3] OES_REV_67	TGAATTTGCTTGAGCACAT	<i>in vitro</i> pull-down assay
T7FWD-2213 RII	TAATACGACTCACTATAGGGCTTCTCTTCAAACCTTTCCG	<i>in vitro</i> dimerization assay
REV-2600 RII	GCAAACGGAAACAGAAAGAC	<i>in vitro</i> dimerization assay
T7FWD-1842 FL	TAATACGACTCACTATAGGGGTTGGGTTCTTAATCAAGATAC	<i>in vitro</i> dimerization assay
REV-2802 FL	AACGTGATCACCATCAATAC	<i>in vitro</i> dimerization assay
Actin5c FWD	TGTGTGACGAAGAAGTTGCTG	qPCR
Actin5c REV	AGGATACCACGCTTGCTCTG	qPCR
[BR12] osk3'UTR FWD	TATCACACAACCTGCCACTTGC	qPCR
[BR13] osk3'UTR REV	CGTCTTTCTGTTTCCGTTTGCA	qPCR
3'UTR FWD #19	TAAGTTGGGTTCTTAATCAAGATAC	Sequencing

## 2.1.8 Oligonucleotides for smFISH probe synthesis

Name:	<i>oskar</i> 24x probe set	Name:	<i>oskar</i> 42x probe set
oskCD#1	GATCCATCAGCGTAAATCG	oskCD#1	GATCCATCAGCGTAAATCG
oskCD#2	CCAACCTAATACTCCAGACTCG	oskCD#2	CCAACCTAATACTCCAGACTCG
oskCD#3	CCAGAACAGATAGGGTTC	oskCD#3	CCAGAACAGATAGGGTTC
oskCD#4	TCGTTGATTAGACAGGAGTG	oskCD#4	TCGTTGATTAGACAGGAGTG

2 Materials and Methods

oskCD#5	ACAATAGTTGCCAGCGG	oskCD#5	ACAATAGTTGCCAGCGG
oskCD#6	TTTGTTAGAATCGGCACCAA	oskCD#6	TTTGTTAGAATCGGCACCAA
oskCD#7	GCATATTGTGCATCTCCTTGA	oskCD#7	GCATATTGTGCATCTCCTTGA
oskCD#8	CTCGATCTGAACCAAAGGC	oskCD#8	CTCGATCTGAACCAAAGGC
oskCD#9	ATAATGTCCACCGATCCGA	oskCD#9	ATAATGTCCACCGATCCGA
oskCD#10	GACGATGATCTGAGTACCC	oskCD#10	GACGATGATCTGAGTACCC
oskCD#11	AGTCCGGATACACAAAGTCC	oskCD#11	AGTCCGGATACACAAAGTCC
oskCD#12	CATTCGGGCGAGATATAGCA	oskCD#12	CATTCGGGCGAGATATAGCA
oskCD#13	CATCGCCCATAAGCGGAAAG	oskCD#13	CATCGCCCATAAGCGGAAAG
oskCD#14	AGATAGGCATCGTAATCCGAG	oskCD#14	AGATAGGCATCGTAATCCGAG
oskCD#15	TCGTCAGCAGAGAATCGTTG	oskCD#15	TCGTCAGCAGAGAATCGTTG
oskCD#16	GTCATTTCTGTGGCGTCTCT	oskCD#16	GTCATTTCTGTGGCGTCTCT
oskCD#17	GCTTTGGGTTCTGCAGCT	oskCD#17	GCTTTGGGTTCTGCAGCT
oskCD#18	GAGCCAAATTGATTGGTTCCTC	oskCD#18	GAGCCAAATTGATTGGTTCCTC
oskCD#19	GCTGTAGATGTTGATGGG	oskCD#19	GCTGTAGATGTTGATGGG
oskCD#20	GCATTTACGCTGGCTTGC	oskCD#20	GCATTTACGCTGGCTTGC
oskCD#21	AATTATCCTGGTAGCACCAG	oskCD#21	AATTATCCTGGTAGCACCAG
oskCD#22	GTTTGAAGGGATTCTTCCAG	oskCD#22	GTTTGAAGGGATTCTTCCAG
osk3'UTR#1	ATCGCGCAAATGCTTCAC	oskCD#23	AGGTGCTCGTGGTATGTTC
osk3'UTR#2	TTAAGGGCAAGTGGCAGG	oskCD#24	TAGTCGCTGGTGCCTCT
		oskCD#25	AGCACCATATCCAGGAGG
		oskCD#26	CGTTCTTCAGGCTCGCTT
		oskCD#27	AAGATCCGCTTACCGGAC
		oskCD#28	CTGCACTCAGCGGTCAACA
		oskCD#29	GGAATGGTCAGCAGGAAA
		oskCD#30	CGTCACGTTGTCTGTCAG
		oskCD#31	AAATGGATTGCCCGTCAG
		oskCD#32	CTTGATGCTCGATATCGTGA
		oskCD#33	TGGGCGTGGCTCAGCAATA
		oskCD#34	CGCGCACCTCACTATCTA
		oskCD#35	ATATTCCTCGCGACGGA
		oskCD#36	ATAGTTGCTCTCGATGATGG
		oskCD#37	TGTTCTCGCTGGTGTTC
		oskCD#38	GTTGTAGGTGATTTCTTGG
		oskCD#39	TCTGAGTGGACGAGAAGAG
		oskCD#40	GCTACGACTTGCAACTGC
		oskCD#41	GAGTTCATGGGCCACCAA
		oskCD#42	CTCCACAACCTCCGCAA

Name:	<i>bicoid</i> 24x porbe set	Name:	<i>gurken</i> 24x probe set
bcd_5UTR_1	TGGCAAAGGAGTGTTGAAAC	grk_A_1	GGAGCTGCTATATGGCCTG
bcd_CD_1	CTGAAGCTGCGGATGTTGG	grk_A_2	CTACACACTTGCATCTCCTTG
bcd_CD_2	TCGAAGGGATTTCCGAATTG	grk_A_3	TCGGCTCGAACACAATCTG
bcd_CD_3	CCATATCTTACCTGGGCTG	grk_A_4	AGCGTATGCTCTCGAGAAG
bcd_CD_4	GTCCTTGTGCTGATCCGAT	grk_A_5	CTCCAGGCGATTGAGCAAC
bcd_CD_5	CTCCACCCAAGCTAAGAGTC	grk_A_6	ATCAGTGATTGGTGTGCTGC

bcd_CD_6	GCGTTGAATGACTCGCTGTAG	grk_A_7	TTTCGGGTGTTGCTACTGTC
bcd_CD_7	TGTGGCCTCCATTGTAGTTG	grk_A_8	TGAATCTCTGTCTCCTTGTCTG
bcd_CD_8	GGTGATTATGGACCTGCTGC	grk_A_9	TGTTGTTCCACCATCGGATGC
bcd_CD_9	GCTGGAAGTCAAAGTGATGG	grk_A_10	GGCAGGAATGGAAGACTGTG
bcd_CD_10	GTAGTACGAGCTGTTGAAGTTG	grk_A_11	AGTCACCATTCCAGCTCTTG
bcd_CD_11	GTGTTAATGGCTCGTAGACC	grk_A_12	CGGAAAGGAGAAGACGATG
bcd_CD_12	CACACAGACTCGGACTTTTCG	grk_A_13	GCGCAACGTAAAGAAATATGG
bcd_CD_13	CTTCTTGCTCGTTCCGTCG	grk_A_14	TCGAGTCGAGTCCCAATCC
bcd_CD_15	CTAAGGCTCTTATCCGGTGC	grk_B_1	GAACGCACACACACGAAAC
bcd_CD_16	CTCCACGATTTCCGGTTCC	grk_B_2	GACCGATTGTCCACCACTAG
bcd_CD_17	GCTTGCATTATCGTATCCATCG	grk_B_3	TCTCCTGGATCTGCTGCTG
bcd_CD_18	CATCCAGGCTAATTGAAGCAG	grk_B_4	CAGGTGTGCGTACTGGATC
bcd_3'UTR_1	ATGAAACTCTTAACACGCCTC	grk_B_5	ACCGCTCTCCATCGTAGTC
bcd_3'UTR_2	GTACAATCAGGAACAACAGTGG	grk_B_6	AGAACGTAGAGCGACGACAG
bcd_3'UTR_3	ACACGGATCTTAGGACTAGACC	grk_B_7	CTGCTTCCGGCGATAATCC
bcd_3'UTR_4	GAATAGCGTATTGCAGGGAAAG	grk_B_8	TGCTTATGCAGGTGTAGTTG
bcd_3'UTR_5	GCCCAAATGGCCTCAAATG	grk_B_9	TGCCATCCAACAAAGAGGAG
bcd_3'UTR_6	CCGAAATGTGGGACGATAAC	grk_B_10	AAGCGAAACAAACGAAACTAAG

Name:	<i>egfp</i> 23x probe set	Name:	<i>patronin</i> 70x probe set*
EGFP#1	TCCTCGCCCTTGCTCACCA	oligo1	AGCCTTTTTTGCCCCGAC
EGFP#2	GTTTACGTCGCCGTCCAGC	oligo2	AGATGCTTGAAGCCTCGC
EGFP#4	CAGCTTGCCGTAGGTGGCA	oligo3	TGGCATCGTCCACGTGAA
EGFP#5	GCCGGTGGTGCAGATGAAC	oligo4	TGCGATTGCAGCTTCACG
EGFP#6	AAGCACTGCACGCCGTAGG	oligo5	CCGGGAGATTTGACACTG
EGFP#7	CTGCTTCATGTGGTCGGGG	oligo6	CATAATCCTCCGAGCTGC
EGFP#8	TGGACGTAGCCTTCGGGCA	oligo7	CAAAGTCGAGATGTGCG
EGFP#9	GCCGTCGTCCTTGAAGAAGA	oligo8	TACCCATGGGCATTCCCA
EGFP#10	GTCGCCCTCGAACTTCACC	oligo9	CGCAAGTTGGTCAACGAC
EGFP#11	TCGATGCCCTTCAGCTCGA	oligo10	GCCTGTACCTGAAACAGG
EGFP#12	CAGGATGTTGCCGTCTCC	oligo11	GCATAAAGCTGCCAGGAC
EGFP#13	AGACGTTGTGGCTGTTGTAG	oligo12	TTGTTCATAAGCGGCGGC
EGFP#14	GTTCTTCTGCTTGTGCGCCA	oligo13	GCAGGTAGAAGTGGTTGG
EGFP#15	GGCGGATCTTGAAGTTCACC	oligo14	AATCGTCGTACACCACGC
EGFP#16	GGGTGTTCTGCTGGTAGTGG	oligo15	TACTGTGGAGTTCGGCCA
EGFP#17	GGGTGCTCAGGTAGTGTTG	oligo16	GGCGAGTGGTTACTGTGA
EGFP#19	CGAACTCCAGCAGGACCATG	oligo17	CCCCGTTGTCGCTGTAAA
EGFP#20	TCGTCCATGCCGAGAGTGA	oligo18	CCATGCTCGTTGACGTAC
EGFP#21	TCTCGTTGGGGTCTTTCG	oligo19	CCAAATCCACGGGATCCA
EGFP#22	CGCTGCCGTCCTCGATGT	oligo20	ATCTTGCGCTTGTCTGCTG
EGFP#23	GGGTGGTACGAGGGTGG	oligo21	ATGCTGCTAGTCGAGGAC
EGFP#24	AAGTTCAGCGTGTCCGGC	oligo22	TCTCCGGATCATAGCCAC
EGFP#25	GTGGTGCCCATCCTGGTC	oligo23	GGAGCGGGAATCGTTGTA
		oligo24	CTGGATAACTGCCACAC
		oligo25	TCAATGGTCAGCTGGGAG
		oligo26	GTTTCATGGATCCGCGCA



2 Materials and Methods

	oligo27	ATCACGGTGTAGGGCAGA
	oligo28	TGAGCAGCGCCAAACAGA
	oligo29	TCGCACAGATCCTGGAAG
	oligo30	TTCTTCGTATGGCCGCCA
	oligo31	ATCACAGACATGTGGGCG
	oligo32	CCGTTTCGGTAATGGGCA
	oligo33	TACAGATTGGCCAGCGTC
	oligo34	AAGGGCTCCTTCAGTTG
	oligo35	ACGCGATTGTTGAACGCC
	oligo36	CCATTTGACGGAAGCACG
	oligo37	CGAGCCTGTCGTATTTCC
	oligo38	CATCGTCCAAGTGATGACG
	oligo39	CACCGGTTTGCTGTTGACA
	oligo40	GGGTATGCGATAGGTGAGA
	oligo41	CTGCTGAAGTTGCTGTTGG
	oligo42	CTCATCAACATCCTCCTCG
	oligo43	CTGCTGTAGTCTTTGTCGC
	oligo44	CTTTCCGTTTCGCGATCC
	oligo45	CTTTCTTGAGTCTGTGCTGC
	oligo46	CGCTCCATCTCATCAACAGA
	oligo47	CGAAGGAGATGTAGAAACCC
	oligo48	CATCATGTCCTCTTGCTGCA
	oligo49	GTTGGACAATTTGCGTTCCC
	oligo50	CCGGGTGTATTTGAAACAGA
	oligo51	GAAATTGCAGACCAGCAGGA
	oligo52	CTCGCTCGGCCTCTTCAA
	oligo53	CTCCTCCTTTTTCCGCGC
	oligo54	TCCTCCTCCTTTTCGCGC
	oligo55	TCTCGTTCTGGGAAGCC
	oligo56	TCCTGTTGCTGGCGACGT
	oligo57	TGCTCTGTTGGAGTCGCG
	oligo58	GCGACATTGGTTGCTGCG
	oligo59	GCTGCGGTGACTGATTGC
	oligo60	AGTTGGATGGGCGGCTCA
	oligo61	GGCCATGGATACTGTGCC
	oligo62	CGACTTCCTGGTGGAGAC
	oligo63	TTGGGTGTTTTGGGCTGC
	oligo64	TTGGATGGAGGGACGGGA
	oligo65	CCGCTGGTGATGTTCCAGC
	oligo66	TGGAGATCATCTCCCCGC
	oligo67	TGGTGCTGCTGCTGCTGT
	oligo68	GCACGCCATTGGATCCAC
	oligo69	GGCCTGTTCCATCCAGGTC
	oligo70	GCTTTTGGTGTGCTGCTGCG

\**patronin* probe set was design by Lucia Cassella.

## 2.1.9 Fly lines

Name:	Genotype:	Source:
BR1	w <sup>-</sup> ; oskar3'UTRWT /CyO; Sb/TM3Ser	This study.
BR2	w <sup>-</sup> ; oskar3'UTRUU /CyO; Sb/TM3Ser	This study.
BR3	w <sup>-</sup> ; oskar3'UTRAA /CyO; Sb/TM3Ser	This study.
D-309	w; Df(3R) pXT103 <sub>rust e ca</sub> /TM3Ser, Sb	DGRC ID 2492
DB	w <sup>-</sup> ; if/CyO; TM3Ser/Sb	
GAL-166	w <sup>-</sup> ; oskar-GAL4/oskar-GAL4; <i>oskar</i> <sup>A87</sup> /TM3Sb	Imre Gaspar
GFP	P{Ubi-GFP.S65T}PAD1	Bloomington; 4888
HJ1	w <sup>-</sup> ; egfp-oskar3'UTRWT/CyO	Helena Jambor
HJ4	w <sup>-</sup> ; egfp-oskar3'UTRAA/CyO	Helena Jambor
HJ5	w <sup>-</sup> ; egfp-oskar3'UTRUU/CyO	Helena Jambor
HJ33.1	w <sup>-</sup> ; oskarUU/CyO	Helena Jambor
HJ33.2	w <sup>-</sup> ; oskarUU (#2)/CyO	Helena Jambor
HJ34.3	w <sup>-</sup> ; oskarAA/CyO	Helena Jambor
osk-spl18	w,oskarWT/oskarWT	Olivier Hachet
RG	w <sup>-</sup> ; nc_osk-166/CyO ; Sb/TM3Ser	Roland Gstir
SJF94	EGFP:Me31B/FM7; Sco/ CyO	Shin-Jung-Fan
	w <sup>-</sup> ; lf/CyO; <i>oskar</i> <sup>attp,3P3-GFP</sup> /TM3Ser	Imre Gaspar
STABLE 1	w <sup>-</sup> ; oskarUU/CyO; <i>oskar</i> <sup>attp,3P3-GFP</sup> /TM3Ser	This study.
STABLE 2	w <sup>-</sup> ; oskarUU/CyO; Df(3R)p-XT103/TM3Ser	This study.
STABLE 3	w <sup>-</sup> ; oskarAA/CyO; <i>oskar</i> <sup>attp,3P3-GFP</sup> /TM3Ser	This study.
STABLE 4	w <sup>-</sup> ; oskarUU (#2)/CyO; <i>oskar</i> <sup>attp,3P3-GFP</sup> /TM3Ser	This study.
STABLE 5	w,oskarWT/oskarWT;; <i>oskar</i> <sup>attp,3P3-GFP</sup> /TM3Ser	This study.
STABLE 6	w,oskarWT/oskarWT;; Df(3R)p-XT103/TM3Ser	This study.
STABLE 7	w <sup>-</sup> ; egfp-oskar3'UTRUU /CyO; Df(3R)p-XT103/TM3Ser	This study.
STABLE 8	w <sup>-</sup> ; egfp-oskar3'UTRUU /CyO; <i>oskar</i> <sup>attp,3P3-GFP</sup> /TM3Ser	This study.
STABLE 9	w <sup>-</sup> ; egfp-oskar3'UTRWT,oskar-GAL4 /CyO; <i>oskar</i> <sup>A87</sup> /TM3Ser	This study.
STABLE 10	w <sup>-</sup> ; egfp-oskar3'UTRAA,oskar-GAL4 /CyO; <i>oskar</i> <sup>A87</sup> /TM3Ser	This study.
STABLE 11	w,EGFP:Me31B/EGFP:Me31B; oskar-GAL4 /CyO <i>oskar</i> <sup>A87</sup> /TM3Ser	This study.
STABLE 12	w <sup>-</sup> ; oskar-GAL4 /CyO; GFP:YPS, <i>oskar</i> <sup>A87</sup> /TM3Ser	This study.
STABLE 13	w <sup>-</sup> ; oskar3'UTRWT /CyO; Df(3R)p-XT103/TM3Ser	This study.
STABLE 14	w <sup>-</sup> ; oskar3'UTRUU /CyO; Df(3R)p-XT103/TM3Ser	This study.
STABLE 15	w <sup>-</sup> ; oskar3'UTRAA /CyO; Df(3R)p-XT103/TM3Ser	This study.
VK18	vas-phi-ZH2A, PBac{y[+]-attP-9A}VK00018	Bellen lab
W[1118]	w <sup>1118</sup>	Bloomington; 3605
	w;; GFP:YPS/TM3Ser	
STABLE 16	w <sup>-</sup> ; oskar-GAL4/oskar-GAL4; GFP:YPS, <i>oskar</i> <sup>A87</sup> /TM3Sb	This study.

## 2.1.10 Software

AdobePhotoshop CC2015.5	AdobeIllustrator CC2015.3
Huygens Essentials	ImageJ/Fiji
R Studio	LAS X
SnapGene Viewer	

## 2.1.11 Online sources

IPknot : <http://rtips.dna.bio.keio.ac.jp/ipknot/>, FlyBase : <http://flybase.org/>

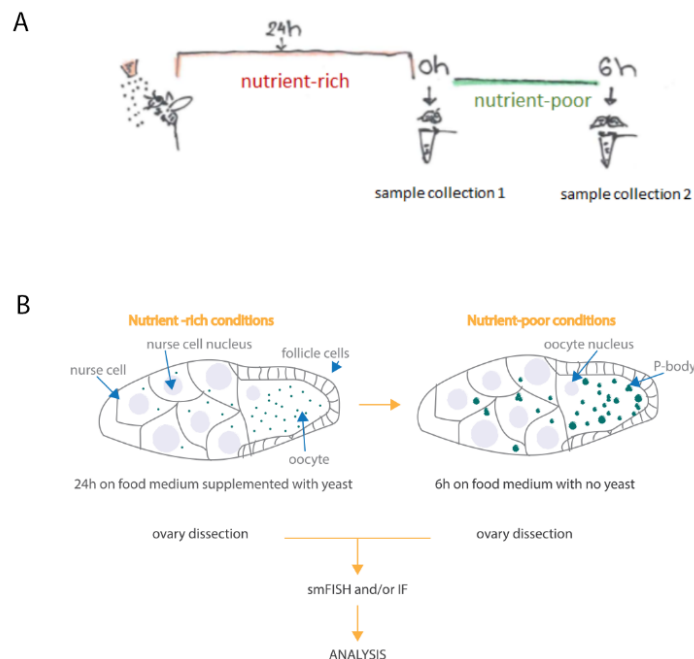
## 2.2 Methods

### 2.2.1 Fly husbandry

All *Drosophila melanogaster* lines were maintained at 18°C or 25°C. Flies were maintained in vials or bottles on standard food (corn-based medium). Prior to the specific experimental procedure, 2-3 day-old flies were kept at 25°C on food supplemented with additional yeast in the form of dry granules or yeast paste.

### 2.2.2 Fly nutrient-deprivation: conditioning flies for promoting P-body formation in the *Drosophila* germline

After eclosing, flies were kept on standard food at 25°C for 24 to 48h. Afterwards, ~2-3 day-old flies were kept on standard food supplemented with additional nutrients (dry yeast granules) for 24h at 25°C (nutrient-rich conditions). Females were collected at 0h (nutrient-rich control) for subsequent experimental procedures. Next, in order to promote P-body formation in the germline, the rest of female flies with male flies were transferred to fresh standard food without dry yeast (nutrient-poor conditions) and kept under this condition for 3h, 6h (Figure 2.1 A and B) or over-night (ON) at 25°C. After each time point, female flies were collected and ovary dissection was performed. The ovaries were then subjected to the next subsequent procedures (Figure 2.1 B). This set-up was applied to each fly line tested.



**2.1 Starvation set up:** **A** Scheme representing conditioning flies under nutrient-rich conditions and nutrient-poor conditions (example for 6h starvation) **B** Scheme of *Drosophila* egg-chambers at oogenic stage 9 without P-bodies (nutrient-rich conditions) (left) and upon P-body formation (nutrient-poor conditions) (right). Experimental set up is presented below.

### 2.2.3 Generation of transgenic fly lines

Transgenic lines referred to as CDS-free *oskar3'UTRWT*, *oskar3'UTRUU*, *oskar3'UTRAA*) were generated by site-specific integration using  $\Phi$ C31 integrase. Usage of  $\Phi$ C31 integrase for genetic transformation of *Drosophila*, requires that the transgene-bearing plasmid contain an attB sequence. When the plasmid is microinjected into *Drosophila* embryos expressing  $\Phi$ C31 integrase, the integrase catalyses recombination between the attB site in the transgene-bearing plasmid and the attP landing site previously integrated in the targeted *Drosophila* genome. This results in insertion of the transgene into the *Drosophila* genome. *oskar3'UTRWT* sequence (amplified from pBS (K+)-*oskar3'UTRWT* plasmid) was cloned in the final expression vector pUASP-attB- $\Delta$ K10 using KpnI and NotI restriction enzymes (Figure 2.1 A). UU and AA mutant plasmids were made by cutting out the region containing mutant SL2b from pUASP-attB- $\Delta$ K10-egfp-*oskar*-UU (made by Helena Jambor) and pUASP-attB-  $\Delta$ K10-egfp-*oskar*-AA (made by Helena Jambor), respectively, using FspAI and NdeI restriction enzymes. Fly injections were performed by Alessandra Reversi. Each plasmid was integrated on the right arm of the second chromosome (cytosite: 532B) (Figure 2.1 B) in the VK18 fly line.

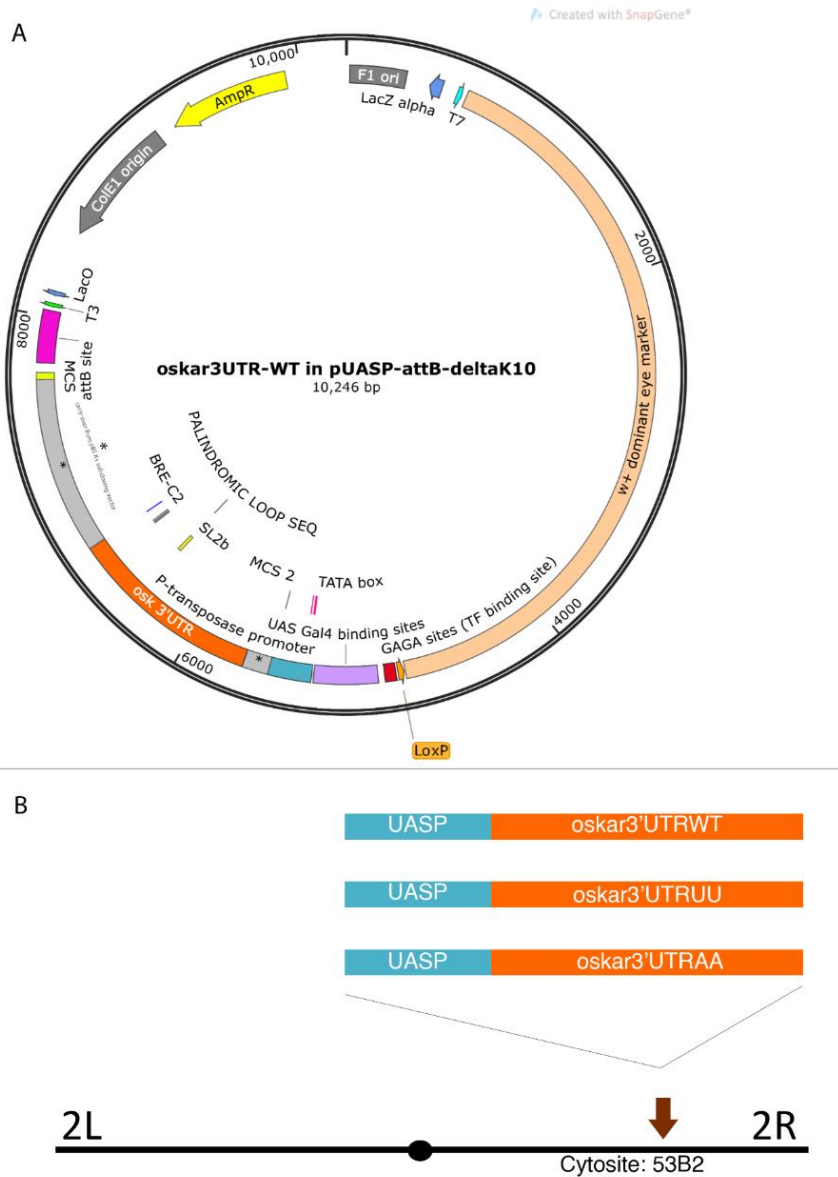


**Figure 2.2 Making CDS-free transgenic fly lines:** **A** Map of the plasmid pUASP-attB- $\Delta$ K10-oskar3'UTR-WT. The map was made using plasmid editors ApE and SnapGene. **B** Simplified schematic representation of CDS-free transgenes: *oskar3'UTRWT*, *oskar3'UTRUU*, *oskar3'UTRAA* and their integration site (cytosite: 53B2) on the right arm of *Drosophila* chromosome II.

### 2.2.4 Genetic crosses

In order to allow expression of each transgene tested in the *oskar* mRNA null background, a number of genetic crosses was performed. Expression of each transgene was driven using the UASP-GAL4 system (Busson and Pret, 2007). Each transgene was under control of UAS promoter(P). Crosses of two generated stable parental lines are shown here. All fly lines that were used are listed in 2.1 Materials.

#### *oskar*WT\*:

*w*<sup>-</sup>, EGFP:Me31B/EGFP:Me31B; *oskar*-GAL4/CyO; *oskar*<sup>A87</sup>/TM3Ser x *oskar*WT/*y*; *w*<sup>-/+</sup> ; *oskar*<sup>attP,3P3-GFP</sup>/TM3Ser

↓

*w*<sup>-</sup>, EGFP:Me31B/*oskar*WT; *oskar*-GAL4/+; *oskar*<sup>A87</sup> / *oskar*<sup>attP,3P3-GFP</sup>

*w*<sup>-</sup>, *oskar*-GAL4/CyO; GFP:YPS, *oskar*<sup>A87</sup>/TM3Ser x *oskar*WT/*y*; *w*<sup>-/+</sup> ; *oskar*<sup>attP,3P3-GFP</sup>/TM3Ser

↓

*w*<sup>-</sup>, +/*oskar*WT; *oskar*-GAL4/+; GFP:YPS, *oskar*<sup>A87</sup> / *oskar*<sup>attP,3P3-GFP</sup>

#### *oskar*UU\*:

*w*<sup>-</sup>, EGFP:Me31B /EGFP:Me31B; *oskar*-GAL4/CyO; *oskar*<sup>A87</sup>/TM3Ser x *w*<sup>-/y</sup>; *oskar*UU/*oskar*UU ; *oskar*<sup>attP,3P3-GFP</sup>/TM3Ser

↓

*w*<sup>-</sup>, EGFP:Me31B /+; *oskar*-GAL4/*oskar*UU; *oskar*<sup>A87</sup> / *oskar*<sup>attP,3P3-GFP</sup>

*w*<sup>-</sup>; *oskar*-GAL4/CyO; GFP:YPS, *oskar*<sup>A87</sup>/TM3Ser x *w*<sup>-/y</sup>; *oskar*UU/*oskar*UU ; *oskar*<sup>attP,3P3-GFP</sup>/TM3Ser

↓

*w*<sup>-</sup>; *oskar*-GAL4/*oskar*UU; GFP:YPS, *oskar*<sup>A87</sup> / *oskar*<sup>attP,3P3-GFP</sup>

#### *oskar*AA\*:

*w*<sup>-</sup>, EGFP:Me31B /EGFP:Me31B; *oskar*-GAL4/CyO; *oskar*<sup>A87</sup>/TM3Ser x *w*<sup>-/y</sup>; *oskar*AA/*oskar*AA ; *oskar*<sup>attP,3P3-GFP</sup>/TM3Ser

↓

*w*<sup>-</sup>, EGFP:Me31B /+; *oskar*-GAL4/*oskar*AA; *oskar*<sup>A87</sup> / *oskar*<sup>attP,3P3-GFP</sup>

#### *egfp-oskar3'UTRWT*:

*egfp-oskar3'UTRWT*, *oskar*-GAL4/CyO; *oskar*<sup>A87</sup>/TM3Ser x *w*<sup>-/y</sup>; + /+; *Df(3R)p-XT103*/TM3Ser,Sb\*

↓

*w*<sup>-</sup>; *egfp-oskar3'UTRWT*, *oskar*-GAL4/+; *oskar*<sup>A87</sup> / *Df(3R)p-XT103*

#### *egfp-oskar3'UTRUU*:

*oskar*-GAL4/*oskar*-GAL4; *oskar*<sup>A87</sup>/TM3Sb x *w*<sup>-/y</sup>; *egfp-oskar3'UTRUU* / *egfp-oskar3'UTRUU*; *Df(3R)p-XT103*/TM3Ser•

↓

*w*<sup>-</sup>; *egfp-oskar3'UTRUU* /*oskar*-GAL4; *oskar*<sup>A87</sup> / *Df(3R)p-XT103*

#### *egfp-oskar3'UTRAA*:

*egfp-oskar3'UTRAA*, *oskar*-GAL4/CyO; *oskar*<sup>A87</sup>/TM3Ser x *w*<sup>-/y</sup>; + /+; *Df(3R)p-XT103*/TM3Ser,Sb\*

↓

*w*<sup>-</sup>; *egfp-oskar3'UTRAA*, *oskar*-GAL4/+; *oskar*<sup>A87</sup> / *Df(3R)p-XT103*

*oskar*3'UTRWT:

*oskar*-GAL4/*oskar*-GAL4; *oskar*<sup>A87</sup>/TM3Sb x *w*-/*y*; *oskar*3'UTRWT/*oskar*3'UTRWT; *Df*(3R)p-XT103/TM3Ser

↓

*w*-; *oskar*3'UTRWT /*oskar*-GAL4; *oskar*<sup>A87</sup> / *Df*(3R)p-XT103

*oskar*3'UTRUU:

*oskar*-GAL4/*oskar*-GAL4; *oskar*<sup>A87</sup>/TM3Sb x *w*-/*y*; *oskar*3'UTRUU/*oskar*3'UTRUU; *Df*(3R)p-XT103/TM3Ser

↓

*w*-; *oskar*3'UTRUU /*oskar*-GAL4; *oskar*<sup>A87</sup> / *Df*(3R)p-XT103

*oskar*3'UTRAA:

*oskar*-GAL4/*oskar*-GAL4; *oskar*<sup>A87</sup>/TM3Sb x *w*-/*y*; *oskar*3'UTRAA/*oskar*3'UTRAA; *Df*(3R)p-XT103/TM3Ser

↓

*w*-; *oskar*3'UTRAA/*oskar*-GAL4; *oskar*<sup>A87</sup> / *Df*(3R)p-XT103

*oskar*UU in *oskar* endogenous background:

*oskar*-GAL4/*oskar*-GAL4/; ; x *w*-/*y*; *oskar*UU/*oskar*UU ; *oskar*<sup>attP,3P3-GFP</sup>/TM3Ser

↓

*oskar*-GAL4/+; *oskar*UU/+; +/TM3Ser

♣ In flies where EGFP:Me31B was not co-expressed, immunostaining for Me31B was performed to detect P-bodies. In the figures (Results section), the fluorescent signal produced by expression of the EGFP:Me31B transgene is annotated as GFP:Me31B.

\* A second *oskar* RNA null line (*if*/CyO; *oskar*<sup>attP,3P3-GFP</sup>/TM3Ser) was also used in some experiments.

• A second *oskar* RNA null line (*if*/CyO; *oskar*<sup>attP,3P3-GFP</sup>/TM3Ser) was also used in some experiments.

## 2.2.5 Ovary dissection and fixation

All experimental steps were performed at room temperature. In order to perform ovary dissection, female flies were selected and anesthetized using CO<sub>2</sub>. Prior to dissection, flies were submerged in 100% ethanol for couple of seconds to remove the cuticle wax and allow easier handling of the specimen. Dissection was performed in a glass dish in PBS using two pairs of tweezers. Next, ovaries were transferred to 1.5 ml tubes containing fixative (see 2.1 Materials) and incubated for 20 min on a nutator.

### 2.2.6 Single molecule fluorescent *in situ* hybridization (smFISH)

All subsequent steps were performed in 1.5 ml tubes on a nutator or a thermo-block. smFISH was performed after ovary fixation. After fixation, two rounds of 10 min washes in PBT were performed. Prior to the hybridization step, ovaries were pre-hybridized in 100 µl of hybridization buffer (HyB) at 42°C. Hybridization was performed in 200µl of HyB containing probe mix (2-3nM per probe) at 42°C for ~2h. After hybridization, the following 5-step washing protocol (a-d) at different temperatures was performed. Each step last 10 min (a-HyB at 42°C, b-1:1 HyB + PBT at 42°C, c-PBT at 42°C, d-pre-warmed PBT (42°C) at room temperature, e-PBT at room temperature). DAPI to a final concentration of 1 µg/ml to stain nuclei was added optionally. After washes, embedding or immunostaining was performed. Hybridization using the *egfp* probe set was performed at 37°C.

### 2.2.7 smFISH: probe design and labeling

To design smFISH probes, an R script ([smFISHprobe\\_finder.Rmd](#)) made by Imre Gaspar was used. Protocol for probe synthesis and labeling, was provided by Gaspar et al., 2017a. For materials and reagents necessary for probe synthesis and labeling see 2.1 Materials.

Overview of the probe labeling protocol:

I	To conjugate ddUTPs with dye-NHS esters, prepare reaction mix and incubate for at least 2 hours at RT protected from light.
II	Dissolve the unlabelled oligonucleotides to obtain ~250µM concentration per individual oligo and prepare reaction mix. Reaction recipe generator is provided in Gaspar et al., 2017.
III	Incubate the reaction at 37°C over-night.
IV	Purify labelled probes by ethanol precipitation.
V	Measure the absorbance of labelled probes and determine the concentration.
VI	Store labelled probes at -20°C.

For detailed protocol see Gaspar et al. (2017a).

### 2.2.8 Immunofluorescence technique

To detect endogenously GFP-tagged proteins, native fluorescence of GFP was visualized. To detect a specific protein in the *Drosophila* ovary, immunostaining was performed usually after smFISH. Primary anti-bodies (see 2.1 Materials) were incubated overnight in 1xβ-casein in PBT at +4°C, followed by three times 10 min washes in PBT at room temperature, and secondary antibody incubation in 1xβ-casein in PBT for 2h at room temperature. After secondary antibody incubation, three times 10 min washes in PBT at room temperature were performed.



### 2.2.9 Ovary mounting and preparation for microscopy

After smFISH and/or immunostaining, ovaries were embedded in 25-50 $\mu$ l of 80% TDE and stored at +4°C for a minimum 24h prior to mounting. Before imaging, ovaries were mounted onto a glass slide and individual ovarioles were gently separated with tungsten needles under a wide-field stereo microscope without spreading too far apart. Subsequently embedded ovaries were covered with a cover glass and sealed.

### 2.2.10 Microscopy

All image acquisitions were performed using a Leica SP8 TCS X confocal laser scanning microscope and LAS X software.

### 2.2.11 Image processing and analysis

All acquired images were processed using Huygens Essentials software and ImageJ. Huygens Essentials software was used for the deconvolution step. Additional processing and further analysis were performed using ImageJ.

mRNA intensities measurement workflow:

I	Select 3D image stack to be analyzed.
II	Subtract background.
III	Sum slices onto a 2D projection.
IV	Select the region of interest (oocyte or the nurse cells compartment).
V	Perform measurements (area, raw integrated density, coordinates, perimeter, mean).
VI	Calculate Volume of the selected compartment: $V = \text{area} * z\text{-step size}$
VII	Calculate mRNA Intensities: $I = \text{raw integrated density} / V$
VIII	Perform these steps for two different conditions: nutrient-rich and nutrient-poor.

Particle segmentation and colocalization analysis:

Colocalization and particle segmentation analyses were performed using plug-ins xsColoc and xsPT developed by Imre Gaspar (Gaspar and Ephrussi, 2017). xsColoc is an object-based co-localization analysis for 2D images. This plug-in allows particle detection in each channel separately based on a nearest neighbour algorithm. The maximum distance between the centroids of the particles is defined by the user (max. dist. in nm). xsPT plug-in works with image sequences (time or space) that contain one or multiple channels. When the image contains multiple channels, one channel is selected as a reference and particles are segmented in this channel exclusively. The outline of these particles is transferred to the other channels and integrated signal intensity values are extracted from all channels in the image.

Quantification of RNA gel images:

In order to measure intensities of the bands of the specific transcripts ran on the gel after *in vitro* dimerization assay ImageJ plugin: GelAnalyzer was used. As a signal read out uncalibrated optical density (OD) was plotted.

Overview of the workflow:

I	Select the image of interest (8-bit .tif).
II	Subtract background.
III	Analyze gel using GelAnalyzer.
IV	Plot measurements of each lane previously analyzed.
V	Select peaks and plot ODs.

**2.2.12 Cloning and bacterial transformation**

To clone and amplify DNA sequence of interest the pBS (K+) plasmid was used. Afterwards, the DNA sequence of interest was cloned in the final expression vector, pUSAP-attB-ΔK10 using restriction enzymes and ligation step. Zero Blunt™ TOPO™ PCR Cloning Kit was used if needed to clone fragments (sequences) of interest to be sent for Sanger sequencing in order to validate the sequence quality. For cloning purposes, the chemical competent XL-1 blue *Escherichia coli* bacterial strain was used. Bacterial transformation was performed using following protocol:

I	Thaw chemical competent XL-1 blue <i>E. coli</i> on ice.
II	Add plasmid of interest (50-100 ng) in 50-100 μl of chemical competent XL-1 blue <i>E. coli</i> and incubate 20 min on ice.
III	Heat-shock for 60-70 sec at 42°C.
IV	Incubate 2 min on ice.
V	Add 400 μl of LB medium and recover at 37°C for 30-45 min with shaking (800rpm).
VI	Spin down at 700 g and discard ~350 μl of LB medium.
VII	Homogenize bacterial pellet with the rest of LB medium and plate transformants on agar plates with antibiotic of interest.
VIII	Incubate over night at 37°C.

**2.2.13 DNA plasmid isolation and purification**

For general DNA plasmid isolation and purification, commercially available QIAprep Spin Miniprep Kit (250) was used. DNA plasmids for injections were prepared using QIAGEN Plasmid Midi Kit (25) followed by additional purification step with QIAquick PCR Purification Kit (50).

### 2.2.14 RNA extraction

Ovary RNA extraction was performed using TRIzol™ LS reagent (Invitrogen). Protocol was provided by manufacturer. For purification (extraction) of *in vitro* synthesized RNA transcripts following protocol was used\*:

I	Add 15 µl of Ammonium-o-acetate stop solution and 115 µl of Rnase, nuclease free water. Mix well and transfer in 1.5 ml tube.
II	Extract with equal amount of phenol/chloroform (acidic, Ambion) then with equal volume of chloroform.
III	Spin (13200rpm) at 4°C for 15 min. The aqueous phase of the supernatant contains RNA.
IV	Precipitate in 100% ethanol at -20°C for 45-60 min.
V	Spin (13200rpm) 45 min at 4°C.
VI	Wash twice with 70% ethanol for 8min.
VII	Discard supernatant and dry the pellet.
VII	Dissolve the pellet in nuclease, Rnase free water.
IX	Store RNA at -80°C.

\*Protocol was optimized and adapted from the manual provided with T7-polymerase MegaShortScript Kit (Invitrogen™).

### 2.2.15 cDNA synthesis

SuperScript III First-Strand Synthesis System SuperMix (Invitrogen™) was used for first-strand cDNA synthesis from purified total RNA extracted from *Drosophila* ovaries.

### 2.2.16 Polymerase chain reaction-PCR

For DNA fragment amplification, Phusion Flash High-Fidelity PCR Master Mix (Thermo Fisher Scientific™) was used.

Short overview of the PCR:

PCR PROGRAM	T(°C)	time
Initial denaturation	98	10s
Denaturation	98	1s
Annealing	Primer dependent	10s
Extension	72	(15s/kb)
Final extension	72	60s

30  
cycles

PCR REACTION	V (µl)
Template	up to 8
FWD primer 10µM	1
REV primer 10µM	1
Phusion Flash MM	10
H <sub>2</sub> O	up to 8*
Total:	20


\*dependent on template V added

### 2.2.17 qPCR

qPCR was performed using StepOnePlus Real-Time PCR Systems (Thermo Fisher Scientific™). To quantify how much DNA has been amplified, DNA intercalating SYBR green fluorescent dye was used. To calculate the relative fold gene expression of samples the delta-delta Ct method, also known as the  $2^{-\Delta\Delta C_t}$  was used.

Overview of qPCR program:

Step	T(°C)	time
Holding stage	95	10min
Cycling stage	95	15sec
	60	1min
Melting Curve	95	15sec
	60	1min
	95	15sec



### 2.2.18 DNA gel electrophoresis

DNA electrophoresis was performed on 1-2% agarose TBE gels in 1xTBE buffer and run at a voltage of 80-90V.

### 2.2.19 RNA *in vitro* transcription

Synthesis of RNAs of interest was performed using a T7-polymerase MegaShortScript Kit (Invitrogen™). A detailed reaction protocol is available in the manual provided with the kit. All primers for *in vitro* transcription are listed in 2.1 Materials. Templates for *in vitro* transcription are listed in the Appendix VI and VII.

### 2.2.20 RNA gel electrophoresis

For native RNA gel electrophoresis, a 1-2% agarose gel was prepared. For RNA quality control after *in vitro* transcription, denaturing polyacrylamide gel electrophoresis (PAGE) was applied. Dependent on the RNA transcript size, commercially available 6% or 10% Urea-TBE gels (Novex™ TBE-Urea Gels, Invitrogen™) were used. Denaturing RNA PAGE was run at +4°C in 1xTBE buffer. For a detailed protocol of RNA PAGE see the commercially available manual provided by ThermoFisher, Scientific (Novex™ TBE-Urea Gels manual, Invitrogen™).

### 2.2.21 *in vitro* dimerization assay

Prior to performing the *in vitro* dimerization assay, PCR fragments that would serve as template for *in vitro* transcription of RNAs of interest were amplified from the following plasmids: pUASP-egfp-

oskar3'UTR-WT, pUASP-egfp-oskar3'UTR-UU, pUASP-egfp-oskar3'UTR-AA. Region 2 (R2) of *oskar* mRNA 3'UTR (Jambor et al., 2014) was transcribed (template sequence provided in the Appendix VI). Protocol for the *in vitro* dimerization assay was adapted from Wagner *et al.*, (2001, 2004) and Laughrea *et al.*, (1999). 1.8 µg of *in vitro* transcribed RNA was diluted in 12µl of ultra-pure H<sub>2</sub>O and incubated at 85°C for 3 min. Next, samples were cooled down gradually to 60°C and appropriate buffers were added (5x of initial sample volume). D1(50mM sodium cacodylate pH 7.5, 300mM KCl, 5mM MgCl<sub>2</sub>) buffer was used to allow dimerization. M1(50mM sodium cacodylate pH 7.5, 50mM KCl, 0.1mM MgCl<sub>2</sub>) buffer was used to prevent dimerization of RNA monomers. After adding the appropriate buffer, samples were incubated 30 min at 25°C. Prior to loading, the samples were chilled on ice. The samples were then loaded on a 1% native agarose gel (in 1xTBE buffer). Prior to loading on the gel, samples were mixed with bromophenol-blue and glycerol as a loading dye. The gel was run at 40-50V for 2-3h. For staining the gel, the HDGreenPlus DNA stain was used.

### 2.2.22 RNA affinity *in vitro* pull-down assay

To obtain an optimal amount of ovary lysate for the pull-down assay, *Oregon-R* flies, raised in ~50 liter cages, were harvested. To ensure the lysates would mainly contain pre-vitellogenic and vitellogenic stages of egg-chambers, sieving steps were included in the harvesting protocol. Each cage usually produced 30-40 g of flies. After harvesting, 3-4 ml of ovaries were obtained per cage, which after lysis resulted in 230-270 mg of total protein. One cage harvested on a specific day was used as one biological replicate for the RNA affinity pull-down assay. Different biological replicates were harvested on different days.

Overview of the harvesting protocol:

I	Grind and collect the flies (+PBS) in 2l beaker.
II	Collection from the previous grinding step run once again through the grinder.
III	Sieving step1-630 µm.
IV	Sieving step2-400 µm.
V	Sieving step3-200 µm.
VI	Repeat sieving step3
VII	Sieving step4-80 µm-now egg-chambers of interest will stay on the mesh of this sieve and from there collect it in PBS in 50 ml falcon tube.
VIII	Spin at 600rpm ~1 min.
XIX	Wash in PBS.
X	Spin at 600rpm ~1 min.
XI	Transfer in 14ml falcon tube the material.
XII	Spin at 700rpm for 1 min.
XII	Discard supernatant.
XIV	Snap-freeze ovaries in liquid nitrogen.
XV	Store at -80°C until continuing with the experiment.

After harvesting, lysis and pull-down were performed. For the pull-down, the same amount of each RNA transcript of interest was used (100 pmol) and each transcript was coupled with the same amount of paramagnetic streptavidin beads (Dynabeads MyOne Streptavidin C1)\*. Per specific transcript pull-down, sample lysate contained 46-54mg of total protein amount.

Transcript:	Amount (pmols)	Amount ( $\mu\text{g}$ )	Volume of beads* ( $\mu\text{l}$ )
WT_359	100	11.54	25
UU_359	100	11.54	25
WT_67	100	2.156	25
UU_67	100	2.156	25

Each transcript was synthesized with random incorporation of biotin-16-UTP (Jena Bioscience): “short” transcripts, WT\_67 and UU\_67 (corresponding to the 67 nucleotide long OES sequence) and “long” transcripts, WT\_359 and UU\_359 (consisting of the 359 nucleotide long distal part of the *oskar* 3’UTR, including the OES, but lacking a polyA tail) (Figure 3.11 B). RNA affinity pull-down protocol was optimized and adapted from Dix et al., 2013; Götze et al., 2017.

#### PROTOCOL WORK FLOW FOR RNA AFFINITY PULL-DOWN:

- I. Couple beads with the RNA for 2h at +4°C in 1.5 ml DNA Lo-binding tubes. Prior to coupling quickly pre-wash beads with the Lysis buffer-complete (LBC) (50-75U of ribolock included).
- II. While step I is ongoing prepare lysate:
  - a. Thaw ovaries.
  - b. Homogenize ovaries in LBC with dounce-homogenizer (all on ice).
  - c. Incubate in LBC for 5 min.
  - d. Spin down for 5 min at 5000rcf to get rid of the debris.
  - e. Transfer lysate to a 15 ml falcon tube.
  - f. Take 0.1% for the total input and measure total protein concentration.
  - g. Pre-clear with avidin-agarose (1/50 of lysate volume) at +4°C for ~30 min (can be prolonged).
  - h. Spin down for 5 min at 5000rcf to get rid of the avidin-agarose.
  - i. Transfer lysate to a 15 ml falcon tube.
  - j. Split lysate in number of tubes corresponding to the number of transcripts that will be tested + no RNA control.
  - k. Take from each sample 0.1-0.2% as a loading input control.
- III. Once coupling RNA to the beads is finished, add coupled RNAs to each lysate sample and add 50-

75U of ribolock.

IV. Incubate 1h at +4°C.

V. After incubation, transfer beads to a 1.5 ml tubes (protein lo-binding tubes).

VI. Wash 3x10 min in Washing buffer

VII. Elute in 10mM Tris-Cl pH 7.5-7.7 buffer for MS analysis; when proceeding with western blot in 1xLDS+10mM DTT. Usually elution is performed for western blot in 60-100 µl of elution buffer. For MS analysis elution is performed in 100 µl of elution buffer

### 2.2.23 Western blot

To detect and analyze proteins from *Drosophila* ovary extracts semi-dry blotting (transfer) was applied. For protein transfer, nitrocellulose membranes were used. Before the transfer gel, membrane and filter papers were submerged in 1 x transfer buffer and assembled into a “transfer sandwich”, using the following order: 1. Three filter papers, 2. Membrane, 3. Protein gel, 4. Three filter papers. Transfer was performed at room temperature for 45-50 min. Amperage was adjusted accordingly:  $\text{mA} = \text{cm}^2 \times \text{cm}^2 \times 2$ ,  $\text{cm}^2 = \text{membrane surface}$ . Following the transfer, membrane was stained with Ponceau for 5 min to estimate sample quality. Next, the membrane was blocked for ~1-2h at room temperature in 5% milk in TBST. Blocking was followed by primary antibody incubation over night at +4°C in the same buffer, after which three 10 min washes in 5% milk in TBST were performed. After washes secondary antibody conjugated with horseradish peroxidase was incubated for 1-2h at room temperature followed by three 10 min washes in TBST. Protein detection was performed using commercially available Immobilon western HRP Substrat (Millipore). Anti-bodies, reagents, chemicals and buffer in use are listed in 2.1 Materials.

### 2.2.24 Protein PAGE

All protein PAGEs were performed using pre-cast NuPAGE™ 4-12% Bis-Tris gels (Invitrogen™). Electrophoresis was performed in 1xMES buffer at room-temperature. For a detailed protocol of protein PAGE see commercially available manual provided by ThermoFisher, Scientific (NuPAGE™ 4-12% Bis-Tris gels manual, Invitrogen™).

### 2.2.25 Sample preparation for mass spectrometry (MS) and TMT labeling

Sample preparation and TMT labeling were performed by **Mandy Rettel** ([Proteomics Core Facility, EMBL](#)) applying following protocol. Reduction of disulphide bridges in cysteine containing proteins was performed with dithiothreitol (56°C, 30 min, 10mM in 50mM HEPES, pH 8.5). Reduced cysteines were alkylated with 2-chloroacetamide (room temperature, in the dark, 30 min, 20mM in 50mM

HEPES, pH 8.5). Samples were prepared using the SP3 protocol (Hughes and Simmonds, 2019; Hughes et al., 2014) with addition of trypsin (sequencing grade, Promega) in an enzyme to protein ratio 1:50 for overnight digestion at 37°C. Next day, peptide recovery in HEPES buffer by collecting the supernatant on magnet and combining with the second elution wash of beads with HEPES buffer was performed. Peptides were labelled with TMT10plex (Werner et al., 2014) Isobaric Label Reagent (ThermoFisher) according to the manufacturer's instructions. In short, 0.8 mg reagent was dissolved in 42 µl acetonitrile (100%) and 4 µl of stock was added and incubated for 1h at room temperature, followed by quenching the reaction with 5% hydroxylamine for 15min at room temperature. Samples were combined for the TMT10plex and for further sample clean-up an OASIS® HLB µElution Plate (Waters) was used. Offline high pH reverse phase fractionation was carried out on an Agilent 1200 Infinity high-performance liquid chromatography system, equipped with a Gemini C18 column (3 µm, 110 Å, 100 x 1.0 mm, Phenomenex) (Reichel et al., 2016).

### Fractionation step in detail:

"Offline high pH reverse phase fractionation was performed using an Agilent 1200 Infinity high-performance liquid chromatography (HPLC) system equipped with a quaternary pump, degasser, variable wavelength UV detector (set to 254 nm), peltier-cooled autosampler, and fraction collector (both set at 10 °C for all samples). The column was a Gemini C18 column (3 µm, 110 Å, 100 x 1.0 mm, Phenomenex) with a Gemini C18, 4 x 2.0 mm SecurityGuard (Phenomenex) cartridge as a guard column. The solvent system consisted of 20 mM ammonium formate (pH 10.0) (A) and 100% acetonitrile as mobile phase (B). The separation was accomplished at a mobile phase flow rate of 0.1 ml/min using the following linear gradient: 100% A for 2 min., from 100% A to 35% B in 59 min., to 85% B in a further 1 min, and held at 85% B for an additional 15 min, before returning to 100% A and re-equilibration for 13 min. Thirty-two fractions were collected along with the LC separation that were subsequently pooled into 6 fractions. As a result the first and the two last fractions of the 32 were not used at all (discarded). Pooled fractions were dried under vacuum centrifugation, reconstituted in 10 µl 1% formic acid, 4% acetonitrile and then stored at -80 °C until LC-MS analysis."

### **2.2.26 Mass spectrometry (MS) data acquisition**

Mass spectrometry data acquisition was performed by Mandy Rettel applying the following protocol. An UltiMate 3000 RSLC nano LC system (Dionex) fitted with a trapping cartridge (µ-Pre-column C18 PepMap 100, 5µm, 300 µm i.d. x 5 mm, 100 Å) and an analytical column (nanoEase™ M/Z HSS T3 column 75 µm x 250 mm C18, 1.8 µm, 100 Å, Waters). Trapping was carried out with a constant flow of solvent A (0.1% formic acid in water) at 30 µl/min onto the trapping column for 6 minutes. Subsequently, peptides were eluted via the analytical column with a constant flow of 0.3 µl/min with



increasing percentage of solvent B (0.1% formic acid in acetonitrile) from 2% to 4% in 4 min, from 4% to 8% in 2 min, then 8% to 28% for a further 96 min, and finally from 28% to 40% in another 10 min. The outlet of the analytical column was coupled directly to a QExactive plus (Thermo) mass spectrometer using the proxeon nanoflow source in positive ion mode.

The peptides were introduced into the QExactive plus via a Pico-Tip Emitter 360  $\mu\text{m}$  OD x 20  $\mu\text{m}$  ID; 10  $\mu\text{m}$  tip (New Objective) and an applied spray voltage of 2.3 kV. The capillary temperature was set at 320°C. Full mass scan was acquired with mass range 350-1400 m/z in profile mode in the FT with resolution of 70000. The filling time was set at maximum of 100 ms with a limitation of  $3 \times 10^6$  ions. Data dependent acquisition (DDA) was performed with the resolution of the Orbitrap set to 35000, with a fill time of 120 ms and a limitation of  $2 \times 10^5$  ions. A normalized collision energy of 32 was applied. A loop count of 10 with count 1 was used and a minimum AGC trigger of  $2e^2$  was set. Dynamic exclusion time of 30 s was used. The peptide match algorithm was set to 'preferred' and charge exclusion 'unassigned', charge states 1, 5 - 8 were excluded. MS<sup>2</sup> data was acquired in profile mode (Strucko et al., 2018).

### 2.2.27 Mass spectrometry (MS) data analysis

Processing of acquired raw data was performed by Mandy Rettel according to the following protocol. IsobarQuant (Franken et al., 2015) and Mascot (v2.2.07) were used to process the acquired data, which was searched against a Uniprot *Drosophila melanogaster* proteome database (UP000000803) containing common contaminants and reversed sequences. The following modifications were included into the search parameters: Carbamidomethyl (C) and TMT10 (K) (fixed modification), Acetyl (Protein N-term), Oxidation (M) and TMT10 (N-term) (variable modifications). For the full scan (MS1) a mass error tolerance of 10 ppm and for MS/MS (MS2) spectra of 0.02 Da was set. Further parameters were set: Trypsin as protease with an allowance of maximum two missed cleavages: a minimum peptide length of seven amino acids; at least two unique peptides were required for a protein identification. The false discovery rate on peptide and protein level was set to 0.01.

Further data analysis was performed by **Frank Stein** (Proteomics Core Facility, EMBL) according to the following protocol. The raw output files of IsobarQuant (protein.txt – files) were processed using the R programming language (ISBN 3-900051-07-0). Only proteins that were quantified with at least two unique peptides were considered for the analysis. Raw TMT reporter ion signals (signal\_sum columns) were first cleaned for batch effects using the removeBatchEffect function from the limma package (Ritchie et al., 2015) and further normalized using vsn (variance stabilization normalization - (Huber et al., 2002)). Proteins were tested for differential expression using the limma package. Proteins were

considered (enriched) hits with a false discovery rate (fdr) smaller 5 % and a fold-change cut-off of 100 % and considered (enriched) candidates with an fdr smaller 20 % and a fold-change cut-off of 50 %.

### 2.2.28 DATA analysis

Quantification of P-body formation was analyzed using the R statistical package (ISBN 3-900051-07-0) or excel (Microsoft). Statistical analysis was performed using the Cochran–Mantel–Haenszel (CMH) test for repeated tests of independence provided in R (ISBN 3-900051-07-0). Where the CMH test was not applicable, the individual Fisher-exact test or Student's t-test were applied. For statistical tests  $\alpha$  value was set to  $\alpha=0.05$ . All plots in this work were obtained using RStudio (<https://www.rstudio.com/>) and ggplot2 library (Wickham, 2009).

Colocalization analysis and particle segmentation analysis of GFP:Me31B RNPs/P-body size were obtained using R scripts generated by Imre Gaspar. Colocalization analysis (Gaspar et al., 2014; Gaspar et al., 2017b) overview: Object-based colocalization for *oskar* mRNPs was performed by measuring the distance between closest-neighbour objects from the *oskarUU* mRNPs (reference channel) and *egfp-oskar3'UTRAA* (target channel) mRNPs within the oocyte. The minimal distance between objects considered to colocalize was set at 250 nm. Random colocalization was addressed by seeding the objects of the target channel randomly into the defined area. This simulation was run hundred times to obtain a distribution of expected (random) colocalization. To calculate fraction of colocalization and to compensate for the huge variability of observed particles per image, reference channel objects were randomly assigned into particle clusters. Observed colocalization within each cluster was compared to the distribution of simulated random values using one-sample Student's *t*-test ( $\alpha = 0.01$ ). To assess biological colocalization, significant values were used to calculate the difference between observed and random colocalization (Gaspar et al., 2017b).

Particle segmentation analysis was performed using xsPT, ImageJ plugin (Gaspar and Ephrussi, 2017) and the R script provided by Imre Gaspar. For each segmented particle, integrated signal intensity values, number of tracks and area were extracted to obtain the particle volume. *oskar* mRNA recruitment to GFP:Me31B positive RNPs in *oskarWT* and *oskarUU* mutant fly lines was presented as correlation of GFP:Me31B and *oskarWT* or GFP:Me31B and *oskarUU* particles' intensities. To compare the difference between the volumes of GFP:Me31B and *oskar* positive RNPs, in *oskarWT* and *oskarUU* mutants Wilcoxon rank-sum test was applied.





## 3 Results

### 3.1 *oskar* mRNA is the part of P-body granules in *Drosophila* female germline

*oskar* mRNA encodes for the Oskar protein, essential for germline determination and proper embryonic development. In addition to its coding function, *oskar* mRNA has several non-coding functions mediated by its 3'UTR (Jambor et al., 2011, 2014; Jenny et al., 2006; Kanke et al., 2015) such as oogenesis progression and completion (Jenny et al., 2006). Interestingly, the *oskar* 3'UTR was shown to dimerize *in vitro* via a stem-loop structure described as stem-loop 2b (SL2b) or dimerizing domain (DD) (Figure 1.5 D and E). Dimerization is mediated via a “kissing-loop” RNA-RNA interaction of the six-nucleotide palindromic sequences present at the top of the SL2b in each of the RNA molecules (Figure 1.5 E). Additionally, this kissing-loop mediated interaction was shown to promote hitchhiking of *oskar* mRNAs *in vivo* (Jambor et al., 2011). In *Drosophila* germline, P-body formation is promoted by nutritional stress (Burn et al., 2015; Shimada et al., 2011). During nutritional stress in *Drosophila* germline cells, both the oocyte and the nurse cells, small RNPs relocate and form large macroscopic RNP aggregates referred to as P-body granules. It is suggested that RNA molecules might have a role as a scaffold and as a consequence promote formation of RNP granules, such as previously mentioned P-bodies (reviewed in Van Treeck and Parker, 2018). Thus, the aim of this work was to investigate the possible function of RNA in P-body assembly using *oskar* mRNA as a paradigm.

#### 3.1.1 P-body distribution in the *Drosophila* germline

To promote nutritional stress response and P-body formation in the germline of *Drosophila* females, wild-type (*w<sup>1118</sup>*) flies were exposed to nutrient-poor conditions (“starved flies”), after which the ovaries were dissected and late previtellogenic and early vitellogenic egg-chambers (stage 6 to 9) were examined for the presence of P-bodies (Figure 3.1 A). P-bodies are identified using immunostaining of the P-body component Me31B (Nakamura 2001) (Figure 3.1 B). When flies were kept under nutrient-rich (“fed flies”) conditions, 24h on the food medium supplemented with additional yeast, nearly 100% of egg-chambers were P-body negative (Figure 3.1 B) and resembled the so-called dispersed phenotype (Snee and Macdonald, 2009). Upon nutrient deprivation for 6 hours on the food medium with no yeast added, the percentage of P-body positive egg-chambers was around 80%, showing that

maintaining the flies under nutrient-poor conditions for this period of time is enough for most of the egg-chambers to sense and respond to the nutritional stress, and form P-bodies (Figure 3.1 B).

#### **3.1.2 *oskar* mRNA localizes in P-bodies upon nutritional stress in the *Drosophila* germline**

An earlier study showed that transgenic GFP:MS2 *oskar* mRNA reporters localize to P-body aggregates in the *Drosophila* germline (Burn et al., 2015). To test whether endogenous *oskar* transcripts localize to P-bodies, *oskar* mRNA smFISH together with immunostaining of Me31B was performed on the egg-chambers from fed and starved females (Figure 3.1 C). This analysis showed that upon starvation *oskar* mRNAs are localized in P-bodies in the *Drosophila* female germline including the oocyte and the nurse cells (Figure 3.1 C).

#### **3.1.3 *oskar* mRNA levels are not affected upon nutritional stress**

P-bodies in yeast and mammalian cells were previously described as sites that harbor mRNAs prior to their degradation. In previous study (Burn et al., 2015), it was reported that no RNA degradation of *Drosophila* maternally deposited RNAs (*oskar*, *gurken* and *bicoid*) is observed. To determine whether there is a change in *oskar* mRNA levels upon nutrient deprivation, we quantified *oskar* mRNA levels prior to and after exposing flies to 6h of nutrient-poor conditions. *oskar* mRNA levels were determined by measuring mRNA intensities of the *oskar* smFISH signal in the oocyte and in the nurse cells independently. Unlike the previous study (Burn et al., 2015) where the abundance of specific transcripts in whole ovaries was analysed using qPCR method, we chose to take advantage of quantitative smFISH and include spatial information to determine the mRNA levels in the two different compartments, the oocyte and the nurse cells. mRNA intensity levels are defined as the measured raw integrated density (the sum of the pixel values provided by the *oskar* smFISH signal in the image) per volume of the selected compartment (the oocyte or the nurse cells). No significant difference in mRNA intensity levels was observed in the oocyte or in the nurse cells (Figure 3.1 D) indicating that there is no significant degradation of *oskar* mRNA in P-bodies.

### 3 Results

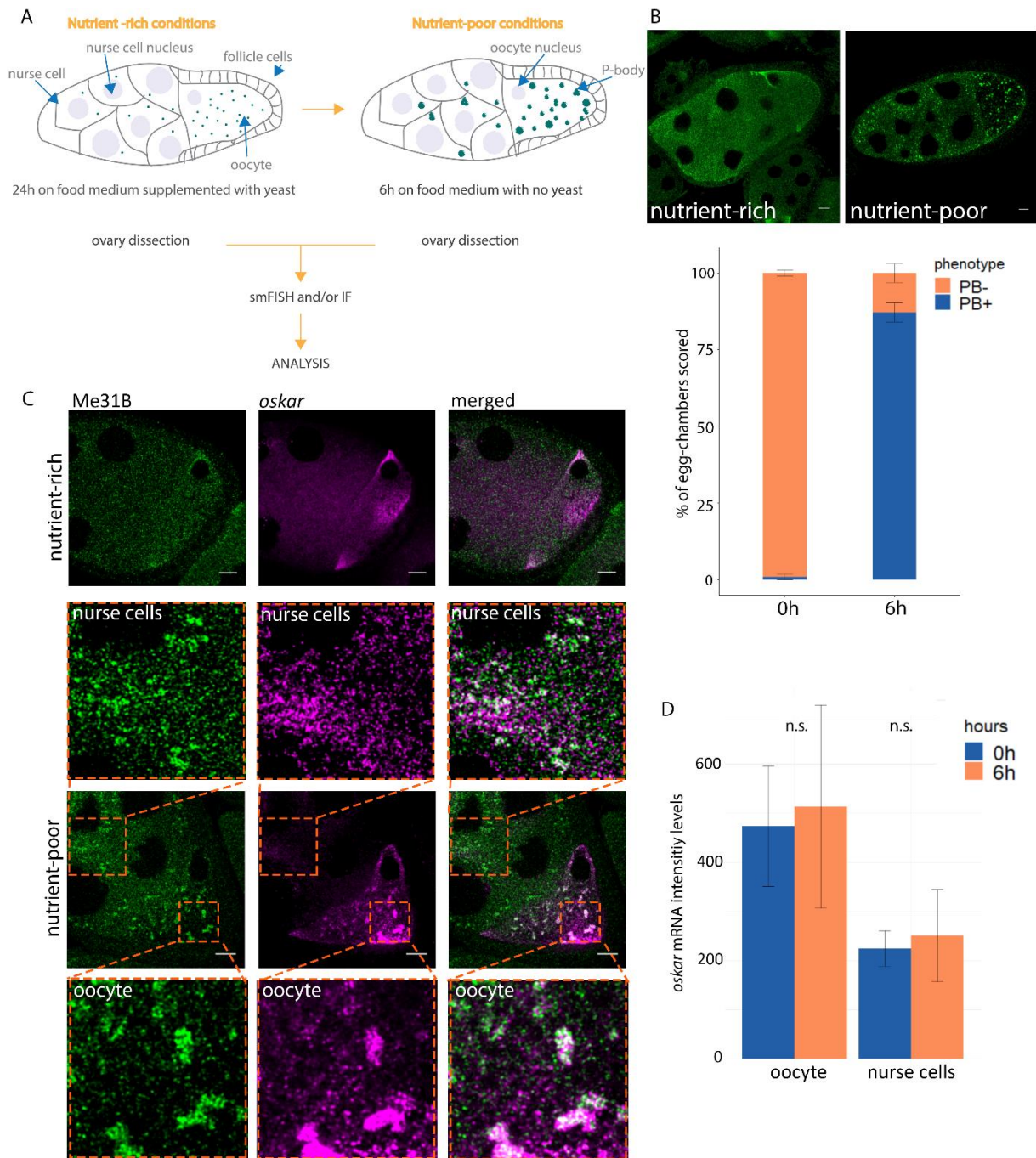


**Figure 3.1 *oskar* mRNAs localize in P-bodies (PBs):** **A** Scheme representing the experimental design. Drawings representing vitellogenic *Drosophila* egg-chambers at oogenic stage 9 prior to (nutrient-rich condition) and after nutrient deprivation (nutrient-poor condition). Prior to nutrient deprivation the flies were kept for 24h on food medium supplemented with yeast. Afterwards the flies were put on food medium with no yeast (nutrient-poor conditions) for 6h prior to ovary dissection. Samples were then processed for smFISH and/or IF (see 2.2 Methods). **B** Top panel: IF detection of Me31B in *Drosophila* egg-chambers (stage 9), under nutrient-rich (left) and nutrient-poor conditions (right), scale bars: 10 $\mu$ m. Bottom panel: graph showing quantification of PBs formed under nutrient-rich (0h) and nutrient-poor (6h) conditions in wild-type flies (*w<sup>1118</sup>*). Oogenic stages responsive to nutrient stress, stage 6 to stage 9, were scored (N:0h =154, N:6h =247), scale bars: 10 $\mu$ m. **C** Co-detection of *oskar* mRNA smFISH (middle) and Me31B IF (left) in *Drosophila* egg-chambers (stage 8) under nutrient-rich and nutrient-poor conditions. In the nutrient-poor panel the insets outlined by orange dashed lines highlight a nurse cell (top) and an oocyte (bottom) compartment with contrast adjusted. Me31B IF signal is shown in green and *oskar* mRNA smFISH signal in magenta. Right panels show the overlay of the two fluorescent signals (merged), scale bars: 10 $\mu$ m. **D** Quantified intensities of *oskar* mRNA smFISH signal under nutrient-rich (0h) and nutrient-poor (6h) conditions in the oocyte and the nurse cells. t-test of significance was used to compare the mean of *oskar* mRNA intensities under nutrient-poor and nutrient-rich conditions.

### 3.2 An intact *oskar* 3'UTR is required for P-body formation and growth

As previously mentioned *oskar* mRNA harbours specific features within 3'UTR which are responsible for its noncoding functions (Jambor et al., 2011, 2014; Jenny et al., 2006; Kanke et al., 2015). For one of these features, *cis*-element SL2b (also referred to as dimerization domain, DD) it has been shown to dimerize *in vitro* (Jambor et al., 2011). In addition, when two nucleotide substitution (e.g. CC to TT, see Appendix I) is introduced in the DD loop the process of dimerization is abolished *in vitro*. Furthermore, mutation in the loop of the DD also affects efficiency of the hitchhiking of *egfp-oskar3'UTR* reporter lines to the endogenous *oskar* mRNAs *in vivo* (Jambor et al., 2011).

#### 3.2.1 A mutation in dimerizing domain of the *oskar* 3'UTR impairs P-body formation

To investigate the possible role of *oskar* mRNA 3'UTR in the assembly of P-bodies as a response to nutritional stress, P-body formation was analysed in flies expressing transgenic wild-type *oskar* (*oskarWT*) or a non-dimerizing *oskar* carrying two nucleotide substitutions (CC to TT, see Appendix I) in the DD loop, referred to as *oskarUU*, in an *oskar* mRNA null genetic background. This genetic background was used in order to provide the system where the obtained phenotype will depend only on the specific transgene, excluding possibility for any additional effect of endogenous *oskar* mRNA transcripts. First, in order to test whether transgenic *oskarWT* flies have the ability to respond to stress and form P-body granules as the wild-type flies (*w<sup>1118</sup>*) P-body formation in these two fly lines was analysed upon 6h of starvation. The analysis showed that transgenic *oskarWT* responded to the nutritional stress and formed P-body granules similarly to the wild-type flies (Appendix III). Next P-body formation analysis performed on *oskarWT* and *oskarUU* mutants showed that the number of egg-chambers scored as P-body positive was significantly lower, ~27% in *oskarUU* compared to ~93% in *oskarWT* females after exposure of the flies to 6h of nutrient-poor conditions (Figure 3.2 A and B). Importantly, expression of the *oskarUU* transgene in wild-type flies (indicted in the Figure 3.2 C as *oskarUU* in endogenous background (in endg.)) did not interfere with P-body formation, and the nutritional stress response with regard to P-body formation was comparable to the wild-type flies (*w<sup>1118</sup>*) not expressing the transgene (Figure 3.2 C). This implies that *oskarUU* does not have a dominant effect on P-body formation. To test if the observed effect of *oskarUU* on P-body formation might be due to the integration site and/or different expression levels of the *oskarUU* and the *oskarWT* transgenes, we assessed P-body formation in another *oskarUU* transgenic line (*oskarUU* #2), integrated at a different location in the genome and with lower mRNA expression (Appendix II). P-body formation was similarly impaired in *oskarUU* #2 (Figure 3.2 D and E), implying that P-body formation depends on an intact sequence in the DD loop of the *oskar* mRNA 3'UTR. These analyses



also indicate that the assembly of cytoplasmic RNP particles into P-body granules might require *oskar* mRNA dimerization.

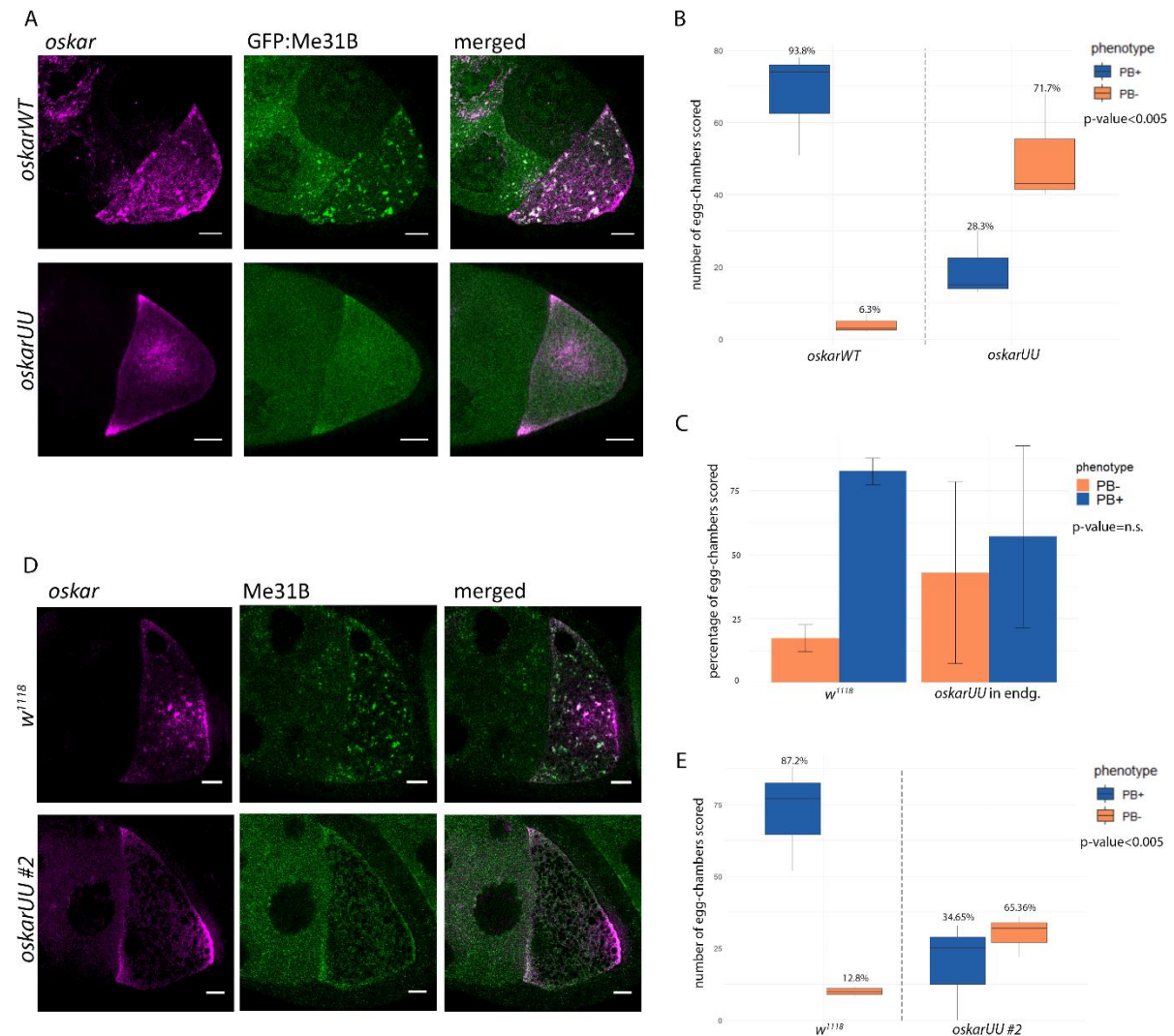


**Figure 3.2 In *oskarUU* non-dimerizing mutants P-body (PB) formation is impaired:** **A** *oskar* mRNA smFISH together with GFP:Me31B detection in *Drosophila* egg-chambers (oogenic stage 8) under nutrient-poor conditions in *oskarWT* (top) and *oskarUU* mutants (bottom). Right panels show an overlay of the two fluorescent signals (merged). Scale bars: 10µm **B** Graph showing the number of PB+ and PB- egg-chambers in *oskarWT* (N=215) and *oskarUU* mutants (N=209). Stages 6 to 9 were scored. In all the box-plots, the mean percentage of screened replicates is indicated above the boxes. Cochran–Mantel–Haenszel (CMH) test for repeated tests of independence was applied. P-values of significance are indicated below the legend of each graph (where the CMH test was not applicable, the Fisher-exact test was applied). **C** Graph showing the number of PB+ and PB- egg-chambers in *w<sup>1118</sup>* (N=221) and *oskarUU* flies (in an *oskar* mRNA endogenous background (endg.) (N=189). t-test of significance was used to compare the mean percentage of PB+ and PB- egg-chambers between *w<sup>1118</sup>* and *oskarUU* in endg. **D** An example of PB formation at stage 8 in *w<sup>1118</sup>* (top) and *oskarUU #2* (bottom) egg-chambers. *oskar* mRNA smFISH signal is shown in magenta and Me31B in green. Right panels show an overlay of the two fluorescent signals (merged). Scale bars: 10µm. **E** Graph showing the number of PB+ and PB- egg-chambers in *w<sup>1118</sup>* (N=247) and *oskarUU #2* (N=148) flies. Stages 6 to 9 were scored. In all the box-plots, the mean percentage of screened replicates is indicated above the boxes. Cochran–Mantel–Haenszel (CMH) test for repeated tests of independence was applied. P-values of significance are indicated below the legend of each graph (where the CMH test was not applicable, the Fisher-exact test was applied). Oogenic stages responsive to nutrient stress, stages 6 to stage 9, were screened for each experimental condition (A-B, C and D-E). All tested *oskar* transgenes, except in C, were expressed in an *oskar* mRNA null background (*oskar<sup>attP,3P3-GFP/oskar<sup>A87</sup></sup>*).

### 3.2.2 A mutation in the *oskar* 3'UTR dimerizing domain affects recruitment of other components into P-bodies

In order to test whether the effect of *oskarUU* non-dimerizing mutants is not exclusive for a single component of P-bodies, Me31B, another established component of these granules, Ypsilon Schachtel (YPS), was used to follow P-body formation, both in the mutant *oskarUU* and the *oskarWT* flies. After being exposed to the nutritional stress for 6h, flies were subjected to ovary dissection and *oskar* smFISH together with GFP:YPS detection was performed. Analysis showed that P-body formation in the *oskarUU* mutant flies co-expressing GFP:YPS was impaired (Figure 3.3 A and B). In addition, recruitment of *patronin* mRNA, identified as a component of P-bodies in an independent study (L. Cassella, unpublished), was analysed. *patronin* mRNA was detected with smFISH in the flies co-expressing P-body marker GFP:Me31B either with *oskarWT* or *oskarUU* mutants. *patronin* mRNA showed similar localization in P-bodies as the *oskar* mRNA (3.3 C, top image panel). Furthermore, number of egg-chambers scored as P-body negative was increased in *oskarUU* mutants compared to *oskarWT* (Figure 3.3 C and D), and *patronin* and GFP:Me31B showed the same dispersed phenotype (Figure 3.3 C, bottom image panel). Thus, these observations indicate that *oskar* mRNA has a global effect on P-body assembly in *Drosophila* germline.

### 3 Results

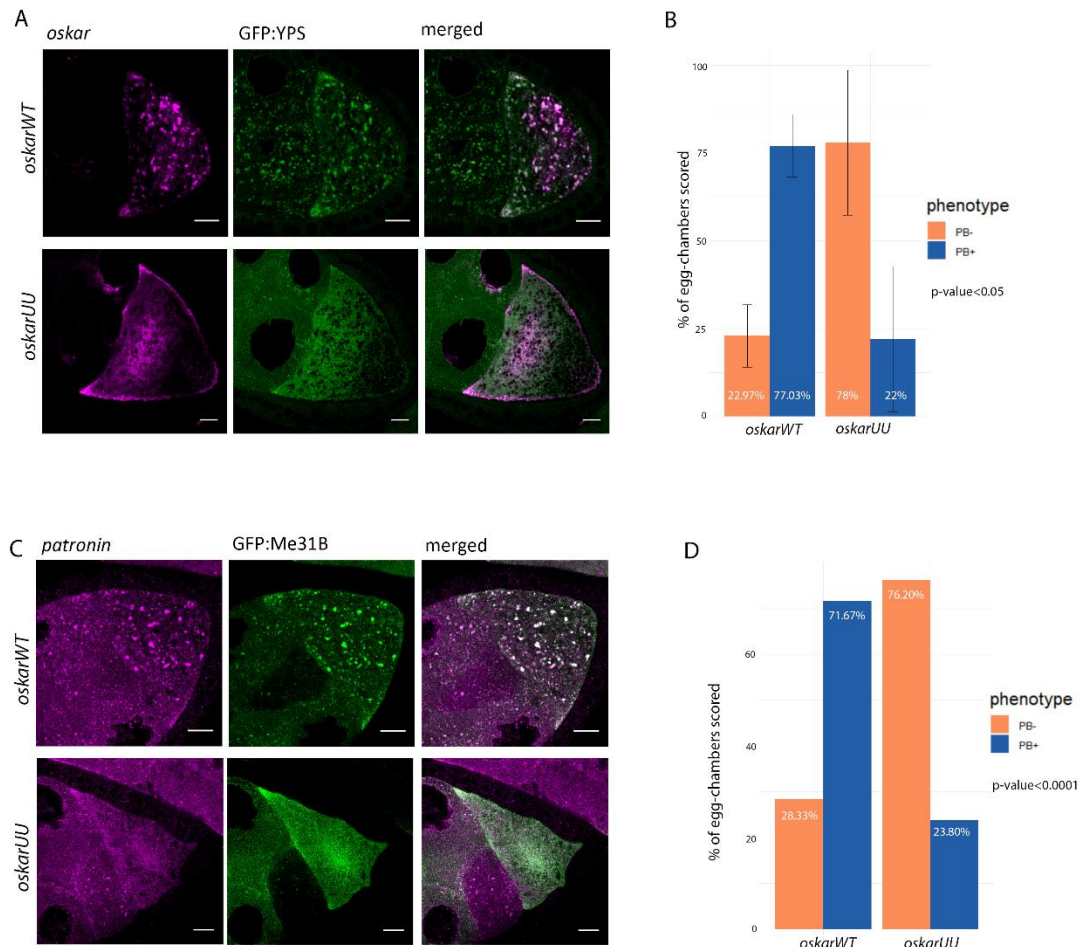


**Figure 3.3** In *oskarUU* mutants, recruitment of P-body components is affected: **A** *oskar* mRNA smFISH (left panels) together with GFP:YPS (middle panels) detection in *oskarWT* (top) and *oskarUU* (bottom) *Drosophila* egg-chambers (oogenic stage 9) under nutrient-poor conditions. *oskar* mRNA smFISH is shown in magenta and GFP:YPS in green. Panels on right show an overlay of the two fluorescent signals (merged). Scale bars: 10 $\mu$ m. **B** Graph showing number of PB+ and PB- *oskarWT* (N=95) and *oskarUU* (N=122) mutant egg-chambers. To compare the difference between the two groups, the t-test was applied. Tested *oskar* transgenes were expressed in *oskar* mRNA null background *oskar<sup>attP,3P3-GFP/oskar<sup>A87</sup></sup>* (A-B). **C** *patronin* mRNA smFISH together with GFP:Me31B detection in *oskarWT* flies (top) and *oskarUU* mutant (bottom) egg-chambers (stage 8) under nutrient-poor conditions. *patronin* mRNA smFISH signal is shown in magenta and GFP:Me31B in green. Right panels show an overlay of the two fluorescent signals (merged). Scale bars: 10 $\mu$ m. **D** Quantification of P-body formation in *oskarWT* (N=60) and *oskarUU* (N=63) mutant egg-chambers. The percentage (%) of P-body positive (blue) and of P-body negative (orange) egg-chambers is indicated. To compare the difference between the two groups, the Fisher-exact test of independence was applied. Tested *oskar* transgenes were expressed in *oskar* mRNA null background *Df(3R)p-XT103/oskar<sup>A87</sup>* (C-D). In each experimental set up (A-B and C-D) PB formation was analysed after 6h of food-deprivation. Oogenic stages responsive to nutrient stress, stages 6 to 9, were screened.

### 3.2.3 *bicoid* and *gurken* do not localize in P-bodies upon nutritional stress in the *Drosophila* germline

Besides *oskar* mRNA, two other maternal determinants, *bicoid* and *gurken*, were reported to be part of P-bodies (Burn et al., 2015; Snee and Macdonald, 2009; Weil et al., 2012). To test these findings we performed independent smFISH for *bicoid* and *gurken* mRNAs in the flies co-expressing GFP:Me31B, P-body marker and *oskar*<sup>WT</sup> in *oskar* mRNA null background, after exposing flies to 6h of nutrient-poor conditions. The analysis of *gurken* and *bicoid* mRNAs localization upon starvation showed that they do not localize to *Drosophila* P-bodies in flies expressing *oskar*<sup>WT</sup> (Figure 3.4 A and B). Few *gurken* or *bicoid* RNPs were observed either in the vicinity of these granules or at their edges. It is important to highlight that most of the sponge-like P-bodies were devoid of both of these RNPs (Figure 3.4 A and B, indicated with arrowheads). These observations differ from those reported by Weil et al. (2012) and Burn et al. (2015). In the first study (Weil et al., 2012), flies were not subjected to nutritional stress, and only the dorsoanterior corner of the oocyte and early embryo were analysed. Furthermore, the particles described by Weil et al. (2012) as P-bodies are small and lack the sponge-like appearance characteristic of the granules formed upon nutritional stress. However, we observed partial colocalization of GFP:Me31B positive RNPs with either *gurken* or *bicoid* in the dorsoanterior region of the oocyte, similar to Weil et al. (2012) (Figure 3.4 A and B, top panels). In addition, it is important to note that in the study of Burn et al. (2015), rather than the endogenous *bicoid* and *gurken* mRNAs, MS2::GFP reporters for each mRNA were analysed. Recent reports indicate that, in yeast, introducing MS2 loops in the *pgk1* mRNA molecules can affect their localization, and cause aberrant enrichment of mRNAs into P-bodies (Heinrich et al., 2017).

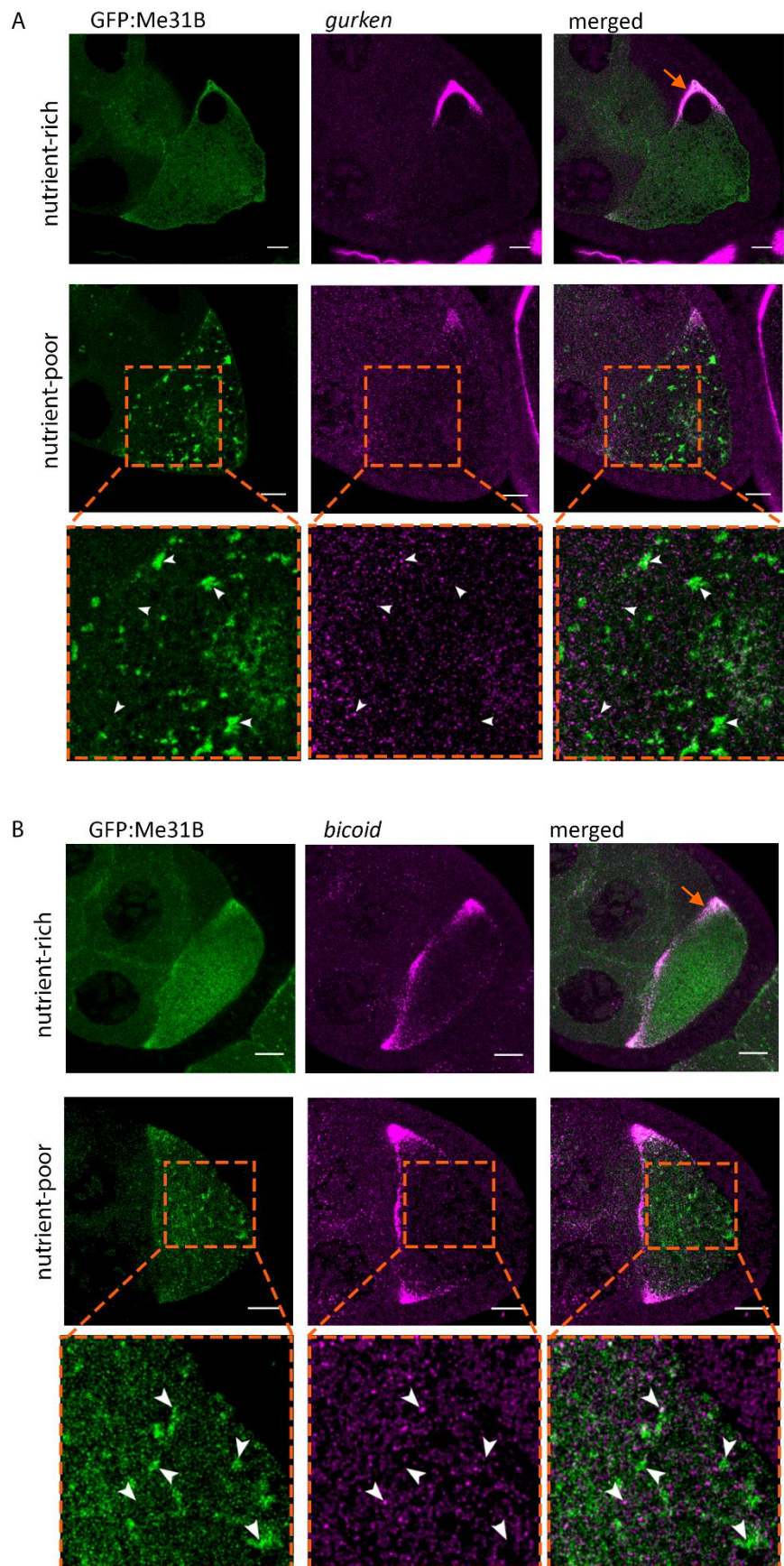


**Figure 3.4 *gurken* and *bicoid* do not localize in P-bodies:** **A** *gurken* mRNA smFISH together with GFP:Me31B detection in egg-chambers (oogenic stage 9) under nutrient-rich (top) and nutrient-poor conditions (bottom) of *oskar*<sup>WT</sup> flies. In the nutrient-rich panel orange arrow indicates dorsoanterior region of the oocyte. In the nutrient-poor panel the inset marked with an orange dashed line highlights a section of the oocyte compartment showing GFP:Me31B (left) and *gurken* mRNA molecules (middle) or overlay of the two fluorescent signals (right, merged). Arrowheads indicate foci with *gurken* and GFP:Me31B where colocalization of these two particles is observed or not. Scale bars: 10µm. GFP:Me31B is in green and *gurken* mRNA smFISH signal in magenta. **B** *bicoid* mRNA smFISH together with GFP:Me31B detection in *oskar*<sup>WT</sup> egg-chambers (oogenic stage 9) under nutrient-rich (top) and nutrient-poor conditions (bottom). In the nutrient-rich panel orange arrow indicates dorsoanterior region of the oocyte. In the nutrient-poor panel the inset marked with an orange dashed line highlights a section of the oocyte compartment showing GFP:Me31B (left) and *bicoid* mRNA molecules (middle) or overlay of the two fluorescent signals (right, merged). Arrowheads indicate foci with *bicoid* and GFP:Me31B where colocalization of these two particles is observed or not. Scale bars: 10µm. GFP:Me31B is in green and *bicoid* mRNA smFISH signal in magenta. PB formation was analysed upon 6h of starvation. Oogenic stages responsive to nutrient stress, stages 6 to stage 9, were screened. All tested *oskar* transgenes were expressed in an *oskar* mRNA null background (*Df(3R)-XT103/oskar*<sup>A87</sup>).

### 3.2.4 A mutation in the *oskar* 3'UTR dimerizing domain hinders P-body growth

Recent studies have described two extreme types of P-body granules depending on the nutritional status of the fly: dispersed P-bodies observed under nutrient-rich conditions and reticulated P-bodies observed under nutrient-poor conditions (Snee and Macdonald, 2009). Dispersed P-bodies correspond to microscopic RNP precursors of the 1-3 µm large so-called reticulated P-body aggregates. Large P-body aggregates are often described as macroscopic cytoplasmic RNP granules formed upon nutritional stress in the *Drosophila* germline and detectable by light microscopy. To investigate in more detail, the dynamics of P-body formation in the *oskar*<sup>UU</sup> non-dimerizing mutants, we analysed P-body formation at different time points (nutrient-rich conditions: 0h; nutrient-poor conditions: 3h, 6h and over-night). After being kept under nutrient-rich conditions for 24h flies were exposed to nutrient-poor conditions for different amount of time. After each time point ovaries were dissected and *oskar* smFISH together with GFP:Me31B detection was performed. Furthermore, P-body formation was analysed in *oskar*<sup>WT</sup> and *oskar*<sup>UU</sup> mutants in *oskar* mRNA null background. The percentage of P-body positive egg-chambers at each hour of maintenance of the flies under nutrient-poor conditions was lower in *oskar*<sup>UU</sup> compared to *oskar*<sup>WT</sup> egg-chambers, including both the oocyte and the nurse cells (Figure 3.5 A). We also tested the recruitment of *oskar* mRNA into P-bodies and estimated P-body size in the oocytes of flies co-expressing *oskar*<sup>UU</sup> or *oskar*<sup>WT</sup> and the P-body marker GFP:Me31B, by particle segmentation analysis using a nearest neighbour algorithm (Gaspar and Ephrussi, 2017). For this analysis we chose the 6h time point of starvation period which showed the highest effect of *oskar*<sup>UU</sup> transgene on P-body formation. Particle segmentation was performed on the oocytes in oogenic stage 8 and 9 of *oskar*<sup>WT</sup> and *oskar*<sup>UU</sup> egg-chambers (Figure 3.5 E). Association

### 3 Results

of *oskar* mRNA with Me31B (here transgenic GFP:Me31B) was not affected in *oskarUU* mutants under nutrient-poor conditions (Figure 3.5 B). However, there was a significant change in the size of GFP:Me31B positive RNP particles in *oskarUU* compared to *oskarWT* expressing flies, with a greater number of smaller RNP particles, and almost complete absence of macroscopic P-bodies (Figure 3.5 C and D). These results suggest that the UU mutation in the *oskar* 3'UTR DD loop impairs P-body growth.

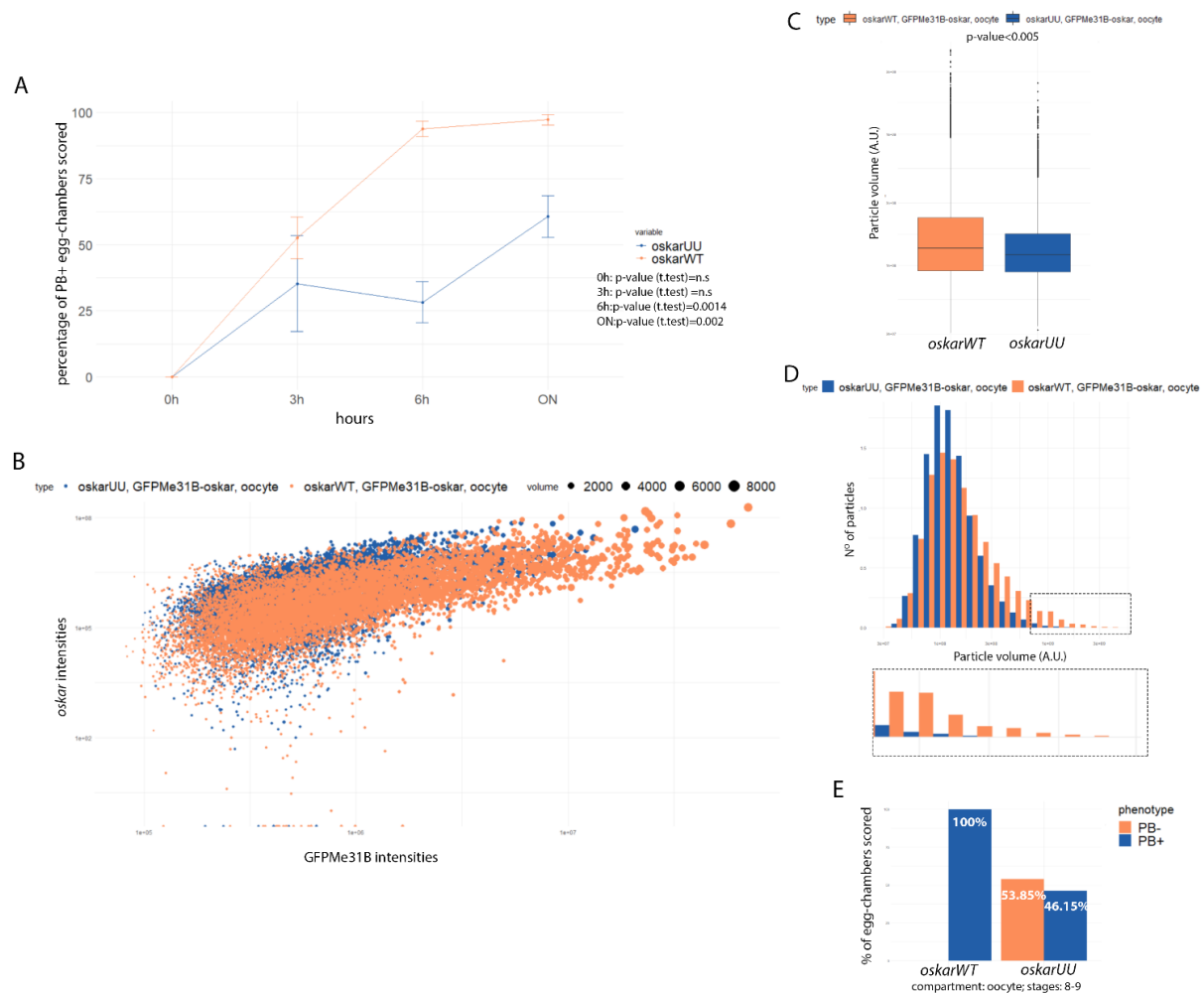


**Figure 3.5 In *oskarUU* mutants P-body (PB) formation is impaired:** **A** Quantification of PB formation under nutrient-rich conditions (0h) and nutrient-poor conditions (3h, 6h and over-night (ON)) in egg-chambers expressing *oskarWT* and *oskarUU* mutant transgenes. Oogenic stages responsive to nutrient stress, stages 6 to stage 9, were scored. To compare the difference between the two groups tested (*oskarWT* vs *oskarUU*) at each time point, a t-test of significance was applied. **B** Scatter plot representing the correlation between GFPMe31B and *oskar* intensities in *oskarWT* and *oskarUU* mutant egg-chambers. **C** Distribution of volumes of GFPMe31B and *oskar* positive RNPs in *oskarWT* and *oskarUU* mutants. To compare the difference of particle volume distribution between *oskarWT* and *oskarUU* mutants, the Wilcoxon rank-sum test was applied. **D** Distribution of GFPMe31B and *oskar* positive RNPs in *oskarWT* and *oskarUU* mutant egg-chambers. The inset marked with the black dashed lines highlights the larger macroscopic RNP granules. For all the particle segmentation analyses (B-D) two populations of egg-chambers (oogenic stages 8 and 9) were analysed: **E** Bar-plot showing the first population, *oskarWT* in which 100% of the egg-chambers were scored as P-body positive (blue) and the second population, *oskarUU* in which ~46% of the egg-chambers were scored as P-body positive (blue) and ~54% as P-body negative (orange). Segmentation analysis was performed in the oocyte compartment of the egg-chambers. All particle segmentation analyses (B-D) were performed on *Drosophila* egg-chambers upon 6h of starvation. All tested *oskar* transgenes were expressed in an *oskar* mRNA null background (*oskar<sup>attP,3P3-GFP/oskar<sup>A87</sup></sup>*).

### 3.3 The effect of *oskar* mRNA dimerization on P-body formation

To test whether the dimerization process *per se* is involved in P-body formation, we co-expressed the *oskarUU* non-dimerizing transgene and another *oskar* transgenic *egfp*-reporter bearing a mutation (GG to AA) complementary to *oskarUU* in the DD domain of the *oskar* 3'UTR (*egfp-oskar3'UTRAA*) (Figure 3.6 A). To analyse P-body formation, flies expressing specific transgenes in the *oskar* mRNA null background were kept under nutrient-poor conditions for 6h. To detect transcripts of interest smFISH was used while P-bodies were detected with endogenously tagged GFP:Me31B. We hypothesized that, should *oskar* mRNA dimerization be central to P-body assembly, restoring dimerization would restore P-body formation comparable to what is observed in the dimerization-competent, transgenic *oskar* wild-type (*oskarWT*) (Figure 3.6 A). However, unlike when *oskarWT* was expressed, impairment of P-body formation was observed in flies (referred to as *oskarUU/AA*) co-expressing *oskarUU* together with *egfp-oskar3'UTRAA* carrying compensatory mutation (Figure 3.6 B). This P-body formation impairment was similar to the one observed when only *oskarUU* transgene was expressed in *oskar* mRNA null background. To exclude the possibility that the observed effect is due to potential inefficient dimerization between the *oskarUU* and *egfp-oskar3'UTRAA* transcripts, the dimerization efficiency of the mutant transcripts in oocytes was assessed. *In vivo* colocalization analysis using smFISH showed that only ~20% of *oskarUU* and *egfp-oskar3'UTRAA* mRNPs colocalize in the diffraction limiting 250 nm radius (Figure 3.6 C). This is in contrast to expected ~100% colocalization of *oskar* wild-type mRNPs, out of which 50% is in the dimeric form (Little et al., 2015). Similar to *in vivo* observation, an *in vitro* dimerization assay showed a lower dimerization efficiency of co-incubated *oskar* 3'UTR region 2 (R2, see Appendix VI) (Figure 3.6 E) UU and AA transcripts, compared to equivalent WT transcripts (Figure 3.6 D and F). Altogether, the *in vivo* colocalization and the *in vitro* dimerization assays indicate that complementarity of AA and UU mutants might not support stable dimer formation to the same extent as WT transcripts. This might explain the impaired P-body formation in flies co-expressing the *oskarUU* and *egfp-oskar3'UTRAA* transgenes. Thus, it is not clear whether *oskar* RNA dimerization is involved in P-body assembly. To test whether the same effect on P-body formation as that observed with *oskarUU* occurs with another *oskar* mRNA non-dimerizing mutant, full-length *oskarAA* transcript, bearing two different nucleotide substitutions (GG to AA, see Appendix I) in the DD domain was tested in *oskar* mRNA null background. Flies expressing *oskarAA* had a nutritional stress response similar to that of flies expressing *oskarUU* and differed significantly from the wild-type (*w<sup>1118</sup>*) with respect to P-body formation (Figure 3.6 G). However, variability among the individual biological replicates tested was quite high, with half of the replicates responding as wild-type for P-body formation and the other half with almost complete impairment of



### 3 Results

P-body assembly. It is important to point out that such high variability among independent replicates was never observed with wild-type flies upon nutritional stress ( $w^{1118}$ ).

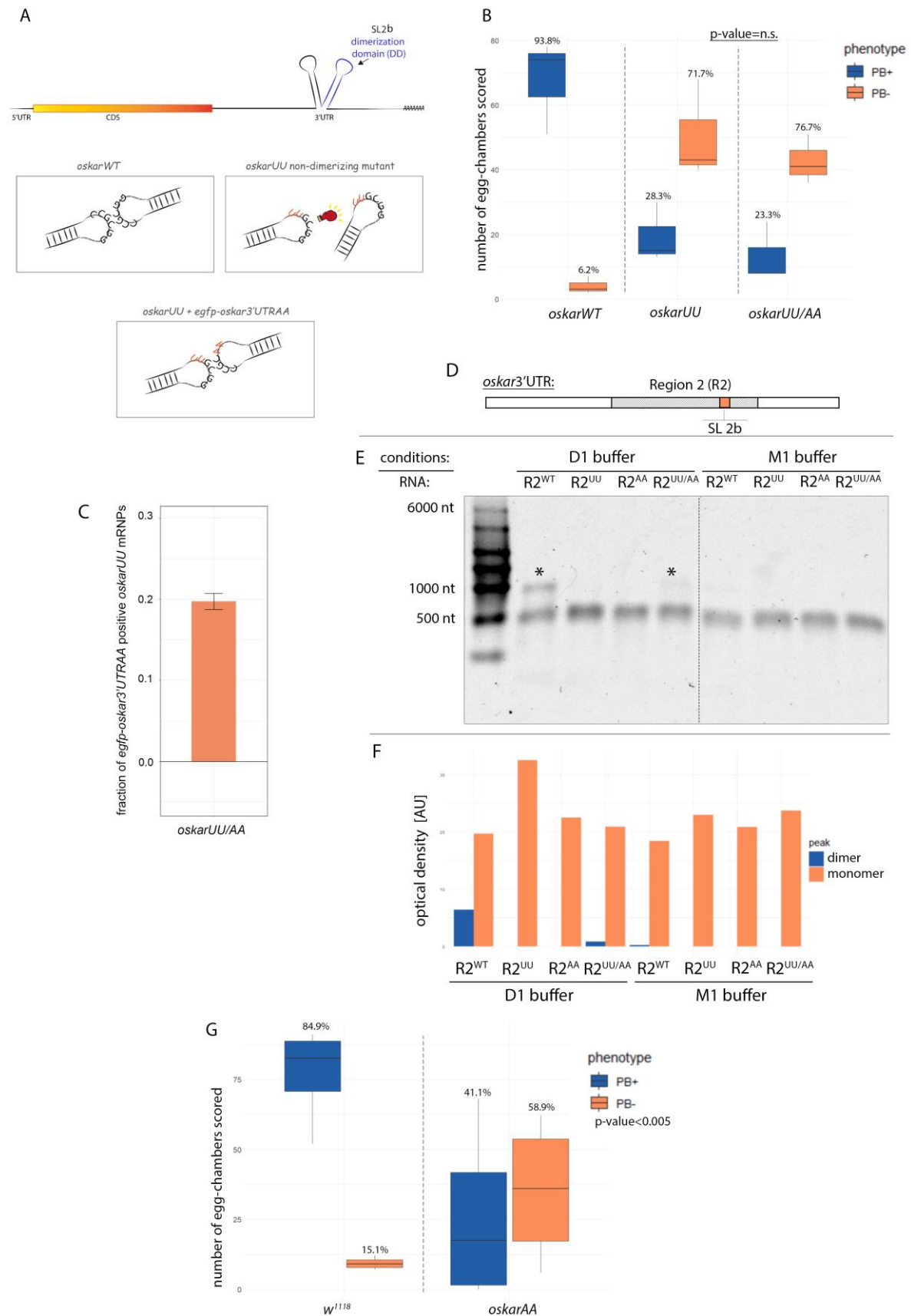


**Figure 3.6 The effect of oskar mRNA dimerization on P-body (PB) formation:** **A** Schematic representation of *oskar* mRNA and the idea behind the “rescue” experimental set up. **B** Graph showing number of PB+ and PB- egg-chambers in *oskar*<sup>WT</sup> (N=215) and *oskar*<sup>UU</sup> (N=209) and *oskar*<sup>UU/AA</sup> mutants (N=168). **C** Quantified fraction of the *oskar*<sup>UU</sup> transcripts colocalizing *egfp-oskar*3'UTRAA complement in *oskar*<sup>UU/AA</sup> mutants. **D** Schematic representation of transcribed R2. **E** Dimerization assay (see 2 Methods) of *in vitro* transcribed *oskar* 3'UTR R2. Each lane corresponds to specific transcript, WT or mutants (UU, AA and co-incubated UU-AA) under dimerization promoting buffer conditions (D1) or monomeric buffer conditions (M1); asterisk on the gel-image indicate dimeric forms of R2 transcripts. **F** Quantified signal intensities of monomeric and dimeric form of RNAs from *in vitro* dimerization assay (C). **G** Graph showing number of PB+ and PB- egg-chambers in *w*<sup>1118</sup> (N=345) and *oskar*<sup>AA</sup> mutants (N=243). PB formation is analysed upon 6h of starvation and oogenic stages 6 to 9 of egg-chambers were scored in each experimental set up. All tested *oskar* transgenes were expressed in *oskar* mRNA null background (*oskar*<sup>attP,3P3-GFP/oskar</sup><sup>A87</sup>). In all the PB formation graphs (B, G), above each phenotype distribution, mean percentage of screened replicates is indicated. To compare difference between the two groups tested, Cochran–Mantel–Haenszel test for repeated tests of independence is used. P-values of significance are indicated in the graph.

### 3.4 Defective repression of mutant non-dimerizing oskar mRNAs does not impair P-body formation

P-bodies are known to be cytoplasmic sites that harbour translationally silent mRNAs (reviewed in Van Treeck and Parker, 2018). For example, global inhibition of translational and stripping ribosomes from mRNAs by puromycin treatment in *Drosophila* S2 cells triggers P-body assembly (Eulalio et al., 2007a). However, the presence of ribosome free mRNAs *per se* is not sufficient to promote P-body formation. If one of the protein components of these granules is depleted through RNAi, even if mRNAs are polysome-free, P-body formation is inhibited (Eulalio et al., 2007a). P-body proteins are mainly proteins involved in translational control and mRNA metabolism, but could also be important building blocks of P-bodies. Currently is not clear if P-body formation is the consequence or the cause of translational repression (Eulalio et al., 2007a; Hubstenberger et al., 2013, 2017). *oskar* mRNA translation is spatially and temporally regulated. *oskar* mRNA is translated at the posterior pole of the oocyte, from oogenic stage 9 onwards. A previous study showed that *oskar*<sup>UU</sup> transcripts are prematurely translated (Jambor, 2008, PhD thesis). Immunohistochemical analysis of Oskar protein in this study, confirmed premature translation of *oskar*<sup>UU</sup> in ~30% of all egg-chambers analysed (Figure 3.7 A and B). This raises the question whether the failure of *oskar*<sup>UU</sup> RNPs to assemble into large P-body granules might be due to “leaky” translation of the mRNAs, prior to localization at the posterior pole.

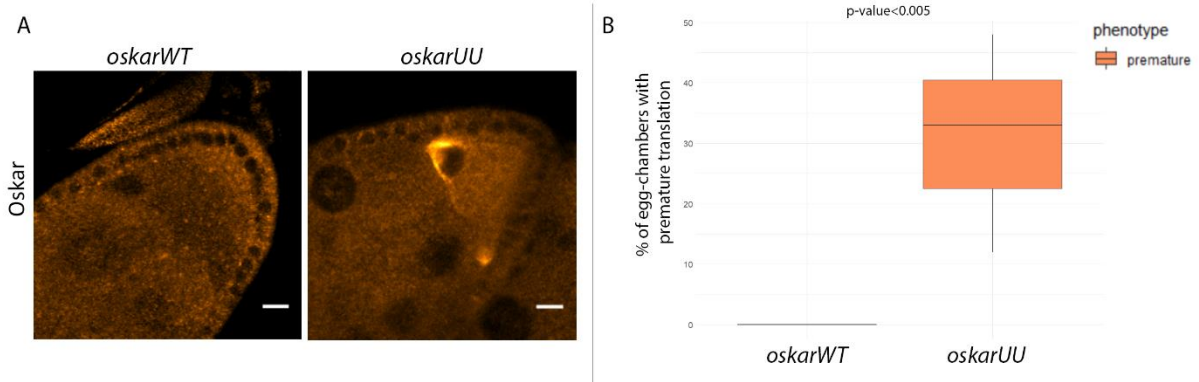


**Figure 3.7 *oskarUU* mutants are translated prematurely:** **A** Oskar protein IF in *Drosophila oskarWT* and *oskarUU* mutant egg-chambers (oogenic stage 8). Oskar protein is shown in orange. Scale bars: 10 $\mu$ m. **B** Graph showing the percentage (%) of egg-chambers in which premature translation was observed. To compare the difference between the two groups of genotypes, the t-test was applied. P-value of the significance is indicated above the groups compared. All tested *oskar* transgenes were expressed in an *oskar* mRNA null background (*oskar<sup>attP,3P3-GFP/oskar<sup>A87</sup></sup>*).

To exclude the possibility that the observed impairment of P-body formation in *oskarUU* mutants is due to its premature translation, *oskar* transgenes lacking the coding sequence (CDS) and consisting only of a wild-type *oskar* 3'UTR (*oskar3'UTRWT*) or an *oskar* 3'UTR carrying the UU mutation (*oskar3'UTRUU*) were expressed in *oskar* mRNA null background flies. In order to analyse P-body formation, wild-type flies and flies expressing *oskar3'UTRWT* and *oskar3'UTRUU* were exposed to 6h of nutrient-poor conditions, after which smFISH for *oskar* mRNA together with Me31B immunostaining on egg-chambers was performed. First it was important to test whether *oskar3'UTRWT* flies behave like the wild-type (*w<sup>1118</sup>*) and display a similar response to nutritional stress by forming P-bodies. Indeed, flies expressing only the *oskar* 3'UTR (*oskar3'UTRWT*) responded to stress similarly to the wild-type control flies (*w<sup>1118</sup>*) (Figure 3.8 A and B), indicating that the absence of *oskar* mRNA translation has not effect on P-body formation. Next, the effect of the UU mutation on P-body assembly was tested in *oskar3'UTRUU* mutants. The analysis showed that compared to *oskar3'UTRWT*, P-body formation was impaired in flies expressing *oskar3'UTRUU*: the number of P-body positive egg-chambers was significantly decreased in UU mutants, compared with the *oskar3'UTRWT* control (Figure 3.8 A and C). Even though the absence of the *oskar* mRNA CDS, thus presumably of ribosomes on the RNA, should have provided a system with translationally inactive *oskar* mRNA, the observation that P-body formation normally occurred in *oskar3'UTRWT* flies, but was impaired in *oskar3'UTRUU* mutants implies that translational inhibition of *oskar* does not suffice to

promote P-body formation. This suggests that features intrinsic to the *oskar* 3'UTR might be important in driving P-body assembly. To further assess the role of the *oskar* 3'UTR in P-body formation, we tested whether P-body formation occurs in UU mutants when ubiquitous and precocious translation of *egfp-oskar3'UTR* reporters was provided. Thus, P-body formation was examined in *oskar* mRNA null flies expressing a transgene consisting of the *egfp* coding sequence fused to either a wild-type (*egfp-oskar3'UTRWT*) or a UU mutant *oskar* 3'UTR (*egfp-oskar3'UTRUU*). Immunostaining for EGFP and western-blot analysis showed that both transcripts were ubiquitously translated in the germline, in the oocyte and the nurse cells respectively (Figure 3.8 D and E). To analyse P-body formation, flies were starved for 6h and smFISH to detect *egfp-cds* in flies expressing *egfp-oskar3'UTRWT* and *egfp-oskar3'UTRUU* or *oskar* mRNA in wild-type flies ( $w^{1118}$ ) was performed together with GFP:Me31B detection or Me31B immunostaining. Flies expressing *egfp-oskar3'UTRWT* showed a similar number of P-body positive egg-chambers as the wild-type flies ( $w^{1118}$ ), (Figure 3.8 F and G). Furthermore, in *egfp-oskar3'UTRUU* mutants the number of P-body positive egg-chambers was significantly reduced compared to *egfp-oskar3'UTRWT* (Figure 3.8 F and H). These results imply that precocious translation of *egfp-oskar3'UTR* transcripts does not hinder P-body formation and that P-body formation impairment is triggered by the presence of the UU mutation in the *oskar* 3UTR. The observation that P-body formation is impaired in the mutant lines both in the absence of *oskar* mRNA translation and in the presence of ubiquitous and precocious translation of *egfp-oskar3'UTR* fusion transcripts implies that P-body formation is independent of *oskar* mRNA translation, hence that P-body impairment is not the consequence of *oskarUU* premature translation (showed in Figure 3.7). Thus, it can be concluded that P-body assembly in the *Drosophila* germline depends on intrinsic features of the 3'UTR of *oskar* mRNA.

### 3 Results

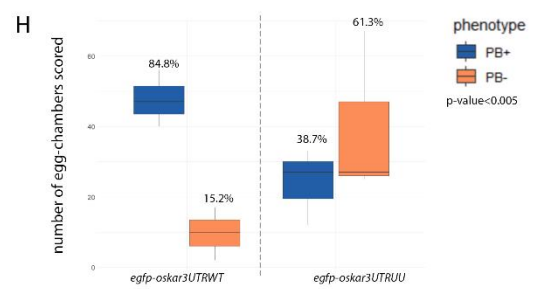
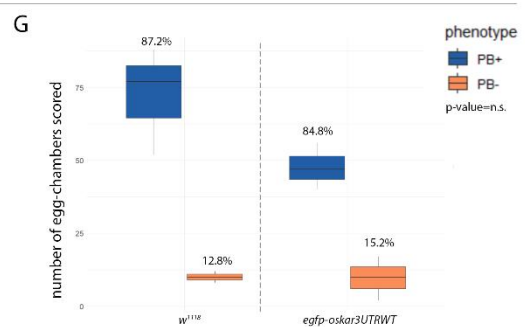
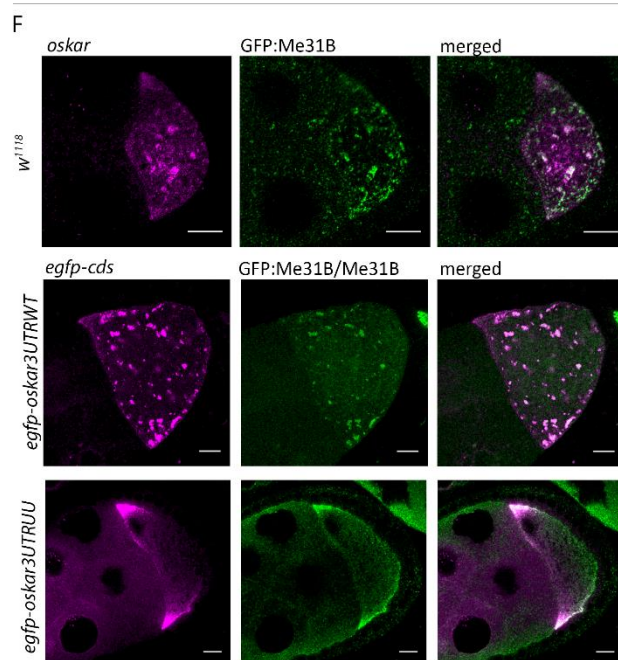
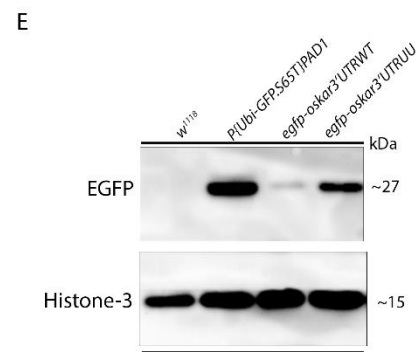
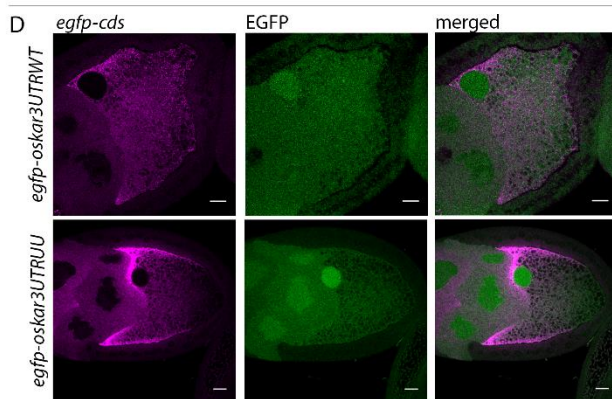
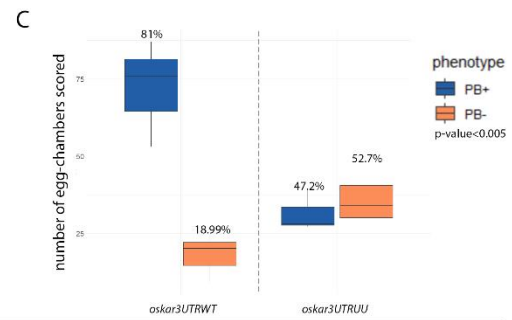
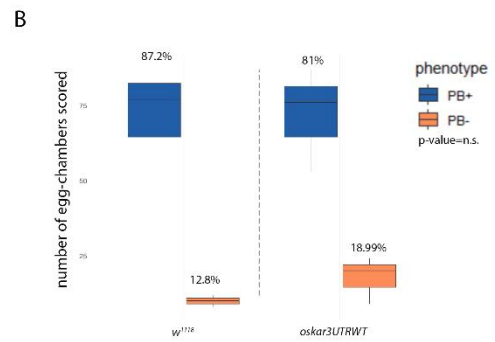
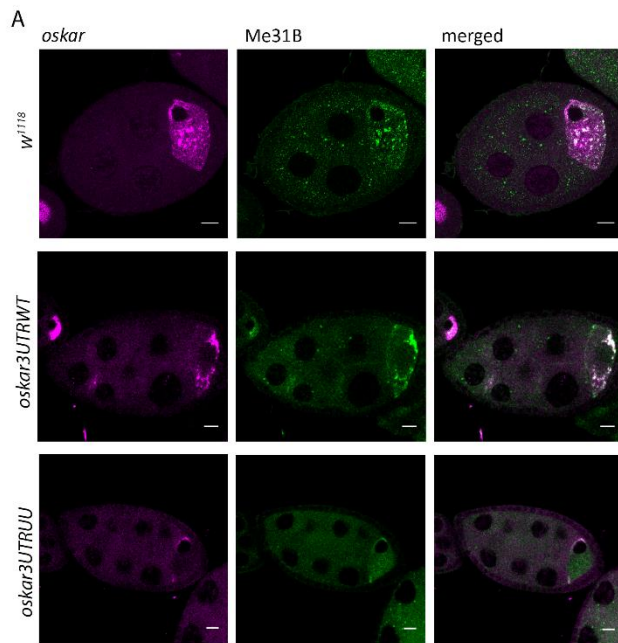


**Figure 3.8 P-body (PB) formation in egg-chambers expressing the *oskar3'UTR* (CDS-free) or *egfp-oskar3'UTR* transgenes:**

**A** Co-detection of *oskar* mRNA smFISH and Me31B IF in nutrient-deprived *w<sup>1118</sup>* (top), *oskar3'UTRWT* (middle) and *oskar3'UTRUU* (bottom) egg-chambers (oogenic stage 8). *oskar* mRNA smFISH signal is in magenta and Me31B IF signal in green. Panels on the right show an overlay of the two fluorescent signals (merged). Scale bars: 10µm. **B** Graph showing the number of PB+ and PB- in *w<sup>1118</sup>* (N=247) and *oskar3'UTRWT* mutant egg-chambers (N=269). **C** Graph showing the number of PB+ and PB- egg-chambers in *oskar3'UTRWT* (N=269) and *oskar3'UTRUU* mutant flies (N=253). PB formation was analysed upon 6h of nutrient deprivation. Oogenic stages responsive to nutrient stress, stages 6 to stage 9, were screened (A-C). In all the graphs (B-C). In all the box-plots, the mean percentage of screened replicates is indicated above the boxes. To compare the difference between the two groups, the Cochran–Mantel–Haenszel test for repeated tests of independence was applied. P-values of significance are indicated below the legend of each graph. **D** Ubiquitous expression of *egfp* in the oocyte and nurse cells (oogenic stage 9) in *egfp-oskar3'UTRWT* (top) and *egfp-oskar3'UTRUU* mutant line (bottom). *egfp-cds* smFISH signal is shown in magenta and EGFP IF signal in green. Panels on the right show an overlay of the two fluorescent signals (merged). Scale bars: 10µm. **E** Immunoblot showing EGFP expression in *egfp-oskar3'UTRWT* (3) and *egfp-oskar3'UTRUU* egg-chambers (4), with *w<sup>1118</sup>* (1) and *P{Ubi-GFP.S65T}PAD1* (2) serving as negative and positive controls, respectively. **F** *oskar* mRNA smFISH together with Me31B IF in *Drosophila* egg-chambers (oogenic stage 8) under nutrient-poor conditions of *w<sup>1118</sup>* (top), *egfp-oskar3'UTRWT* (middle) and *oskar3'UTRUU* (bottom) flies. *oskar* mRNA smFISH signal is in magenta and Me31B IF signal is in green. Panels on the right show an overlay of the two fluorescent signals (merged). Scale bars: 10µm. **G** Graph showing the number of PB+ and PB- *w<sup>1118</sup>* (N=247) and *oskar3'UTRWT* mutant (N=172) egg-chambers. **H** Graph showing the number of PB+ and PB- *egfp-oskar3'UTRWT* (N=172) and *egfp-oskar3'UTRUU* mutant egg-chambers (N=191). PB formation was analysed upon 6h of starvation. Oogenic stages responsive to nutrient stress, stage 6 to stage 9, were screened (F-H). In all the graphs (G-H). In all the box-plots, the mean percentage of screened replicates is indicated above the boxes. To compare the difference between the two groups tested, the Cochran–Mantel–Haenszel test for repeated tests of independence was applied. P-values of significance are indicated below the legend of each graph. All tested *oskar* transgenes were expressed in an *oskar* mRNA null background *oskar<sup>attP,3P3-GFP/oskar<sup>A87</sup></sup>* (A-C and F-H) or *Df(3R)p-XT103/oskar<sup>A87</sup>* (D-E).

### 3.5 *oskar* 3'UTR is sufficient to support P-body formation

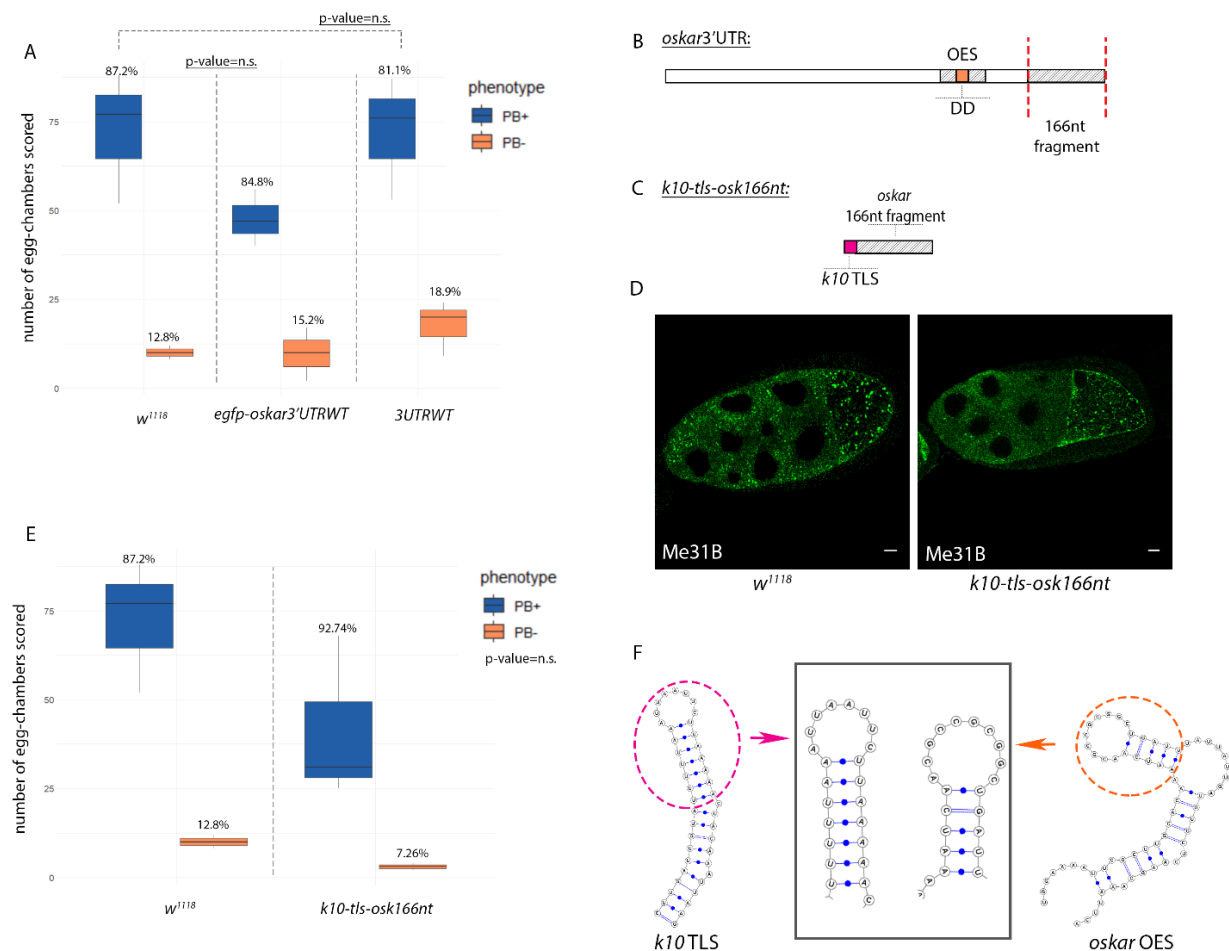
The above experiments (section 3.4) indicate that the wild-type *oskar* 3'UTR is sufficient to support P-body formation. When expressed in an *oskar* mRNA null background, both *oskar3'UTRWT* and *egfp-oskar3'UTRWT* show a similar distribution of P-body positive and negative egg-chambers as do wild-type flies (*w<sup>1118</sup>*) upon exposure to nutrient-poor conditions (Figure 3.9 A). Most importantly in both *oskar3'UTRUU* and *egfp-oskar3'UTRUU* mutants expressed in *oskar* mRNA null flies P-body formation is impaired (look at the Section 3.4, Figure 3.8 C and H). This shows that changes within the *oskar* 3'UTR affect P-body formation and implies that the 3'UTR of *oskar* has properties important for P-body assembly.

#### 3.5.1 Flies expressing a *oskar* 3'UTR rescue fragment form P-bodies upon nutrient deprivation

The ability of *oskar* mRNA to support P-body formation and the observation that in *oskar* non-dimerizing mutants P-body formation is impaired suggests that *oskar* mRNA on its own might promote in P-body assembly in the *Drosophila* germline. To test the importance and requirement of *oskar* mRNA in P-body assembly one approach would be to assess if P-body formation occurs in the flies that express no endogenous *oskar* mRNA. Such “*oskar* mRNA null” flies exist, but manifest a phenotype that complicates their use as such: the flies arrest oogenesis at stage 7 and germline cells display morphological abnormalities (Jenny et al., 2006; Kanke et al., 2015). As egg-chambers that respond to nutritional stress and form P-bodies are mid-previtellogenic to early vitellogenic stages 8 and 9 (Burn et al., 2015; Shimada et al., 2011), the problem of oogenesis arrest of the mRNA null flies must be circumvented. This can be achieved by expressing a 3'-terminal fragment of the *oskar* 3'UTR, which when fused to the TLS of *K10* mRNA, is imported into the oocyte and supports the progression of oogenesis (Jambor et al., 2014; Kanke et al., 2015). We therefore made use of this strategy to analyse the role of the *oskar* RNA molecule in P-body formation. Wild-type flies (*w<sup>1118</sup>*) and flies expressing the 166 nucleotide long 3'-terminal fragment of the *oskar* 3'UTR fused to *K10* TLS, *k10-tls-osk166nt* transgene (Gstir, 2012), (Figure 3.9 B and C), were exposed to nutrient-poor conditions for 6h after which immunostaining for Me31B was performed on the egg-chambers. Surprisingly, no effect on P-body formation upon nutrient deprivation was observed in *k10-tls-osk166nt* flies, which formed P-bodies just as the wild-type control, (Figure 3.9 D and E). Since mutations in *oskar* RNA that impair P-body formation reside within the 3'UTR dimerization domain, we assumed that P-body formation would be affected in *k10-tls-osk166nt* transgenic flies, in which the *oskar* DD was completely absent. The puzzling observation that the *k10-tls-osk166nt* transgene supports P-body formation led us to

### 3 Results

analyse in more detail the sequence of the *K10* TLS, which has been reported to share features with the *oskar* OES (Jambor et al., 2014; Lehmann, 2016; Serano and Cohen, 1995). RNA secondary structure prediction analysis obtained using iPKnot web server for predicting RNA secondary structure and pseudoknots (*Graduate School of Information Science, Nara Institute of Science and Technology (NAIST), Japan; Department of Biosciences and Informatics, Keio University, Japan*) confirmed that the *oskar* OES (DD) and the *K10* TLS have similar structural features in the upper region of the stem-loop (Figure 3.9 F), which might explain the wild-type like P-body formation observed in *k10-tls-osk166nt* expressing flies. Another interesting observation is that transgenic flies expressing *oskar* non-dimerizing RNAs, and in which the *K10* mRNA is normally expressed, P-body formation is nevertheless impaired. This implies, that the *K10* TLS and the *oskar* 3'UTR must be coupled in *cis* to promote P-body formation. It is possible that the *oskar* DD or any other alien domain with a similar predicted stem-loop structure (in this case the *K10* TLS) and the 3' oogenesis rescuing piece of *oskar* 3'UTR together provide a scaffold or a specific environment that could promote RNA-RNA and RNA-protein interactions necessary for P-body formation. The mutation in this domain (e.g. CC to TT; see section 3.2) could affect both *in cis* and *in trans* interactions of the *oskar* 3'UTR with components required for P-body assembly.





---

**Figure 3.9 *oskar* 3'UTR is sufficient to promote P-body (PB) formation:** **A** Graph showing the number of PB+ and PB- egg-chambers in *w<sup>1118</sup>* (N=247), *egfp-oskar3UTRWT*(N=172) and *3UTRWT* flies (N=269). **B** Schematic representation of the *oskar* 3'UTR. Dimerization domain (DD) is highlighted in orange. Oogenesis-rescuing 166 nucleotide (nt) fragment is marked with red dashed lines. **C** Scheme of the *k10-tls-osk166nt* construct (Appendix XII). **D** Egg-chambers at oogenic stage 9 showing Me31B IF in wild-type (*w<sup>1118</sup>*) and *k10-tls-osk166nt* flies upon nutrient deprivation. **E** Graph showing the number of PB+ and PB- egg-chambers in *w<sup>1118</sup>* (N=247) and *k10-tls-osk166nt* and *3UTRWT* mutants (N=133). PB formation was analysed upon 6h of starvation and for each experimental set up stages 6 to 9 were screened (A, D, E). In all the images the PB marker Me31B is in green. Scale bars: 10µm. Above each box-plot, the mean percentage of screened replicates is indicated. To compare the difference between the two groups tested, the Cochran–Mantel–Haenszel test for repeated tests of independence was used. P-values of significance are indicated in the graph. All transgenes were expressed in an *oskar* mRNA null background (*oskar<sup>attP,3P3-GFP/oskar<sup>A87</sup></sup>*). **F** Secondary structure predictions of the *K10* TLS and *oskar* OES. For secondary structure predictions, the iPKnot web server for predicting RNA secondary structure and pseudoknots was used (*Graduate School of Information Science, Nara Institute of Science and Technology (NAIST), Japan; Department of Biosciences and Informatics, Keio University, Japan*).

---

### 3.6 Introducing mutations in the *oskar* 3'UTR affects RBP recruitment

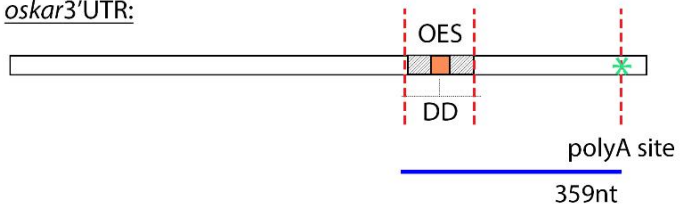
In this study it was observed that an *oskar* 3'UTR expressed in *oskar* mRNA null flies is sufficient to drive P-body assembly (see sections 3.4 and 3.5) and that introducing mutations in the *oskar* 3'UTR DD loop hinders P-body formation in *Drosophila* female germline. The inability to restore dimerization *in vivo* and *in vitro* (see section 3.3) prevented us from addressing the importance of dimerization as an initial step in P-body assembly. Whether the kissing-loop mediated dimerization of two *oskar* molecules via six-nucleotide palindromic sequence in the DD loop could be an important step in triggering P-body formation needs to be further investigated. The assembly of P-bodies could also involve interactions between *oskar* mRNA and RBPs. In order to investigate whether the P-body interfering mutations introduced in the *oskar* 3'UTR might affect recruitment of interacting proteins, RNA affinity pull-down assay was applied, followed by candidate based or mass spectrometry (MS) analysis.

#### 3.6.1 Introducing a mutation in the DD loop of *oskar* 3'UTR affects recruitment of Bruno

As previously mentioned, many *oskar* translational regulators were reported to be components of *Drosophila* P-bodies (e.g. PTB, dGe-1, Bruno, Me31B, Hrp48) (Besse et al., 2009; Fan et al., 2011; Snee and Macdonald, 2009). For a number of these components such as Bruno and PTB, binding sites within the *oskar* 3'UTR were identified (Besse et al., 2009; Kim-Ha et al., 1995; Micklem et al., 2000; Reveal et al., 2010; St Johnston et al., 1991; Tian and Mathews, 2003), whilst for many others not. The observed impairment of P-body formation in *oskarUU* non-dimerizing mutants could be due to the compromised interaction of *oskarUU* 3'UTR with proteins that are necessary for proper P-body assembly. The inefficient or unstable RNA-protein interactions could lead to inhibition of P-body formation in *oskar* non-dimerizing mutants. Secondary structure RNA predictions of a 359 nt *oskar* 3'UTR fragment (Figure 3.10 A) showed additional long-range intramolecular interactions occurring between the *oskar* DD loop containing the UU mutation and a distal region of the *oskar* 3'UTR (Figure 3.10 C). These intramolecular interactions were not observed in the WT 3'UTR (Figure 3.10 B). New interactions formed in the UU mutant involve the so-called C region of the *oskar* 3'UTR which includes BREs, Type II Bruno binding sites and putative binding sites of another *oskar* translational regulator, bicoid stability factor (BSF), (Ryu and Macdonald, 2015), (Figure 3.10 C). These predicted interactions could have an effect on Bruno and BSF recruitment to *oskar* mRNA. Bruno was shown to be a component of *Drosophila* P-bodies (Snee and Macdonald, 2009), hence affecting its recruitment to *oskar* might also affect P-body assembly.

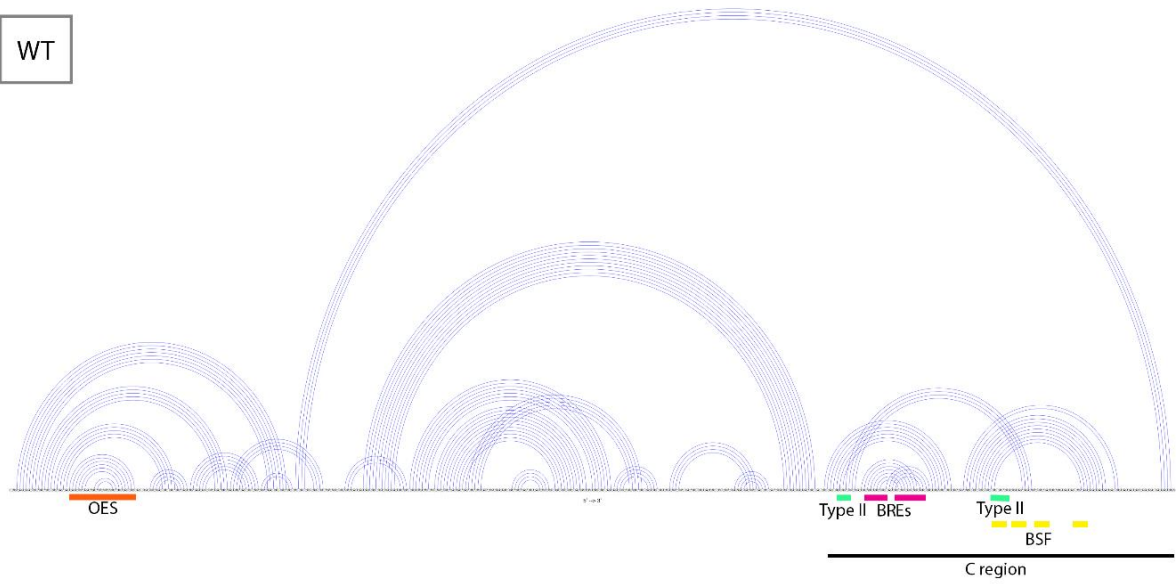
### 3 Results

A *oskar*3'UTR:



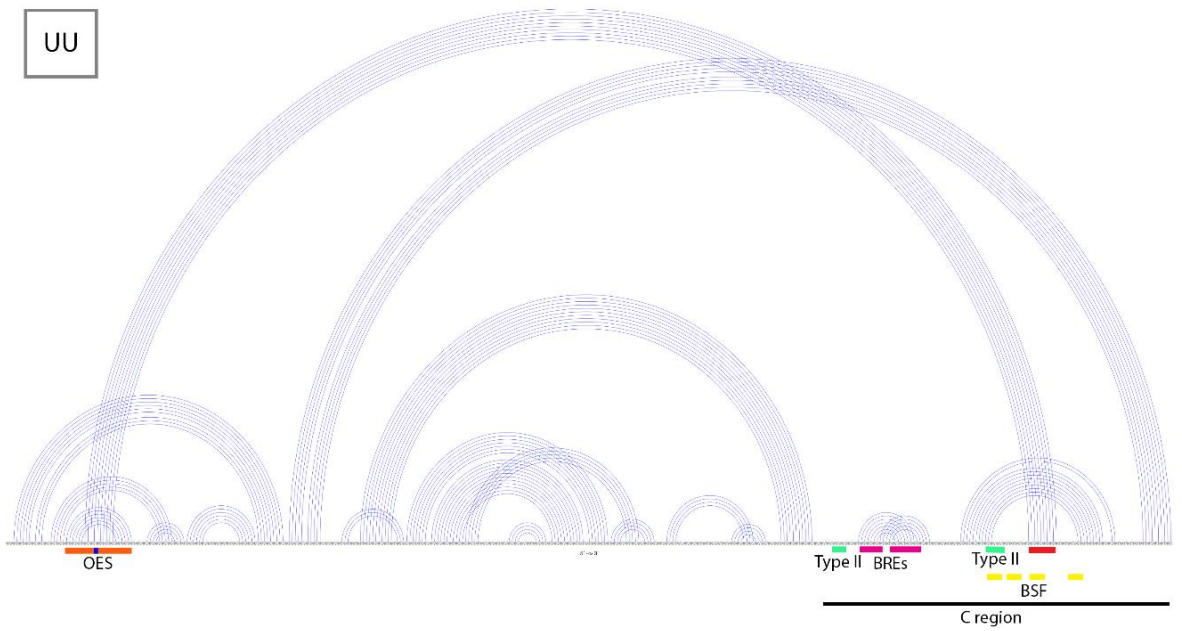
B

WT



C

UU



---

**Figure 3.10 *oskar* 3'UTR secondary structure prediction:** **A** Schematic representation of the *oskar* 3'UTR. Red dashed lines highlight OES (with DD loop region in orange). PolyA site is indicated with a green asterisk. Blue line below the 3'UTR marks the 359 nucleotide long region used for RNA secondary predictions. **B** Secondary structure prediction of the 359 nucleotide long region of WT *oskar* 3'UTR. **C** Secondary structure prediction of the 359 nucleotide long region of the *oskar* UU mutant 3'UTR. UU mutation is indicated with blue square within the OES region (marked in orange, B and C). Red line indicates additional intramolecular interaction formed in UU mutants. Bruno binding sites are indicated with green lines (Type II) and magenta (BREs) (B and C). Putative BSF binding sites are indicated with yellow lines. Region C is indicated with black line (B and C). For secondary structure predictions, the iPKnot web server for predicting RNA secondary structure and pseudoknots was used (Graduate School of Information Science, Nara Institute of Science and Technology (NAIST), Japan; Department of Biosciences and Informatics, Keio University, Japan).

---

In order to address the question whether the DD mutations in the *oskar* 3'UTR could affect recruitment of Bruno, an RNA affinity pull-down assay from ovarian extract was performed (Figure 3.11 A). Immunoblotting analysis of pull-downs of *in vitro* synthesized transcripts revealed that Bruno recruitment is affected in pulldowns using *oskar* UU\_359 mutant transcripts, compared to corresponding *oskar* wild-type WT\_359 transcripts (Figure 3.11 C, one representative replicate is shown, see Appendix VIII for the rest). As expected, no Bruno was detected in the pull-downs with WT\_67 and UU\_67 transcripts which do not contain Bruno binding sites. The decreased amount of Bruno detected in the UU\_359 pull-down indicates that changes in the 3'UTR of *oskar* might affect Bruno recruitment. As suggested by RNA secondary structure predictions (Figure 3.10), new intramolecular interactions in *oskar* 3'UTR caused by introducing UU mutation in the DD loop could interfere with Bruno binding to *oskar*. As Bruno is known to be a repressor of *oskar* translation (Chekulaeva et al., 2006; Kim-Ha et al., 1995; Nakamura et al., 2004; Wilhelm et al., 2003), inefficient binding of Bruno to the UU\_359 transcripts might explain premature translation in *oskarUU* mutants. Also, as Bruno was shown to be component of *Drosophila* P-bodies (Snee and Macdonald, 2009), inefficient binding of Bruno to *oskar* UU\_359 mutant transcript might explain the impairment of P-body formation in *oskarUU* non-dimerizing mutants.

### 3 Results

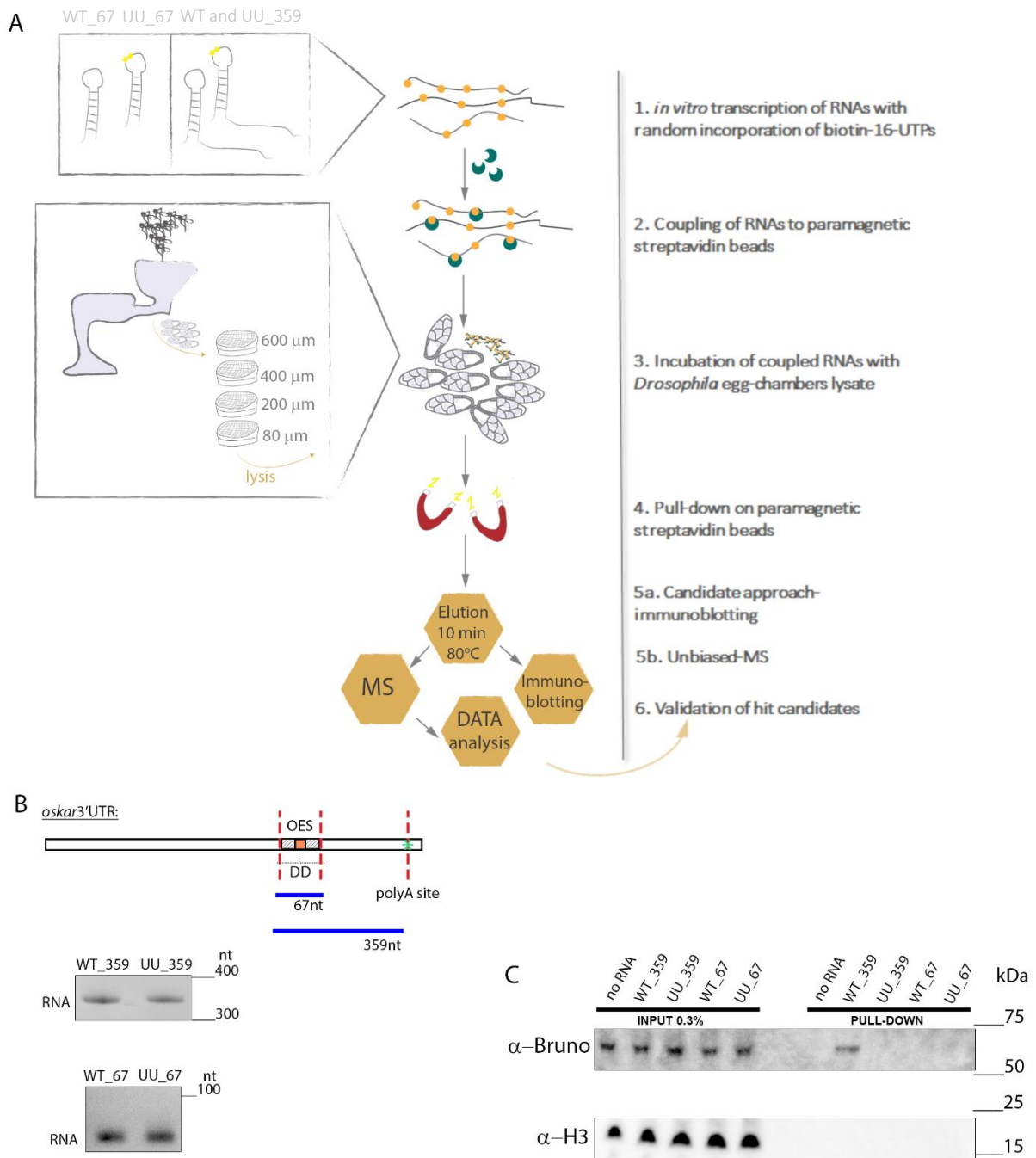
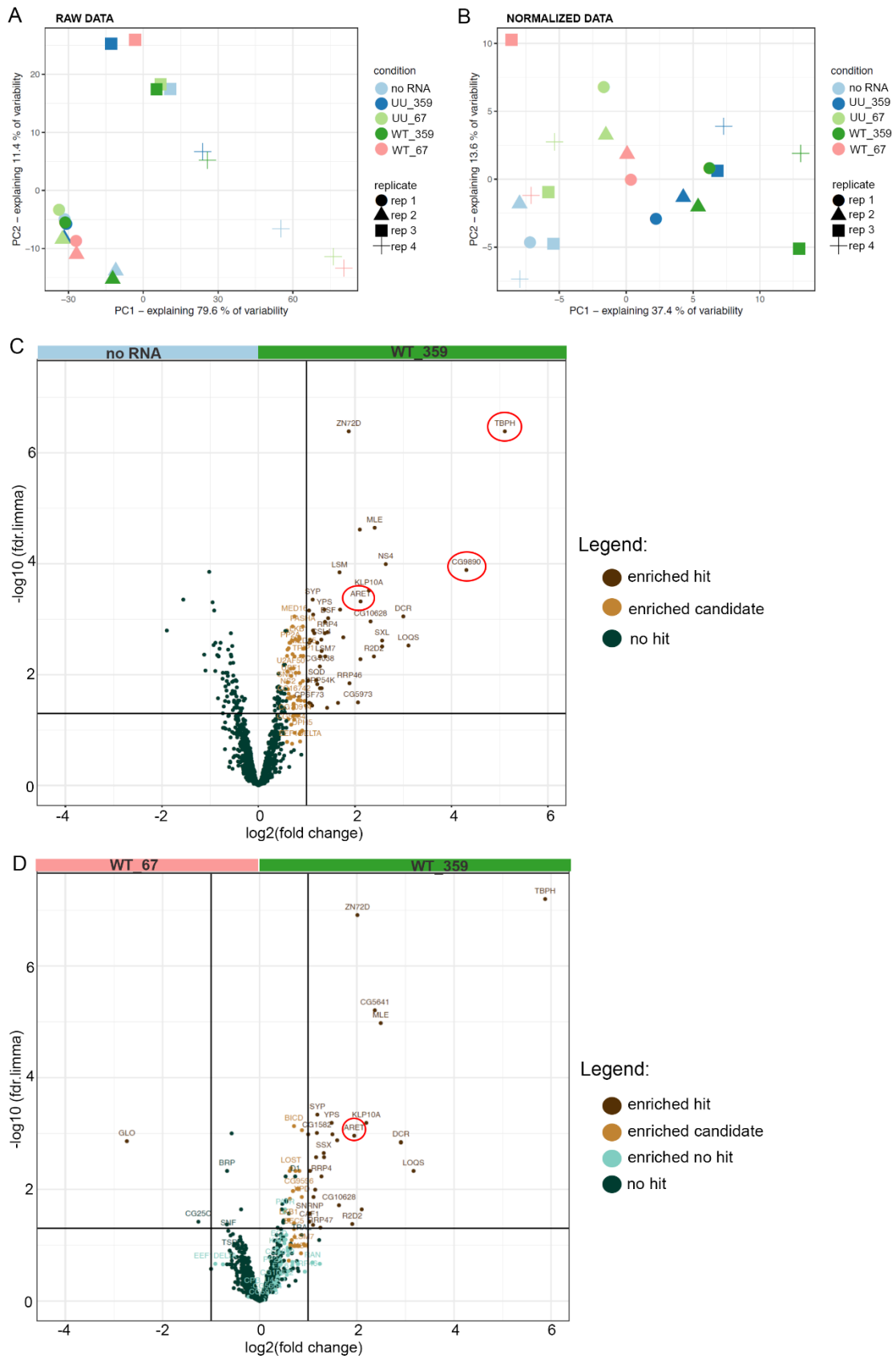


**Figure 3.11 *oskar* specific RNA affinity pull-down reveals differences in Bruno affinity for *oskar* WT and UU mutant 3'UTR transcripts:** **A** Schematic representation of experimental work-flow for the RNA affinity pull-down assay. **B** At the top, schematic representation of the *oskar* 3'UTR with regions of the 3'UTR used for the pull down indicated (blue lines: 67 nt long and 359 nt long region, see Appendix VII). Red dashed lines highlight OES (with DD loop region in orange). PolyA site is indicated with the green asterisk. (top). Middle and bottom panel show *in vitro* transcribed *oskar* 3'UTR fragments. **C** Immunoblot showing loss of Bruno in UU\_359 pull-down, compared to WT\_359. In addition to the no RNA control, WT\_67 and UU\_67, which lack Bruno binding sites were used further as negative controls. 33.3% of each pull-down sample was loaded on the gel.

### 3.6.2 The *oskar* 3'UTRWT vs. *oskar* 3'UTRUU proteome

In order to obtain broader insight into possible differences in protein interactors between the *oskar* mRNA WT 3'UTR and the UU mutant 3'UTR, after RNA affinity pull-downs TMT-labeling quantitative LC-MS/MS was performed (Figure 3.12 A). Four biological replicates were prepared in independent experiments and quantified in two different MS runs (run 1: replicate 1 and 2, run 2: replicate 3 and 4). Each biological replicate was prepared at different day by harvesting Oregon-R flies to obtain lysates for the pull-downs. (see 2 Materials and Methods). Pull-down samples were prepared and LC-MS/MS Data analysis of MS measurements was performed in a collaboration with Frank Stein (Proteomics Core Facility, EMBL) Prior to differential expression data analysis, a complete data set was obtained by the merging of MS measurements of four replicates, and normalization including an imputation step to replace absent with substituted values was applied (see 2 Material and Methods). Principal component analysis (PCA) was performed before and after normalization to assess variability of the data (Figure 3.12 A and B). After the normalization step, PCA showed that the sample variability could be explained by different pull-down conditions (Figure 3.12 B). To identify the proteins that bind *oskar* 3'UTR WT transcripts we analysed the protein set obtained from the WT\_359 RNA pull-down (Figure 3.12 C). Around one hundred proteins (see table 1, Appendix IX) were identified as enriched hits compared to the "no RNA" control. These include the known *oskar* binder Bruno (ARET) and a number of proteins (e.g. YPS, GLO, BSF, SQD, Hrp48) shown to be involved in *oskar* translational control, components of *Drosophila* P-bodies (Huynh et al., 2004; Kalifa et al., 2009; Mansfield et al., 2002; Ryu and Macdonald, 2015; Yano et al., 2004), or part of *oskar* RNPs (Nakamura et al., 2001; Snee and Macdonald, 2009; Wilhelm et al., 2000; Yano et al., 2004; Frank Wippich, personal communication). In addition, few potential novel *oskar* binders such as the hnRNP family members, TBPH and CG9890 were identified (Figure 3.12 C). As identified Bruno binding sites are included only in the WT\_359 *oskar* 3'UTR transcripts but not in the WT\_67 transcripts, we performed differential enrichment analysis to test selectivity of the long fragment for Bruno, as well as to gain insight into new candidates binding to one or another *oskar* 3'UTR region. The analysis confirmed Bruno as a significantly enriched hit in the WT\_359 compared to the WT\_67 pull-downs (Figure 3.12 D), and revealed a number of additional candidates as significantly enriched hits in the WT\_359 pulldowns (Figure 3.12 D, see table 2, Appendix X).

### 3 Results



---

**Figure 3.12 Differential enrichment MS data analysis of RNA affinity pull-downs:** **A** PCA plot showing data variability of raw data set of MS runs. **B** PCA plot showing data variability of data set of MS runs after batch effect removal, data normalization and imputation step. **C** Volcano plot showing logFC values ( $\log_2(\text{fold change})$ ) and  $\text{fdr.limma}$  p-values ( $\log_{10}(\text{fdr.limma})$ ) of differential enrichment analysis of WT\_359 vs. “no RNA control” data set. Putative novel *oskar* mRNA binders TBPH and CG9890 and known *oskar* RBP, Bruno (ARET) are highlighted with red ellipses. **D** Volcano plot showing logFC values ( $\log_2(\text{fold change})$ ) and  $\text{fdr.limma}$  p-values ( $\log_{10}(\text{fdr.limma})$ ) of differential enrichment analysis of WT\_359 vs. WT\_67 data set with “no RNA control” subtracted. The known *oskar* RBP, Bruno (ARET) is highlighted with red ellipse. Proteins were considered enriched hits with a false discovery rate (fdr) smaller 5 % and a fold-change cut-off of 100 % and considered enriched candidates with an fdr smaller 20 % and a fold-change cut-off of 50 %. Proteins were considered as enriched no hits if they were enriched in one of the conditions but did not satisfy parameters of statistical significance.

---

To address the question whether the mutation in the DD loop of *oskar* 3'UTR could have a global effect on recruitment of proteins to *oskar* mRNA, WT\_359 and UU\_359 pull-downs were compared. Differential enrichment analysis revealed in total ~100 enriched proteins (see table 3, Appendix XI). After applying statistical analysis (see 2 Materials and Methods) only one protein candidate, CG9890 was identified as a significantly enriched hit in the WT\_359 compared to UU\_359 data set ( $p(\text{fdr})\text{-value} \leq 0.05$ ,  $\log_{2}(\text{FC}) \geq 2$ ) (Figure 3.13). CG9890 was identified in this study as a potential novel *oskar* binder (Figure 3.12 C). Interestingly Bruno was enriched in the WT\_359 compared to UU\_359 pull-downs. However, it did not satisfy parameters of statistical significance and therefore could not be validated as an enriched hit. Importantly, the observation in the MS analysis correlates with the previous observation obtained with immunoblotting, whereby Bruno was less enriched in UU\_359 compared to WT\_359 pull-downs (Figure 3.11 C). Similar to Bruno, a number of interesting protein candidates (not identified as hits after differential enrichment analysis) such as a new potential *oskar* binder TBPH, the known translational regulators Hrp48 (also referred as HRB27C), GLO, YPS, and the *oskar* mRNA transport machinery component BICD, showed decreased enrichment in the UU\_359 compared to WT\_359 pull-downs (Figure 3.13, see table 3, Appendix XI). A number of these protein candidates such as Hrp48, Bruno, Yps were shown to be part of *Drosophila* P-bodies and involved in the transport of *oskar* mRNPs (e.g. BICD). Taken together, these findings suggest that inefficient binding of protein interactors to the 3'UTR of *oskar* mRNA with a mutation in the DD loop might explain the effect of the mutation on P-body assembly and growth.



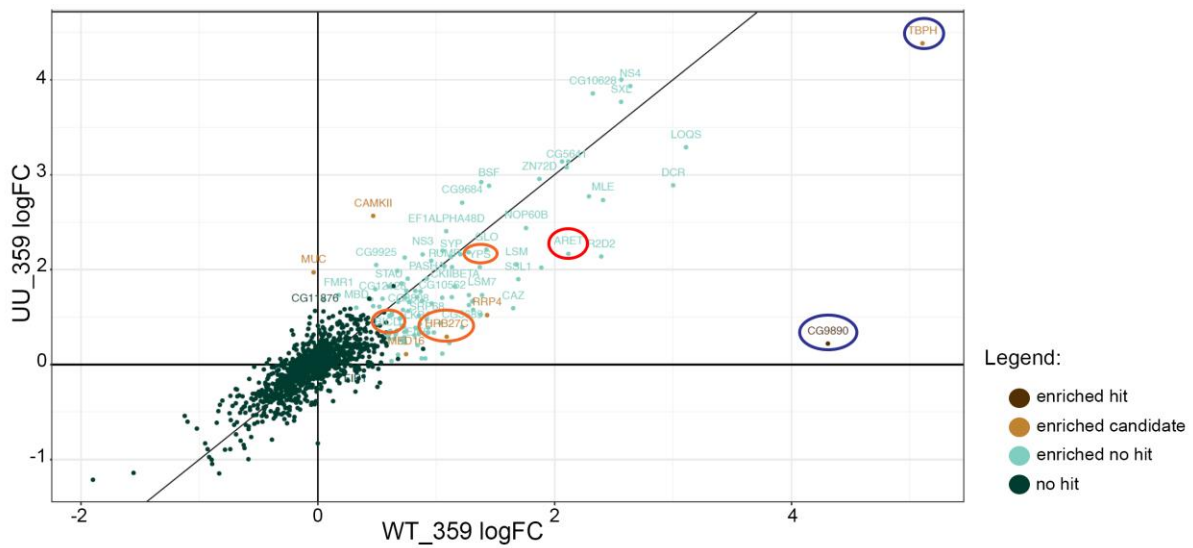


**Figure 3.13 Differential enrichment MS data analysis of UU\_359 vs WT\_359 pull-down:** Correlation of  $\log_2(\text{fold change})$  ( $\log\text{FC}$ ) of UU\_359 protein set and WT\_359 protein set with “no RNA” control subtracted. Putative novel *oskar* mRNA binders TBPH and CG9890 are highlighted with blue ellipses. The known *oskar* mRNA binder, Bruno (ARET) is highlighted with red ellipse. Number of components found to be part of *oskar* mRNPs (YPS, BICD, Hrp48 (HRB27C)) are highlighted with orange ellipses. Proteins were considered enriched hits with a false discovery rate (fdr) smaller 5 % and a fold-change cut-off of 100 % and considered enriched candidates with an fdr smaller 20 % and a fold-change cut-off of 50 %. Proteins were considered as enriched no hits if they were enriched in one of the conditions but did not satisfy parameters of statistical significance.



## 4 Discussion

### 4.1 *oskar* mRNA is a component of P-bodies in the *Drosophila* germline

P-bodies are formed in response to stress in many organisms, starting from yeast to mammals (reviewed in Standart and Weil, 2018). In *Drosophila*, upon nutrient deprivation, P-bodies are assembled in the female germline. Recent studies revealed the transcriptome of mammalian P-bodies and SG with long mRNAs mainly enriched in each of these RNP granules (Hubstenberger et al., 2017; Khong et al., 2017). mRNAs enriched in mammalian P-bodies were described to be involved in RNA control, cell division and development (Hubstenberger et al., 2017). In contrast, not much is known about transcriptome of *Drosophila* P-bodies. Studies indicate that maternally deposited mRNAs such as *gurken*, *bicoid* and *oskar* localize to *Drosophila* P-bodies (Burn et al., 2015; Weil et al., 2012). However, in the study of Burn et al., MS2:GFP reporters were used as a proxy for each mRNA and it has been shown previously in yeast that MS2 loops promote relocalization from the cytosol to P-bodies (Heinrich et al., 2017), implying possible drawbacks of this system. Weil et al., showed that *gurken* and *bicoid* localize in P-bodies in dorsoanterior region of the oocyte (Weil et al., 2012). In this study I have shown that *oskar* mRNA is an integral component of *Drosophila* P-bodies. Upon nutrient deprivation the majority of *oskar* mRNAs relocalize into so-called reticulated P-bodies. I also observed that unlike *oskar*, other maternal determinants, *bicoid* and *gurken* do not localize in these granules but are rather observed in their vicinity. This observation is not supported by the study of Weil et al., (2012). However, the main difference comes from the fact that P-body formation in the present study was analysed upon nutritional stress compared, in contrast to the study of Weil et al., where flies were not conditioned. I also showed that under nutrient-rich conditions all three mRNAs, *oskar*, *bicoid* and *gurken*, are found in the dispersed, microscopic precursors of reticulated stress induced P-bodies. This suggests that *oskar* or *bicoid* and *gurken* may form independent RNP particles which could undergo different fates under stress conditions, with *oskar* predominantly localizing into macroscopic P-bodies. In this work I showed that another maternally deposited mRNA, *patronin*, localizes into nutrient stress induced P-bodies, implying that this phenomenon is not unique to *oskar*. To summarise, I showed that two maternally deposited mRNAs localize to P-bodies upon nutrient deprivation during *Drosophila* oogenesis. Thus, this study can be a stepping stone for the future studies of *Drosophila* P-bodies such as characterization of P-body composition and function.

## 4.2 *oskar* mRNA drives P-body assembly in the *Drosophila* germline

Main building blocks of P-bodies are mRNA molecules and proteins. In order to be formed P-bodies require pools of non-translating mRNAs (Liu et al., 2005; Pillai et al., 2005; Sheth and Parker, 2003; Teixeira et al., 2005). After being exported to the cytoplasm, exogenous RNAs can also trigger the formation of P-body related RNP granules such as SGs (Mahadevan et al., 2013). These and many other findings (reviewed in Van Treeck and Parker, 2018; Garcia-Jove Navarro *et al.*, 2019) imply the possible role of RNA molecules in RNP granule formation. In the present work, I have shown that introducing a mutation in the loop of the *oskar* 3'UTR dimerization domain (DD) impairs P-body formation. This impairment seems not to be sequence specific, since introducing different nucleotide substitutions in different parts of the DD loop (CC to TT or GG to AA, see Appendix I) leads to a similar effect. It was previously reported that *oskar* mRNAs dimerize *in vitro* and that introducing the same mutations in the DD loop abolished this process (Jambor et al., 2011). Thus, it could be hypothesized that disrupting the dimerization might be the cause of P-body formation impairment. mRNA dimerization in eukaryotic systems is not often studied and not a fully understood process. To date, mRNA dimerization has been shown to occur in the *Drosophila* germline between two *bicoid* mRNAs (Ferrandon et al., 1997) or two *oskar* mRNAs (Jambor et al., 2011). *bicoid* dimerization is mediated via double loop-loop and *oskar* dimerization is mediated via kissing-loop interactions with Watson-Crick base pairing between two interacting mRNA molecules (*bicoid* or *oskar*) (Ferrandon et al., 1997; Jambor et al., 2011). Kissing-loop mediated dimerization, such as that described for *oskar* mRNA (Jambor et al., 2011), has mostly been studied in viruses. As it has been shown for HIV-1, RNA dimerization is an important initial step for virion packaging (Dubois et al., 2018; Ferrer et al., 2016; Paillart et al., 1996b, 1996a). Dimerization of two *oskar* molecules could be a crucial step in initiating P-body formation in *Drosophila*. Since *oskar* molecules are transported in the form of dimers that oligomerize in higher order RNP particles once they reach the posterior pole of the oocyte (Glotzer et al., 1997; Little et al., 2015), dimeric *oskar* molecules could also be the nucleating centre for P-body assembly (Figure 4.1). It is possible that once the dimers are formed, kissing-loop mediated interaction between two *oskar* mRNAs might be reinforced by *oskar* interacting proteins. Important interactors could be for example Bruno, which has been shown to promote *oskar* RNP oligomerization (Chekulaeva et al., 2006) or Me31B, whose orthologue in *C. elegans* has been shown to be important for P-body assembly (Hubstenberger et al., 2013). In this work I showed that Bruno recruitment to non-dimerizing *oskar* transcripts was negatively affected by introducing two-nucleotide substitution in the 3'UTR of *oskar*. HIV-1 proteins, nucleocapsid (NC) and gag have been shown to be required to stabilize RNA dimerization (Chen et al., 2016; Feng et al., 1996; Fu et al., 2006; Laughrea et al., 2001; Muriaux et al., 1996). Similarly, Bruno might have a role in stabilizing *oskar* dimers and subsequently

promoting *oskar* RNP oligomerization and P-body formation (Figure 4.1). The inability to restore the dimerization process *in vivo* by co-expressing two complementary *oskar* mutant transgenes left open the question of the importance of *oskar* mRNA dimerization in P-body assembly. In addition, an *in vitro* dimerization assay showed a reduced dimerization efficiency of complementary mutant transcripts compared to WT transcripts, thus supporting the *in vivo* observation.

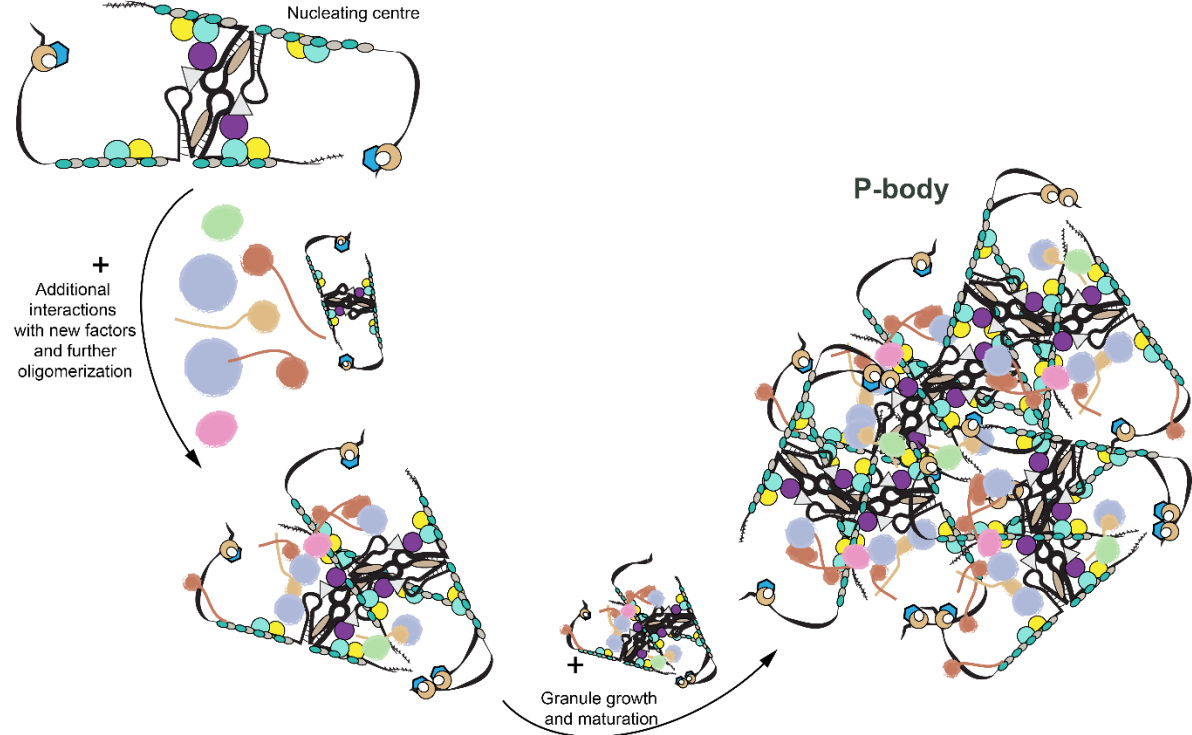
Besides hindering P-body formation, the *oskarUU* non-dimerizing mutants have been shown to be prematurely translated. Even though it is still not clear whether P-bodies are the cause or the consequence of translational inhibition, the observation that *oskarUU* mutants were prematurely translated led to the question of whether premature translation could be the cause of P-body formation impairment in the *Drosophila* germline. In this work I showed that, in an *in vivo* system in which no translation of *oskar* occurs, CDS free *oskar3'UTRUU* mutants also showed P-body formation impairment. In addition, when an *egfp-oskar3'UTRUU* reporter was ubiquitously translated in the germline, a similar phenotype was observed. These observations imply that P-body formation in the *Drosophila* germline can be uncoupled from the event of translational inhibition. Inhibition of translation *per se* might not be sufficient to promote P-body assembly and therefore intrinsic features within the 3'UTR of *oskar* might play an important role in formation of P-bodies. I also showed that on its own the 3'UTR of *oskar* is sufficient to drive P-body formation, and that replacing the *oskar* dimerization domain (DD) with another orthogonal stem-loop (in this study, the *K10* TLS) had no effect on P-body assembly. Importantly, interaction of the *K10* TLS or possibly any other stem-loop with similar features to the DD must be *in cis* with the distal fragment of *oskar* 3'UTR in order to support P-body formation, implying that the context of the intramolecular RNA interaction could be an important step in determining the fate of RNP granule assembly. These intramolecular interactions might be affected by the introduction of nucleotide substitutions in the *oskarUU* mutants. Altered intramolecular interactions within the *oskar* 3'UTR could be one of the causes of hindered P-body assembly. Altogether, P-body formation in *Drosophila* could be a multistep process, requiring dimerization between two *oskar* molecules, followed by stabilization *in trans* by interactions with *oskar* binders and/or P-body components (e.g. Bruno, Me31B, Hrp48, PTB). This step would be followed by an oligomerization step promoted by additional intermolecular interactions of *oskar* RNPs and possibly other *trans*-factors leading to formation and growth of mature P-body assemblies (Figure 4.1). Perturbing the system by introducing mutations in the 3'UTR of *oskar*, specifically in the DD loop, could lead to loss of dimerization. Subsequently, new intramolecular interactions could be formed, which could lead to inefficient recruitment of components necessary for triggering *oskar* RNP packaging and as a consequence hindering P-body assembly (Figure 4.1). The exact mechanism how

#### 4 Discussion

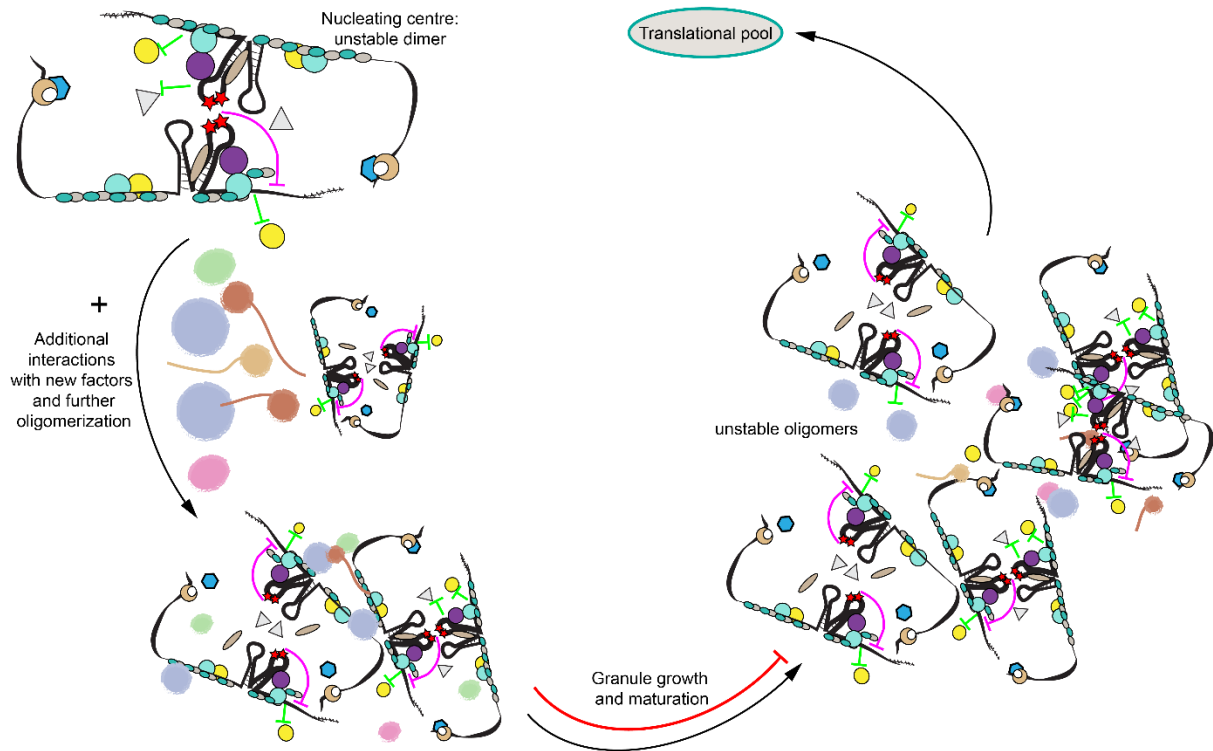
P-bodies are formed in *Drosophila* remains to be investigated in more detail, but it is clear that *oskar* mRNA plays an important role in this process.

## 4 Discussion

### Wild-type



### Mutant



---

**Figure 4.1 Hypothetical model of *oskar* mRNA dependent P-body formation upon nutrient deprivation in *Drosophila*:** When the wild-type flies are kept under nutrient-poor conditions, P-body formation is triggered. P-body assembly could start from microscopic mRNP precursors with *oskar* dimers playing a role as a scaffold and nucleating centre for P-body biogenesis, followed by the step of oligomerization. The oligomerization step would include establishing new RNA-RNA, RNA-protein and protein-protein *in cis* and/or *in trans* interactions which could additionally stabilize *oskar* dimers and further promote growth of RNP oligomers into mature P-body. When the system is perturbed by introducing a mutation (e.g. two nucleotide substitutions) in the 3'UTR of *oskar*, the process of P-body assembly could be affected. Introduced mutation could lead to forming of new intramolecular interactions within the 3'UTR of *oskar* mRNA and therefore affecting recruitment of a number of *trans* factors (e.g. Bruno). New intramolecular interactions could be a cause of *oskar* dimers' instability, which could lead to an inefficient oligomerization step. Thus, P-body growth and maturation could be impaired. In addition, a population of *oskar* mRNPs that would escape packaging into P-bodies, would reenter rounds of translation.

---



### 4.3 P-bodies: a protective harbors of maternal mRNAs

Due to the identification of 5'-3' RNA decay machinery in P-bodies, P-bodies were thought to be predominantly involved in mRNA turnover (Sheth and Parker, 2003). Subsequent studies identified several translational regulators (e.g. CPEB1 and 4E-T) to be a part of P-bodies and it has been shown that P-body mRNAs can reenter translation, suggesting P-bodies to be a potential storage of silenced mRNAs (Aizer et al., 2014; Bhattacharyya et al., 2006; Ferraiuolo et al., 2005; Wilczynska et al., 2005). New studies of mammalian P-bodies, and monitoring mRNA decay events in live cells revealed that there is no accumulation of decay machinery components in P-bodies (Hubstenberger et al., 2017; Standart and Weil, 2018), supporting their function in storing mRNA molecules. Similar RNP granules are also found in other organisms such as *C. elegans* and *Drosophila*. In eukaryotes, P-bodies share a number of common components, such as a putative DEAD box helicase, DDX6, and translational regulators from CPEB and Y-box protein family (A. Schisa, 2012). Since most of the studies regarding P-bodies were performed in cell lines or yeast, not much is known about their biological function in multicellular organisms. In *C. elegans* and *Drosophila*, P-bodies were identified in the germline (Jud et al., 2008; Wilsch-Bräuninger et al., 1997). P-bodies in *C. elegans* contribute to oogenesis and protect specific maternal mRNAs (Boag et al., 2008). Similarly, in *Drosophila* it could be assumed that these RNP granules store maternal mRNAs and other components necessary for oocyte development during stress conditions. In this study I showed that the key germline determinant *oskar* did not undergo degradation after applying stress conditions (nutrient deprivation). Also when stress conditions were overcome, P-bodies disassemble (Shimada et al., 2011; Snee and Macdonald, 2009). This suggests that, in *Drosophila*, P-bodies might have a role in protecting maternal mRNAs during oogenesis. However, the function of these RNP granules needs to be explored in more detail. It would be valuable to the field to identify the transcriptome of *Drosophila* P-bodies especially during different steps of P-body assembly. This could provide a new information about the biological function of P-bodies.

#### 4.4 RNA as a scaffold in RNP granule formation

Eukaryotic cells contain many non-membranous organelles described as RNA-protein granules. Many studies nowadays stress the importance of RNA molecules in forming these cytoplasmic compartments. Both intra- and intermolecular RNA interactions could be important for RNP granule formation (Van Treeck and Parker, 2018) and also other cellular processes such as regulation of the p53 pathway (Uroda et al., 2019). Dimerization of *bicoid* or *oskar* mRNAs was shown to be required for their recruitment into RNP particles during *Drosophila* oogenesis (Ferrandon et al., 1997; Jambor et al., 2011). In this study I observed that in *oskarUU* non-dimerizing mutants, P-body formation is impaired, thus indicating a possible importance of kissing-loop mediated dimerization of two *oskar* molecules in P-body assembly. Interestingly, a recent study showed that intramolecular kissing-loop *cis* interactions between the two motifs of the lncRNA, MEG3 are required for MEG3-dependent p53 stimulation in human cells (Uroda et al., 2019). These observations indicate that RNA molecules and their intrinsic features can have important functions in different cellular processes. Importantly, it is believed that RNA molecules are always accompanied by RNA binding proteins. Therefore, RNA molecules could provide a scaffold for both RNA and protein interactors in order to promote RNP granule biogenesis. Intra- and intermolecular RNA interactions could provide such an environment which would promote the binding of different proteins important for RNP granule assembly. It has been previously reported that changing the RNA environment (e.g. by changing the secondary structure of mRNAs) affects RNAs' recruitment into specific RNP granules, possibly by changing the accessibility of binding sites for proteins necessary for the recruitment (Langdon et al., 2018). To summarize, it can be assumed that RNAs can be a platform for RNA-RNA and RNA-protein interactions which drive RNP granule assembly. Once specific RNA features are perturbed, all downstream processes, including both *cis* and *trans* interactions, could be affected and as a consequence, RNP granule formation could be impaired. Here I showed that introducing only two nucleotide substitutions in the 3'UTR of *oskar* mRNA was sufficient to perturb the system and impair P-body formation in the *Drosophila* germline.

## 4.5 Importance of RNP granule formation in response to stress

RNP granule assembly and remodelling can be triggered in response to aging, meiotic arrest or different environmental stresses (Bhattacharyya et al., 2006; Jud et al., 2007; Noble et al., 2008; Shimada et al., 2011; Snee and Macdonald, 2009; Teixeira et al., 2005). Formation of RNP granules such as SG and P-bodies in response to stress is conserved among eukaryotes. In yeast and mammalian cells, SG and P-body formation can be promoted by, for example heat-shock, hypoxia, osmotic changes and amino-acid deprivation. What could be the advantage of forming RNP granules during stress conditions is not clearly understood. Nevertheless, in yeast, P-bodies seem to be important for viability (Lavut and Raveh, 2012) and survival of G0 cells (Ramachandran et al., 2011). During oogenesis (e.g. in *C. elegans* and *Drosophila*), RNP granule composition and remodelling is highly dependent on environmental changes. In *C. elegans*, large RNP granules form in response to meiotic arrest or heat shock (Jud et al., 2008) while in *Drosophila*, formation of large so-called reticulated P-bodies is promoted upon nutritional stress (Snee and Macdonald, 2009). RNP granule formation in response to stress occurs in a very short time period, implying the importance of this process under non-homeostatic conditions. In *C. elegans*, large RNP granules assemble in the oocyte within 2h after heat shock and in *Drosophila*, the same time is needed for the formation of P-bodies upon nutritional stress (Jud et al., 2008; Snee and Macdonald, 2009). This process is reversible and the moment the stress is overcome, RNP granules return to their so called dispersed state (Shimada et al., 2011; Snee and Macdonald, 2009). The reason for RNP granule remodelling due to environmental changes during oogenesis remains not well explored. One of the reasons could be to protect maternal mRNAs during stress conditions. For example, component of P-bodies in *C. elegans* has been shown to protect specific mRNAs during oogenesis (Boag et al., 2008). On the other hand, in *Drosophila* during nutrient deprivation, females halt egg production to increase the chances of the progeny developing when stress is overcome. This could be achieved by slowing down development of previtellogenic and young vitellogenic egg-chambers (Drummond-Barbosa and Spradling, 2001; Shimada et al., 2011). During this time P-body formation is also observed. P-body formation could be one of the mechanisms to sequester and protect a subset of maternal mRNAs and other components which would be important for further development when environmental conditions allow it. In summary, RNP granule formation in cells could be a mechanism to compartmentalize and locally limit different cellular processes (e.g. rRNAs synthesis and processing in the nucleolus). Furthermore, formation of specific RNP granules in the germline of different organisms when they are exposed to stress could be a way to halt development and increase chances for survival of the future embryos.



## Bibliography

3-900051-07-0, I. R Development Core Team (2008). R: A language and environment Computing, statistical computing. R Foundation for Statistical Vienna, Austria. URL <http://www.R-project.org>.

A. Schisa, J. (2012). Chapter seven - New Insights into the Regulation of RNP Granule Assembly in Oocytes. K.W.B.T.-I.R. of C. and M.B. Jeon, ed. (Academic Press), pp. 233–289.

Ables, E.T., Hwang, G.H., Finger, D.S., Hinnant, T.D., and Drummond-Barbosa, D. (2016). A Genetic Mosaic Screen Reveals Ecdysone-Responsive Genes Regulating <em>Drosophila</em> Oogenesis. *G3 Genes | Genomes | Genetics* 6, 2629 LP – 2642.

Aizer, A., Kalo, A., Kafri, P., Shraga, A., Ben-Yishay, R., Jacob, A., Kinor, N., and Shav-Tal, Y. (2014). Quantifying mRNA targeting to P-bodies in living human cells reveals their dual role in mRNA decay and storage. *J. Cell Sci.* 127, 4443 LP – 4456.

Anderson, P., and Kedersha, N. (2006). RNA granules. *J. Cell Biol.* 172, 803–808.

Anderson, D.M., Anderson, K.M., Chang, C.-L., Makarewich, C.A., Nelson, B.R., McAnally, J.R., Kasaragod, P., Shelton, J.M., Liou, J., Bassel-Duby, R., et al. (2015). A micropeptide encoded by a putative long noncoding RNA regulates muscle performance. *Cell* 160, 595–606.

Andrei, M.A., Ingelfinger, D., Heintzmann, R., Achsel, T., Rivera-Pomar, R., and Lührmann, R. (2005). A role for eIF4E and eIF4E-transporter in targeting mRNPs to mammalian processing bodies. *RNA* 11, 717–727.

Ashe, M.P., De Long, S.K., and Sachs, A.B. (2000). Glucose depletion rapidly inhibits translation initiation in yeast. *Mol. Biol. Cell* 11, 833–848.

Ayache, J., Bénard, M., Ernoult-Lange, M., Minshall, N., Standart, N., Kress, M., and Weil, D. (2015). P-body assembly requires DDX6 repression complexes rather than decay or Ataxin2/2L complexes. *Mol. Biol. Cell* 26, 2579–2595.

Babu, K., Cai, Y., Bahri, S., Yang, X., and Chia, W. (2004). Roles of Bifocal, Homer, and F-actin in anchoring Oskar to the posterior cortex of *Drosophila* oocytes. *Genes Dev.* 18, 138–143.

Becalska, A.N., and Gavis, E.R. (2009). Lighting up mRNA localization in *Drosophila* oogenesis. *Development* 136, 2493–2503.

Berleth, T., Burri, M., Thoma, G., Bopp, D., Richstein, S., Frigerio, G., Noll, M., and Nüsslein-Volhard, C. (1988). The role of localization of bicoid RNA in organizing the anterior pattern of the *Drosophila* embryo. *EMBO J.* 7, 1749–1756.

Besse, F., and Ephrussi, A. (2008). Translational control of localized mRNAs: restricting protein synthesis in space and time. *Nat. Rev. Mol. Cell Biol.* 9, 971.

Besse, F., López de Quinto, S., Marchand, V., Trucco, A., and Ephrussi, A. (2009). *Drosophila* PTB promotes formation of high-order RNP particles and represses oskar translation. *Genes Dev.* *23*, 195–207.

Bhattacharyya, S.N., Habermacher, R., Martine, U., Closs, E.I., and Filipowicz, W. (2006). Relief of microRNA-Mediated Translational Repression in Human Cells Subjected to Stress. *Cell* *125*, 1111–1124.

Boag, P.R., Atalay, A., Robida, S., Reinke, V., and Blackwell, T.K. (2008). Protection of specific maternal messenger RNAs by the P body protein CGH-1 (Dhh1/RCK) during *Caenorhabditis elegans* oogenesis. *J. Cell Biol.* *182*, 543 LP – 557.

Brendza, R.P., Serbus, L.R., Duffy, J.B., and Saxton, W.M. (2000). A function for kinesin I in the posterior transport of oskar mRNA and Stauf protein. *Science* *289*, 2120–2122.

Bregues, M., Teixeira, D., and Parker, R. (2005). Movement of Eukaryotic mRNAs Between Polysomes and Cytoplasmic Processing Bodies. *Science* (80-. ). *310*, 486 LP – 489.

Brown E.H., K.R.. (1964). Studies on the events resulting in the formation of an egg chamber in *Drosophila melanogaster*. *Growth* 41–81.

Broyer, R.M., Monfort, E., and Wilhelm, J.E. (2017). Cup regulates oskar mRNA stability during oogenesis. *Dev. Biol.* *421*, 77–85.

Buchan, J.R., and Parker, R. (2009). Eukaryotic stress granules: the ins and outs of translation. *Mol. Cell* *36*, 932–941.

Buchan, J.R., Kolaitis, R.-M., Taylor, J.P., and Parker, R. (2013). Eukaryotic stress granules are cleared by autophagy and Cdc48/VCP function. *Cell* *153*, 1461–1474.

Buchberger, A., Bukau, B., and Sommer, T. (2010). Protein Quality Control in the Cytosol and the Endoplasmic Reticulum: Brothers in Arms. *Mol. Cell* *40*, 238–252.

Bullock, S.L., and Ish-Horowicz, D. (2001). Conserved signals and machinery for RNA transport in *Drosophila* oogenesis and embryogenesis. *Nature* *414*, 611–616.

Burn, K.M., Shimada, Y., Ayers, K., Vemuganti, S., Lu, F., Hudson, A.M., and Cooley, L. (2015). Somatic insulin signaling regulates a germline starvation response in *Drosophila* egg chambers. *Dev. Biol.* *398*, 206–217.

Busson, D., and Pret, A.-M. (2007). GAL4/UAS Targeted Gene Expression for Studying *Drosophila* Hedgehog Signaling BT - Hedgehog Signaling Protocols. J.I. Horabin, ed. (Totowa, NJ: Humana Press), pp. 161–201.

Chang, J.S., Tan, L., and Schedl, P. (1999). The *Drosophila* CPEB Homolog, Orb, Is Required for Oskar Protein Expression in Oocytes. *Dev. Biol.* *215*, 91–106.

Chekulaeva, M., Hentze, M.W., and Ephrussi, A. (2006). Bruno Acts as a Dual Repressor of oskar

Translation, Promoting mRNA Oligomerization and Formation of Silencing Particles. *Cell* 124, 521–533.

Chen, F., Evans, A., Pham, J., and Plosky, B. (2010). Cellular Stress Responses: A Balancing Act. *Mol. Cell* 40, 175.

Chen, J., Rahman, S.A., Nikolaitchik, O.A., Grunwald, D., Sardo, L., Burdick, R.C., Plisov, S., Liang, E., Tai, S., Pathak, V.K., et al. (2016). HIV-1 RNA genome dimerizes on the plasma membrane in the presence of Gag protein. *Proc. Natl. Acad. Sci.* 113, E201 LP-E208.

Ciccia, A., and Elledge, S.J. (2010). The DNA Damage Response: Making It Safe to Play with Knives. *Mol. Cell* 40, 179–204.

Clemson, C.M., Hutchinson, J.N., Sara, S.A., Ensminger, A.W., Fox, A.H., Chess, A., and Lawrence, J.B. (2009). An architectural role for a nuclear noncoding RNA: NEAT1 RNA is essential for the structure of paraspeckles. *Mol. Cell* 33, 717–726.

Cougot, N., Babajko, S., and Séraphin, B. (2004). Cytoplasmic foci are sites of mRNA decay in human cells. *J. Cell Biol.* 165, 31–40.

Dahlgard, K., Raposo, A.A.S.F., Niccoli, T., and St Johnston, D. (2007). Capu and Spire assemble a cytoplasmic actin mesh that maintains microtubule organization in the *Drosophila* oocyte. *Dev. Cell* 13, 539–553.

Damgaard, C.K., and Lykke-Andersen, J. (2011). Translational coregulation of 5' TOP mRNAs by TIA-1 and TIAR. *Genes Dev.* 25, 2057–2068.

Decker, C.J., and Parker, R. (2012). P-bodies and stress granules: possible roles in the control of translation and mRNA degradation. *Cold Spring Harb. Perspect. Biol.* 4, a012286–a012286.

Decker, C.J., Teixeira, D., and Parker, R. (2007). Edc3p and a glutamine/asparagine-rich domain of Lsm4p function in processing body assembly in *Saccharomyces cerevisiae*; *J. Cell Biol.* 179, 437 LP – 449.

Dienstbier, M., Boehl, F., Li, X., and Bullock, S.L. (2009). Egalitarian is a selective RNA-binding protein linking mRNA localization signals to the dynein motor. *Genes Dev.* 23, 1546–1558.

Dix, C.I., Soundararajan, H.C., Dzhindzhev, N.S., Begum, F., Suter, B., Ohkura, H., Stephens, E., and Bullock, S.L. (2013). Lissencephaly-1 promotes the recruitment of dynein and dynactin to transported mRNAs. *J. Cell Biol.* 202, 479 LP – 494.

Doi, M., Shimatani, H., Atobe, Y., Murai, I., Hayashi, H., Takahashi, Y., Fustin, J.-M., Yamaguchi, Y., Kiyonari, H., Koike, N., et al. (2019). Non-coding cis-element of *Period2* is essential for maintaining organismal circadian behaviour and body temperature rhythmicity. *Nat. Commun.* 10, 2563.

Drummond-Barbosa, D., and Spradling, A.C. (2001). Stem Cells and Their Progeny Respond to Nutritional Changes during *Drosophila* Oogenesis. *Dev. Biol.* 231, 265–278.

Dubois, N., Marquet, R., Paillart, J.-C., and Bernacchi, S. (2018). Retroviral RNA Dimerization:

From Structure to Functions . Front. Microbiol. 9, 527.

Ephrussi, A., and Lehmann, R. (1992). Induction of germ cell formation by oskar. *Nature* 358, 387–392.

Ephrussi, A., Dickinson, L.K., and Lehmann, R. (1991). oskar organizes the germ plasm and directs localization of the posterior determinant nanos. *Cell* 66, 37–50.

Eulalio, A., Behm-Ansmant, I., Schweizer, D., and Izaurralde, E. (2007a). P-body formation is a consequence, not the cause, of RNA-mediated gene silencing. *Mol. Cell Biol.* 27, 3970–3981.

Eulalio, A., Behm-Ansmant, I., and Izaurralde, E. (2007b). P bodies: at the crossroads of post-transcriptional pathways. *Nat. Rev. Mol. Cell Biol.* 8, 9.

Fan, S.-J., Marchand, V., and Ephrussi, A. (2011). Drosophila Ge-1 promotes P body formation and oskar mRNA localization. *PLoS One* 6, e20612–e20612.

Feng, Y.X., Copeland, T.D., Henderson, L.E., Gorelick, R.J., Bosche, W.J., Levin, J.G., and Rein, A. (1996). HIV-1 nucleocapsid protein induces “maturation” of dimeric retroviral RNA in vitro. *Proc. Natl. Acad. Sci.* 93, 7577 LP – 7581.

Ferraiuolo, M.A., Basak, S., Dostie, J., Murray, E.L., Schoenberg, D.R., and Sonenberg, N. (2005). A role for the eIF4E-binding protein 4E-T in P-body formation and mRNA decay. *J. Cell Biol.* 170, 913 LP – 924.

Ferrandon, D., Koch, I., Westhof, E., and Nüsslein-Volhard, C. (1997). RNA-RNA interaction is required for the formation of specific bicoid mRNA 3' UTR-STAUFIN ribonucleoprotein particles. *EMBO J.* 16, 1751–1758.

Ferrer, M., Clerté, C., Chamontin, C., Basyuk, E., Lainé, S., Hottin, J., Bertrand, E., Margeat, E., and Mougel, M. (2016). Imaging HIV-1 RNA dimerization in cells by multicolor super-resolution and fluctuation microscopies. *Nucleic Acids Res.* 44, 7922–7934.

Fox, A.H., Lam, Y.W., Leung, A.K.L., Lyon, C.E., Andersen, J., Mann, M., and Lamond, A.I. (2002). Paraspeckles: A Novel Nuclear Domain. *Curr. Biol.* 12, 13–25.

Frankel, L.B., Lubas, M., and Lund, A.H. (2017). Emerging connections between RNA and autophagy. *Autophagy* 13, 3–23.

Franken, H., Mathieson, T., Childs, D., Sweetman, G.M.A., Werner, T., Tögel, I., Doce, C., Gade, S., Bantscheff, M., Drewes, G., et al. (2015). Thermal proteome profiling for unbiased identification of direct and indirect drug targets using multiplexed quantitative mass spectrometry. *Nat. Protoc.* 10, 1567.

Fu, W., Dang, Q., Nagashima, K., Freed, E.O., Pathak, V.K., and Hu, W.-S. (2006). Effects of Gag mutation and processing on retroviral dimeric RNA maturation. *J. Virol.* 80, 1242–1249.

Gall, J.G. (2000). Cajal Bodies: The First 100 Years. *Annu. Rev. Cell Dev. Biol.* 16, 273–300.



Galluzzi, L., Yamazaki, T., and Kroemer, G. (2018a). Linking cellular stress responses to systemic homeostasis. *Nat. Rev. Mol. Cell Biol.* *19*, 731–745.

Galluzzi, L., Vitale, I., Aaronson, S.A., Abrams, J.M., Adam, D., Agostinis, P., Alnemri, E.S., Altucci, L., Amelio, I., Andrews, D.W., et al. (2018b). Molecular mechanisms of cell death: recommendations of the Nomenclature Committee on Cell Death 2018. *Cell Death Differ.* *25*, 486–541.

Garcia-Jove Navarro, M., Kashida, S., Chouaib, R., Souquere, S., Pierron, G., Weil, D., and Gueroui, Z. (2019). RNA is a critical element for the sizing and the composition of phase-separated RNA–protein condensates. *Nat. Commun.* *10*, 3230.

Gaspar, I., and Ephrussi, A. (2017). Ex vivo Ooplasmic Extract from Developing *Drosophila* Oocytes for Quantitative TIRF Microscopy Analysis. *Bio-Protocol* *7*, e2380.

Gaspar, I., Yu, Y. V, Cotton, S.L., Kim, D.-H., Ephrussi, A., and Welte, M.A. (2014). Klar ensures thermal robustness of *oskar* localization by restraining RNP motility. *J. Cell Biol.* *206*, 199 LP – 215.

Gaspar, I., Wippich, F., and Ephrussi, A. (2017). Enzymatic production of single-molecule FISH and RNA capture probes. *RNA* *23*, 1582–1591.

Gaspar, I., Hövelmann, F., Chamiolo, J., Ephrussi, A., and Seitz, O. (2018). Quantitative mRNA Imaging with Dual Channel qFIT Probes to Monitor Distribution and Degree of Hybridization. *ACS Chem. Biol.* *13*, 742–749.

Gáspár, I., Sysoev, V., Komissarov, A., and Ephrussi, A. (2017). An RNA-binding atypical tropomyosin recruits kinesin-1 dynamically to *oskar* mRNPs. *EMBO J.* *36*, 319–333.

Gebauer, F., and Hentze, M.W. (2004). Molecular mechanisms of translational control. *Nat. Rev. Mol. Cell Biol.* *5*, 827–835.

Gebauer, F., Preiss, T., and Hentze, M.W. (2012). From cis-regulatory elements to complex RNPs and back. *Cold Spring Harb. Perspect. Biol.* *4*, a012245–a012245.

Ghosh, S., Marchand, V., Gáspár, I., and Ephrussi, A. (2012). Control of RNP motility and localization by a splicing-dependent structure in *oskar* mRNA. *Nat. Struct. & Mol. Biol.* *19*, 441.

Gilks, N., Kedersha, N., Ayodele, M., Shen, L., Stoecklin, G., Dember, L.M., and Anderson, P. (2004). Stress Granule Assembly Is Mediated by Prion-like Aggregation of TIA-1. *Mol. Biol. Cell* *15*, 5383–5398.

Glotzer, J.B., Saffrich, R., Glotzer, M., and Ephrussi, A. (1997). Cytoplasmic flows localize injected *oskar* RNA in *Drosophila* oocytes. *Curr. Biol.* *7*, 326–337.

Götze, M., Dufourt, J., Ihling, C., Rammelt, C., Pierson, S., Sambrani, N., Temme, C., Sinz, A., Simonelig, M., and Wahle, E. (2017). Translational repression of the *Drosophila nanos* mRNA involves the RNA helicase Belle and RNA coating by Me31B and Trailer hitch. *RNA* *23*, 1552–1568.

- Gstir, R. (2012). A non-coding function of oskar mRNA in oogenesis of *Drosophila melanogaster*.
- Hachet, O., and Ephrussi, A. (2004). Splicing of oskar RNA in the nucleus is coupled to its cytoplasmic localization. *Nature* 428, 959–963.
- Hebert, M.D., and Matera, A.G. (2000). Self-association of Coilin Reveals a Common Theme in Nuclear Body Localization. *Mol. Biol. Cell* 11, 4159–4171.
- Heinrich, S., Sidler, C.L., Azzalin, C.M., and Weis, K. (2017). Stem-loop RNA labeling can affect nuclear and cytoplasmic mRNA processing. *RNA* 23, 134–141.
- Hentze, M.W., Castello, A., Schwarzl, T., and Preiss, T. (2018). A brave new world of RNA-binding proteins. *Nat. Rev. Mol. Cell Biol.* 19, 327.
- Hershey, J.W.B., Sonenberg, N., and Mathews, M.B. (2012). Principles of translational control: an overview. *Cold Spring Harb. Perspect. Biol.* 4, a011528.
- Hetz, C., and Papa, F.R. (2018). The Unfolded Protein Response and Cell Fate Control. *Mol. Cell* 69, 169–181.
- Hinnebusch, A.G., and Lorsch, J.R. (2012). The mechanism of eukaryotic translation initiation: new insights and challenges. *Cold Spring Harb. Perspect. Biol.* 4, a011544.
- Huang, P., Sahai-Hernandez, P., Bohm, R.A., Welch, W.P., Zhang, B., and Nystul, T. (2014). Enhancer-Trap Flippase Lines for Clonal Analysis in the *Drosophila* Ovary. *G3 Genes|Genomes|Genetics* 4, 1693 LP – 1699.
- Hubé, F., and Francastel, C. (2018). Coding and Non-coding RNAs, the Frontier Has Never Been So Blurred. *Front. Genet.* 9, 140.
- Huber, W., von Heydebreck, A., Sültmann, H., Poustka, A., and Vingron, M. (2002). Variance stabilization applied to microarray data calibration and to the quantification of differential expression. *Bioinformatics* 18, S96–S104.
- Hubstenberger, A., Noble, S.L., Cameron, C., and Evans, T.C. (2013). Translation repressors, an RNA helicase, and developmental cues control RNP phase transitions during early development. *Dev. Cell* 27, 161–173.
- Hubstenberger, A., Courel, M., Bénard, M., Souquere, S., Ernoult-Lange, M., Chouaib, R., Yi, Z., Morlot, J.-B., Munier, A., Fradet, M., et al. (2017). P-Body Purification Reveals the Condensation of Repressed mRNA Regulons. *Mol. Cell* 68, 144-157.e5.
- Hughes, S.C., and Simmonds, A.J. (2019). *Drosophila* mRNA Localization During Later Development: Past, Present, and Future . *Front. Genet.* 10, 135.
- Hughes, C.S., Foehr, S., Garfield, D.A., Furlong, E.E., Steinmetz, L.M., and Krijgsveld, J. (2014). Ultrasensitive proteome analysis using paramagnetic bead technology. *Mol. Syst. Biol.* 10, 757.
- Huynh, J.-R., Munro, T.P., Smith-Litière, K., Lepesant, J.-A., and Johnston, D.S. (2004). The

Drosophila hnRNPA/B Homolog, Hrp48, Is Specifically Required for a Distinct Step in *osk* mRNA Localization. *Dev. Cell* 6, 625–635.

Jain, S., Wheeler, J.R., Walters, R.W., Agrawal, A., Barsic, A., and Parker, R. (2016). ATPase-Modulated Stress Granules Contain a Diverse Proteome and Substructure. *Cell* 164, 487–498.

Jakymiw, A., Lian, S., Eystathiou, T., Li, S., Satoh, M., Hamel, J.C., Fritzler, M.J., and Chan, E.K.L. (2005). Disruption of GW bodies impairs mammalian RNA interference. *Nat. Cell Biol.* 7, 1267–1274.

Jambor, H. (2008). Characterization of *oskar* 3'UTR RNA domains involved in early RNA localization and translational repression. Heidelberg University.

Jambor, H., Brunel, C., and Ephrussi, A. (2011). Dimerization of *oskar* 3' UTRs promotes hitchhiking for RNA localization in the *Drosophila* oocyte. *RNA* 17, 2049–2057.

Jambor, H., Mueller, S., Bullock, S.L., and Ephrussi, A. (2014). A stem-loop structure directs *oskar* mRNA to microtubule minus ends. *RNA* 20, 429–439.

Jenny, A., Hachet, O., Závorszky, P., Cyrklaff, A., Weston, M.D.J., Johnston, D.S., Erdélyi, M., and Ephrussi, A. (2006). A translation-independent role of *oskar* RNA in early *Drosophila* oogenesis. *Development* 133, 2827 LP – 2833.

Jud, M., Razelun, J., Bickel, J., Czerwinski, M., and Schisa, J.A. (2007). Conservation of large foci formation in arrested oocytes of *Caenorhabditis* nematodes. *Dev. Genes Evol.* 217, 221–226.

Jud, M.C., Czerwinski, M.J., Wood, M.P., Young, R.A., Gallo, C.M., Bickel, J.S., Petty, E.L., Mason, J.M., Little, B.A., Padilla, P.A., et al. (2008). Large P body-like RNPs form in *C. elegans* oocytes in response to arrested ovulation, heat shock, osmotic stress, and anoxia and are regulated by the major sperm protein pathway. *Dev. Biol.* 318, 38–51.

Kalifa, Y., Armenti, S.T., and Gavis, E.R. (2009). Glorund interactions in the regulation of *gurken* and *oskar* mRNAs. *Dev. Biol.* 326, 68–74.

Kamenska, A., Simpson, C., Vindry, C., Broomhead, H., Bénard, M., Ernoult-Lange, M., Lee, B.P., Harries, L.W., Weil, D., and Standart, N. (2016). The DDX6-4E-T interaction mediates translational repression and P-body assembly. *Nucleic Acids Res.* 44, 6318–6334.

Kanke, M., Jambor, H., Reich, J., Marches, B., Gstir, R., Ryu, Y.H., Ephrussi, A., and Macdonald, P.M. (2015). *oskar* RNA plays multiple noncoding roles to support oogenesis and maintain integrity of the germline/soma distinction. *RNA* 21, 1096–1109.

Karapetyan, A.R., Buiting, C., Kuiper, R.A., and Coolen, M.W. (2013). Regulatory Roles for Long ncRNA and mRNA. *Cancers (Basel)*. 5, 462–490.

Kato, Y., and Nakamura, A. (2012). Roles of cytoplasmic RNP granules in intracellular RNA localization and translational control in the *Drosophila* oocyte. *Dev. Growth Differ.* 54, 19–31.

Kedersha, N., Stoecklin, G., Ayodele, M., Yacono, P., Lykke-Andersen, J., Fritzler, M.J., Scheuner,

D., Kaufman, R.J., Golan, D.E., and Anderson, P. (2005). Stress granules and processing bodies are dynamically linked sites of mRNP remodeling. *J. Cell Biol.* *169*, 871 LP – 884.

Kedersha, N., Panas, M.D., Achorn, C.A., Lyons, S., Tisdale, S., Hickman, T., Thomas, M., Lieberman, J., McInerney, G.M., Ivanov, P., et al. (2016). G3BP–Caprin1–USP10 complexes mediate stress granule condensation and associate with 40S subunits. *J. Cell Biol.* *212*, 845 LP – 860.

Kedersha, N.L., Gupta, M., Li, W., Miller, I., and Anderson, P. (1999). RNA-binding proteins TIA-1 and TIAR link the phosphorylation of eIF-2 alpha to the assembly of mammalian stress granules. *J. Cell Biol.* *147*, 1431–1442.

Khong, A., Matheny, T., Jain, S., Mitchell, S.F., Wheeler, J.R., and Parker, R. (2017). The Stress Granule Transcriptome Reveals Principles of mRNA Accumulation in Stress Granules. *Mol. Cell* *68*, 808-820.e5.

Kiebler, M.A., and Bassell, G.J. (2006). Neuronal RNA Granules: Movers and Makers. *Neuron* *51*, 685–690.

Kim-Ha, J., Smith, J.L., and Macdonald, P.M. (1991). oskar mRNA is localized to the posterior pole of the *Drosophila* oocyte. *Cell* *66*, 23–35.

Kim-Ha, J., Kerr, K., and Macdonald, P.M. (1995). Translational regulation of oskar mRNA by Bruno, an ovarian RNA-binding protein, is essential. *Cell* *81*, 403–412.

Kim, G., Pai, C.-I., Sato, K., Person, M.D., Nakamura, A., and Macdonald, P.M. (2015). Region-specific activation of oskar mRNA translation by inhibition of Bruno-mediated repression. *PLoS Genet.* *11*, e1004992–e1004992.

King, R.C. (1957). Oogenesis in adult *Drosophila melanogaster*. II. Stage distribution as a function of age. *Growth* *21*, 95–102.

Kloc, M., Wilk, K., Vargas, D., Shirato, Y., Bilinski, S., and Etkin, L.D. (2005). Potential structural role of non-coding and coding RNAs in the organization of the cytoskeleton at the vegetal cortex of *Xenopus* oocytes. *Development* *132*, 3445 LP – 3457.

Koch, E.A., and King, R.C. (1969). Further studies on the ring canal system of the ovarian cystocytes of *Drosophila melanogaster*. *Zeitschrift Für Zellforsch. Und Mikroskopische Anat.* *102*, 129–152.

Koch, E.A., Smith, P.A., and King, R.C. (1967). The division and differentiation of *Drosophila* cystocytes. *J. Morphol.* *121*, 55–70.

Kroemer, G., Mariño, G., and Levine, B. (2010). Autophagy and the Integrated Stress Response. *Mol. Cell* *40*, 280–293.

Kumari, P., and Sampath, K. (2015). cncRNAs: Bi-functional RNAs with protein coding and non-coding functions. *Semin. Cell Dev. Biol.* *47–48*, 40–51.

Langdon, E.M., Qiu, Y., Ghanbari Niaki, A., McLaughlin, G.A., Weidmann, C.A., Gerbich, T.M., Smith, J.A., Crutchley, J.M., Termini, C.M., Weeks, K.M., et al. (2018). mRNA structure determines specificity of a polyQ-driven phase separation. *Science* *360*, 922–927.

Laughrea, M., Shen, N., Jetté, L., and Wainberg, M.A. (1999). Variant Effects of Non-Native Kissing-Loop Hairpin Palindromes on HIV Replication and HIV RNA Dimerization: Role of Stem–Loop B in HIV Replication and HIV RNA Dimerization. *Biochemistry* *38*, 226–234.

Laughrea, M., Shen, N., Jetté, L., Darlix, J.-L., Kleiman, L., and Wainberg, M.A. (2001). Role of Distal Zinc Finger of Nucleocapsid Protein in Genomic RNA Dimerization of Human Immunodeficiency Virus Type 1; No Role for the Palindrome Crowning the R-U5 Hairpin. *Virology* *281*, 109–116.

Lavut, A., and Raveh, D. (2012). Sequestration of Highly Expressed mRNAs in Cytoplasmic Granules, P-Bodies, and Stress Granules Enhances Cell Viability. *PLOS Genet.* *8*, e1002527.

Lehmann, R. (2016). Germ Plasm Biogenesis--An Oskar-Centric Perspective. *Curr. Top. Dev. Biol.* *116*, 679–707.

Liao, G., Mingle, L., Van De Water, L., and Liu, G. (2015). Control of cell migration through mRNA localization and local translation. *Wiley Interdiscip. Rev. RNA* *6*, 1–15.

Lin, M.-D., Fan, S.-J., Hsu, W.-S., and Chou, T.-B. (2006). Drosophila Decapping Protein 1, dDcp1, Is a Component of the oskar mRNP Complex and Directs Its Posterior Localization in the Oocyte. *Dev. Cell* *10*, 601–613.

Ling, S.H.M., Decker, C.J., Walsh, M.A., She, M., Parker, R., and Song, H. (2008). Crystal Structure of Human Edc3 and Its Functional Implications. *Mol. Cell. Biol.* *28*, 5965 LP – 5976.

Little, S.C., Sinsimer, K.S., Lee, J.J., Wieschaus, E.F., and Gavis, E.R. (2015). Independent and coordinate trafficking of single Drosophila germ plasm mRNAs. *Nat. Cell Biol.* *17*, 558–568.

Liu, J., Valencia-Sanchez, M.A., Hannon, G.J., and Parker, R. (2005). MicroRNA-dependent localization of targeted mRNAs to mammalian P-bodies. *Nat. Cell Biol.* *7*, 719–723.

Lu, W., Lakonishok, M., Serpinskaya, A.S., Kirchenbuechler, D., Ling, S.-C., and Gelfand, V.I. (2018). Ooplasmic flow cooperates with transport and anchorage in Drosophila oocyte posterior determination. *J. Cell Biol.* *217*, 3497–3511.

Mager, W.H., and Ferreira, P.M. (1993). Stress response of yeast. *Biochem. J.* *290* ( Pt 1, 1–13.

Mahadevan, K., Zhang, H., Akef, A., Cui, X.A., Gueroussov, S., Cenik, C., Roth, F.P., and Palazzo, A.F. (2013). RanBP2/Nup358 potentiates the translation of a subset of mRNAs encoding secretory proteins. *PLoS Biol.* *11*, e1001545–e1001545.

Majmundar, A.J., Wong, W.J., and Simon, M.C. (2010). Hypoxia-Inducible Factors and the Response to Hypoxic Stress. *Mol. Cell* *40*, 294–309.

Mansfield, J.H., Wilhelm, J.E., and Hazelrigg, T. (2002). Ypsilon Schachtel, a

<em>Drosophila</em>; Y-box protein, acts antagonistically to Orb in the <em>oskar</em> mRNA localization and translation pathway. *Development* *129*, 197 LP – 209.

Mao, Y.S., Sunwoo, H., Zhang, B., and Spector, D.L. (2011a). Direct visualization of the co-transcriptional assembly of a nuclear body by noncoding RNAs. *Nat. Cell Biol.* *13*, 95–101.

Mao, Y.S., Zhang, B., and Spector, D.L. (2011b). Biogenesis and function of nuclear bodies. *Trends Genet.* *27*, 295–306.

Markussen, F.H., Michon, A.M., Breitwieser, W., and Ephrussi, A. (1995). Translational control of oskar generates short OSK, the isoform that induces pole plasma assembly. *Development* *121*, 3723 LP – 3732.

Martin, K.C., and Ephrussi, A. (2009). mRNA Localization: Gene Expression in the Spatial Dimension. *Cell* *136*, 719–730.

Martin, S.G., Leclerc, V., Smith-Litière, K., and Johnston, D.S. (2003). The identification of novel genes required for <em>Drosophila</em> anteroposterior axis formation in a germline clone screen using GFP-Staufen. *Development* *130*, 4201 LP – 4215.

Mazzalupo, S., and Cooley, L. (2006). Illuminating the role of caspases during *Drosophila* oogenesis. *Cell Death Differ.* *13*, 1950–1959.

McCann, C., Holohan, E.E., Das, S., Dervan, A., Larkin, A., Lee, J.A., Rodrigues, V., Parker, R., and Ramaswami, M. (2011). The Ataxin-2 protein is required for microRNA function and synapse-specific long-term olfactory habituation. *Proc. Natl. Acad. Sci. U. S. A.* *108*, E655–E662.

McClintock, M.A., Dix, C.I., Johnson, C.M., McLaughlin, S.H., Maizels, R.J., Hoang, H.T., and Bullock, S.L. (2018). RNA-directed activation of cytoplasmic dynein-1 in reconstituted transport RNPs. *Elife* *7*, e36312.

Micklem, D.R., Adams, J., Grünert, S., and St Johnston, D. (2000). Distinct roles of two conserved Staufen domains in oskar mRNA localization and translation. *EMBO J.* *19*, 1366–1377.

Mittag, T., and Parker, R. (2018). Multiple Modes of Protein–Protein Interactions Promote RNP Granule Assembly. *J. Mol. Biol.* *430*, 4636–4649.

Muriaux, D., De Rocquigny, H., Roques, B.-P., and Paoletti, J. (1996). NCp7 Activates HIV-1 RNA Dimerization by Converting a Transient Loop-Loop Complex into a Stable Dimer. *J. Biol. Chem.* *271*, 33686–33692.

Nakamura, A., Amikura, R., Hanyu, K., and Kobayashi, S. (2001). Me31B silences translation of oocyte-localizing RNAs through the formation of cytoplasmic RNP complex during <em>Drosophila</em> oogenesis. *Development* *128*, 3233 LP – 3242.

Nakamura, A., Sato, K., and Hanyu-Nakamura, K. (2004). *Drosophila* Cup Is an eIF4E Binding

Protein that Associates with Bruno and Regulates oskar mRNA Translation in Oogenesis. *Dev. Cell* 6, 69–78.

Nam, J.-W., Choi, S.-W., and You, B.-H. (2016). Incredible RNA: Dual Functions of Coding and Noncoding. *Mol. Cells* 39, 367–374.

Navarro, C., Puthalakath, H., Adams, J.M., Strasser, A., and Lehmann, R. (2004). Egalitarian binds dynein light chain to establish oocyte polarity and maintain oocyte fate. *Nat. Cell Biol.* 6, 427–435.

Neves, J., Demaria, M., Campisi, J., and Jasper, H. (2015). Of flies, mice, and men: evolutionarily conserved tissue damage responses and aging. *Dev. Cell* 32, 9–18.

Noble, S.L., Allen, B.L., Goh, L.K., Nordick, K., and Evans, T.C. (2008). Maternal mRNAs are regulated by diverse P body-related mRNP granules during early *Caenorhabditis elegans* development. *J. Cell Biol.* 182, 559 LP – 572.

Olexiuk, V., Crappé, J., Verbruggen, S., Verhegen, K., Martens, L., and Menschaert, G. (2016). sORFs.org: a repository of small ORFs identified by ribosome profiling. *Nucleic Acids Res.* 44, D324–D329.

Paillart, J.C., Skripkin, E., Ehresmann, B., Ehresmann, C., and Marquet, R. (1996a). A loop-loop “kissing” complex is the essential part of the dimer linkage of genomic HIV-1 RNA. *Proc. Natl. Acad. Sci.* 93, 5572 LP – 5577.

Paillart, J.C., Berthoux, L., Ottmann, M., Darlix, J.L., Marquet, R., Ehresmann, B., and Ehresmann, C. (1996b). A dual role of the putative RNA dimerization initiation site of human immunodeficiency virus type 1 in genomic RNA packaging and proviral DNA synthesis. *J. Virol.* 70, 8348–8354.

Parker, R., and Sheth, U. (2007). P Bodies and the Control of mRNA Translation and Degradation. *Mol. Cell* 25, 635–646.

Parton, R.M., Davidson, A., Davis, I., and Weil, T.T. (2014). Subcellular mRNA localisation at a glance. *J. Cell Sci.* 127, 2127 LP – 2133.

Pauley, K.M., Eystathiou, T., Jakymiw, A., Hamel, J.C., Fritzler, M.J., and Chan, E.K.L. (2006). Formation of GW bodies is a consequence of microRNA genesis. *EMBO Rep.* 7, 904–910.

Pestova, T. V., Kolupaeva, V.G., Lomakin, I.B., Pilipenko, E. V, Shatsky, I.N., Agol, V.I., and Hellen, C.U. (2001). Molecular mechanisms of translation initiation in eukaryotes. *Proc. Natl. Acad. Sci. U. S. A.* 98, 7029–7036.

Pillai, R.S., Bhattacharyya, S.N., Artus, C.G., Zoller, T., Cougot, N., Basyuk, E., Bertrand, E., and Filipowicz, W. (2005). Inhibition of Translational Initiation by Let-7 MicroRNA in Human Cells. *Science* (80-. ). 309, 1573 LP – 1576.

Preiss, T., and W. Hentze, M. (2003). Starting the protein synthesis machine: eukaryotic translation initiation. *BioEssays* 25, 1201–1211.

Pritchett, T.L., Tanner, E.A., and McCall, K. (2009). Cracking open cell death in the *Drosophila* ovary. *Apoptosis* 14, 969–979.

Protter, D.S.W., and Parker, R. (2016). Principles and Properties of Stress Granules. *Trends Cell Biol.* 26, 668–679.

Protter, D.S.W., Rao, B.S., Van Treeck, B., Lin, Y., Mizoue, L., Rosen, M.K., and Parker, R. (2018). Intrinsically Disordered Regions Can Contribute Promiscuous Interactions to RNP Granule Assembly. *Cell Rep.* 22, 1401–1412.

Ramachandran, V., Shah, K.H., and Herman, P.K. (2011). The cAMP-Dependent Protein Kinase Signaling Pathway Is a Key Regulator of P Body Foci Formation. *Mol. Cell* 43, 973–981.

Reichel, M., Liao, Y., Rettel, M., Ragan, C., Evers, M., Alleaume, A.-M., Horos, R., Hentze, M.W., Preiss, T., and Millar, A.A. (2016). In Planta Determination of the mRNA-Binding Proteome of *Arabidopsis* Etiolated Seedlings. *Plant Cell* 28, 2435 LP – 2452.

Reveal, B., Yan, N., Snee, M.J., Pai, C.-I., Gim, Y., and Macdonald, P.M. (2010). BREs mediate both repression and activation of oskar mRNA translation and act in trans. *Dev. Cell* 18, 496–502.

Richter, K., Haslbeck, M., and Buchner, J. (2010). The Heat Shock Response: Life on the Verge of Death. *Mol. Cell* 40, 253–266.

Riechmann, V., and Ephrussi, A. (2001). Axis formation during *Drosophila* oogenesis. *Curr. Opin. Genet. Dev.* 11, 374–383.

Ritchie, M.E., Phipson, B., Wu, D., Hu, Y., Law, C.W., Shi, W., and Smyth, G.K. (2015). limma powers differential expression analyses for RNA-sequencing and microarray studies. *Nucleic Acids Res.* 43, e47–e47.

Rongo, C., Gavis, E.R., and Lehmann, R. (1995). Localization of oskar RNA regulates oskar translation and requires Oskar protein. *Development* 121, 2737 LP – 2746.

Ruiz-Orera, J., Messeguer, X., Subirana, J.A., and Alba, M.M. (2014). Long non-coding RNAs as a source of new peptides. *Elife* 3, e03523–e03523.

Ryu, Y.H., and Macdonald, P.M. (2015). RNA sequences required for the noncoding function of oskar RNA also mediate regulation of Oskar protein expression by Bicoid Stability Factor. *Dev. Biol.* 407, 211–223.

Sengupta, S., Peterson, T.R., and Sabatini, D.M. (2010). Regulation of the mTOR Complex 1 Pathway by Nutrients, Growth Factors, and Stress. *Mol. Cell* 40, 310–322.

Serano, T.L., and Cohen, R.S. (1995). A small predicted stem-loop structure mediates oocyte localization of *Drosophila* K10 mRNA. *Development* 121, 3809 LP – 3818.

Serbus, L.R., Cha, B.-J., Theurkauf, W.E., and Saxton, W.M. (2005). Dynein and the actin cytoskeleton control kinesin-driven cytoplasmic streaming in *Drosophila* oocytes. *Development* 132,



3743–3752.

Sheth, U., and Parker, R. (2003). Decapping and decay of messenger RNA occur in cytoplasmic processing bodies. *Science* *300*, 805–808.

Shimada, Y., Burn, K.M., Niwa, R., and Cooley, L. (2011). Reversible response of protein localization and microtubule organization to nutrient stress during *Drosophila* early oogenesis. *Dev. Biol.* *355*, 250–262.

Shpilka, T., and Haynes, C.M. (2017). The mitochondrial UPR: mechanisms, physiological functions and implications in ageing. *Nat. Rev. Mol. Cell Biol.* *19*, 109.

Simon, B., Masiewicz, P., Ephrussi, A., and Carlomagno, T. (2015). The structure of the SOLE element of oskar mRNA. *RNA* *21*, 1444–1453.

Snee, M.J., and Macdonald, P.M. (2009). Dynamic organization and plasticity of sponge bodies. *Dev. Dyn.* *238*, 918–930.

Spriggs, K.A., Bushell, M., and Willis, A.E. (2010). Translational Regulation of Gene Expression during Conditions of Cell Stress. *Mol. Cell* *40*, 228–237.

St Johnston, D., Beuchle, D., and Nüsslein-Volhard, C. (1991). *staufer*, a gene required to localize maternal RNAs in the *Drosophila* egg. *Cell* *66*, 51–63.

Standart, N., and Weil, D. (2018). P-Bodies: Cytosolic Droplets for Coordinated mRNA Storage. *Trends Genet.* *34*, 612–626.

Stroberg, W., and Schnell, S. (2017). On the origin of non-membrane-bound organelles, and their physiological function. *J. Theor. Biol.* *434*, 42–49.

Strucko, T., Zirngibl, K., Pereira, F., Kafkia, E., Mohamed, E.T., Rettel, M., Stein, F., Feist, A.M., Jouhten, P., Patil, K.R., et al. (2018). Laboratory evolution reveals regulatory and metabolic trade-offs of glycerol utilization in *Saccharomyces cerevisiae*. *Metab. Eng.* *47*, 73–82.

Tanaka, T., and Nakamura, A. (2008). The endocytic pathway acts downstream of Oskar in *Drosophila*; germ plasm assembly. *Development* *135*, 1107 LP – 1117.

Tang, H., Hornstein, E., Stolovich, M., Levy, G., Livingstone, M., Templeton, D., Avruch, J., and Meyuhas, O. (2001). Amino acid-induced translation of TOP mRNAs is fully dependent on phosphatidylinositol 3-kinase-mediated signaling, is partially inhibited by rapamycin, and is independent of S6K1 and rpS6 phosphorylation. *Mol. Cell. Biol.* *21*, 8671–8683.

Teixeira, D., Sheth, U., Valencia-Sanchez, M.A., Brengues, M., and Parker, R. (2005). Processing bodies require RNA for assembly and contain nontranslating mRNAs. *RNA* *11*, 371–382.

Tian, B., and Mathews, M.B.B.T.-P. in N.A.R. and M.B. (2003). Phylogenetics and Functions of the Double-Stranded RNA-Binding Motif: A Genomic Survey. (Academic Press), pp. 123–158.

Tourrière, H., Chebli, K., Zekri, L., Courselaud, B., Blanchard, J.M., Bertrand, E., and Tazi, J.

(2003). The RasGAP-associated endoribonuclease G3BP assembles stress granules. *J. Cell Biol.* *160*, 823 LP – 831.

Van Treeck, B., and Parker, R. (2018). Emerging Roles for Intermolecular RNA-RNA Interactions in RNP Assemblies. *Cell* *174*, 791–802.

Van Treeck, B., Protter, D.S.W., Matheny, T., Khong, A., Link, C.D., and Parker, R. (2018). RNA self-assembly contributes to stress granule formation and defining the stress granule transcriptome. *Proc. Natl. Acad. Sci. U. S. A.* *115*, 2734–2739.

Uroda, T., Anastasakou, E., Rossi, A., Teulon, J.-M., Pellequer, J.-L., Annibale, P., Pessey, O., Inga, A., Chillón, I., and Marcia, M. (2019). Conserved Pseudoknots in lncRNA MEG3 Are Essential for Stimulation of the p53 Pathway. *Mol. Cell* *75*, 982-995.e9.

Vanzo, N.F., and Ephrussi, A. (2002). Oskar anchoring restricts pole plasm formation to the posterior of the *Drosophila* oocyte. *Development* *129*, 3705 LP – 3714.

Vanzo, N., Oprins, A., Xanthakis, D., Ephrussi, A., and Rabouille, C. (2007). Stimulation of Endocytosis and Actin Dynamics by Oskar Polarizes the *Drosophila* Oocyte. *Dev. Cell* *12*, 543–555.

Voronina, E., Seydoux, G., Sassone-Corsi, P., and Nagamori, I. (2011). RNA granules in germ cells. *Cold Spring Harb. Perspect. Biol.* *3*, a002774.

Voronina, E., Paix, A., and Seydoux, G. (2012). The P granule component PGL-1 promotes the localization and silencing activity of the PUF protein FBF-2 in germline stem cells. *Development* *139*, 3732–3740.

Wagner, C., Palacios, I., Jaeger, L., St Johnston, D., Ehresmann, B., Ehresmann, C., and Brunel, C. (2001). Dimerization of the 3'UTR of bicoid mRNA involves a two-step mechanism<sup>11</sup>Edited by J. Doudna. *J. Mol. Biol.* *313*, 511–524.

Wagner, C., Ehresmann, C., Ehresmann, B., and Brunel, C. (2004). Mechanism of Dimerization of Bicoid mRNA: INITIATION AND STABILIZATION. *J. Biol. Chem.* *279*, 4560–4569.

Wang, C., Schmich, F., Srivatsa, S., Weidner, J., Beerenwinkel, N., and Spang, A. (2018). Context-dependent deposition and regulation of mRNAs in P-bodies. *Elife* *7*, e29815.

Wang, J.T., Smith, J., Chen, B.-C., Schmidt, H., Rasoloson, D., Paix, A., Lambrus, B.G., Calidas, D., Betzig, E., and Seydoux, G. (2014). Regulation of RNA granule dynamics by phosphorylation of serine-rich, intrinsically disordered proteins in *C. elegans*. *Elife* *3*, e04591.

Webster, P.J., Liang, L., Berg, C.A., Lasko, P., and Macdonald, P.M. (1997). Translational repressor bruno plays multiple roles in development and is widely conserved. *Genes Dev.* *11*, 2510–2521.

Weil, T.T. (2014). mRNA localization in the *Drosophila* germline. *RNA Biol.* *11*, 1010–1018.

Weil, T.T., Parton, R.M., Hoppers, B., Soetaert, J., Veenendaal, T., Xanthakis, D., Dobbie, I.M.,

Halstead, J.M., Hayashi, R., Rabouille, C., et al. (2012). *Drosophila* patterning is established by differential association of mRNAs with P bodies. *Nat. Cell Biol.* *14*, 1305–1313.

Wellen, K.E., and Thompson, C.B. (2010). Cellular Metabolic Stress: Considering How Cells Respond to Nutrient Excess. *Mol. Cell* *40*, 323–332.

Werner, T., Sweetman, G., Savitski, M.F., Mathieson, T., Bantscheff, M., and Savitski, M.M. (2014). Ion Coalescence of Neutron Encoded TMT 10-Plex Reporter Ions. *Anal. Chem.* *86*, 3594–3601.

Wickham, H. (2009). *ggplot2: elegant graphics for data analysis*. (New York: Springer).

Wilczynska, A., Aigueperse, C., Kress, M., Dautry, F., and Weil, D. (2005). The translational regulator CPEB1 provides a link between dcp1 bodies and stress granules. *J. Cell Sci.* *118*, 981 LP – 992.

Wilhelm, J.E., Mansfield, J., Hom-Booher, N., Wang, S., Turck, C.W., Hazelrigg, T., and Vale, R.D. (2000a). Isolation of a ribonucleoprotein complex involved in mRNA localization in *Drosophila* oocytes. *J. Cell Biol.* *148*, 427–440.

Wilhelm, J.E., Vale, R.D., and Hegde, R.S. (2000b). Coordinate control of translation and localization of Vg1 mRNA in *Xenopus* oocytes. *Proc. Natl. Acad. Sci.* *97*, 13132 LP – 13137.

Wilhelm, J.E., Hilton, M., Amos, Q., and Henzel, W.J. (2003). Cup is an eIF4E binding protein required for both the translational repression of *oskar* and the recruitment of Barentsz. *J. Cell Biol.* *163*, 1197–1204.

Wilsch-Bräuninger, M., Schwarz, H., and Nüsslein-Volhard, C. (1997). A Sponge-like Structure Involved in the Association and Transport of Maternal Products during *Drosophila* Oogenesis. *J. Cell Biol.* *139*, 817 LP – 829.

Yamashita, Y.M. (2018). Subcellular Specialization and Organelle Behavior in Germ Cells. *Genetics* *208*, 19 LP – 51.

Yamazaki, T., Souquere, S., Chujo, T., Kobelke, S., Chong, Y.S., Fox, A.H., Bond, C.S., Nakagawa, S., Pierron, G., and Hirose, T. (2018). Functional Domains of NEAT1 Architectural lncRNA Induce Paraspeckle Assembly through Phase Separation. *Mol. Cell* *70*, 1038-1053.e7.

Yano, T., de Quinto, S.L., Matsui, Y., Shevchenko, A., Shevchenko, A., and Ephrussi, A. (2004). Hrp48, a *Drosophila* hnRNPA/B Homolog, Binds and Regulates Translation of *oskar* mRNA. *Dev. Cell* *6*, 637–648.

Yu, J.H., Yang, W.-H., Gulick, T., Bloch, K.D., and Bloch, D.B. (2005). Ge-1 is a central component of the mammalian cytoplasmic mRNA processing body. *RNA* *11*, 1795–1802.

Zimyanin, V.L., Belaya, K., Pecreaux, J., Gilchrist, M.J., Clark, A., Davis, I., and St Johnston, D. (2008). In vivo imaging of *oskar* mRNA transport reveals the mechanism of posterior localization. *Cell* *134*, 843–853.

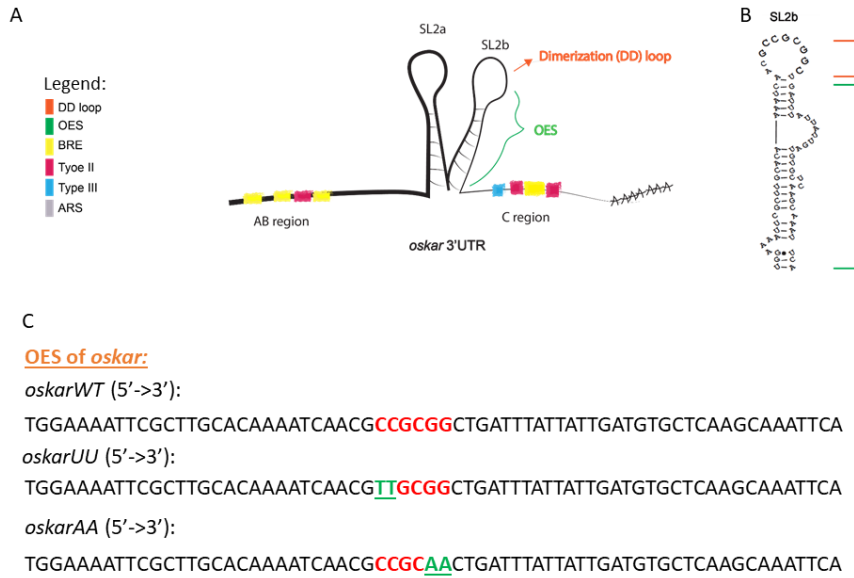


## List of figures

I.	Figure 1.1 Cellular response to stress.....	4
II.	Figure 1.2 Model of the “mRNA cycle” .....	6
III.	Figure 1.3 RNP granule assembly.....	9
IV.	Figure 1.4 <i>Drosophila</i> oogenesis and nutrient stress induced P-body formation.....	11
V.	Figure 1.5 <i>oskar</i> mRNA.....	14
VI.	Figure 1.6 <i>oskar</i> localization and translation.....	16
VII.	Figure 2.1 Starvation set up.....	33
VIII.	Figure 2.2 Making CDS-free transgenic fly lines.....	35
IX.	Figure 3.1 <i>oskar</i> mRNAs localize in P-bodies (PBs) .....	53
X.	Figure 3.2 In <i>oskarUU</i> non-dimerizing mutants P-body (PB) formation is impaired.....	55
XI.	Figure 3.3 In <i>oskarUU</i> mutants, recruitment of P-body components is affected.....	57
XII.	Figure 3.4 <i>gurken</i> and <i>bicoid</i> do not localize in P-bodies.....	59
XIII.	Figure 3.5 In <i>oskarUU</i> mutants P-body (PB) formation is impaired.....	61
XIV.	Figure 3.6 The effect of <i>oskar</i> mRNA dimerization on P-body (PB) formation.....	63
XV.	Figure 3.7 <i>oskarUU</i> mutants are translated prematurely.....	65
XVI.	Figure 3.8 P-body (PB) formation in egg-chambers expressing the <i>oskar3’UTR</i> (cds-free) or <i>egfp-oskar3’UTR</i> transgenes.....	67
XVII.	Figure 3.9 <i>oskar</i> 3’UTR is sufficient to promote P-body (PB) formation.....	70
XVIII.	Figure 3.10 <i>oskar</i> 3’UTR secondary structure prediction.....	73
XIX.	Figure 3.11 <i>oskar</i> specific RNA affinity pull-down reveals differences in Bruno affinity for <i>oskar</i> WT and UU mutant 3’UTR transcripts.....	75
XX.	Figure 3.12 Differential enrichment MS data analysis of RNA affinity pull-downs.....	77
XXI.	Figure 3.13 Differential enrichment MS data analysis of UU_359 vs WT_359 pull-down.....	79
XXII.	Figure 4.1 Hypothetical model of <i>oskar</i> mRNA dependent P-body formation upon nutrient deprivation in <i>Drosophila</i> .....	85

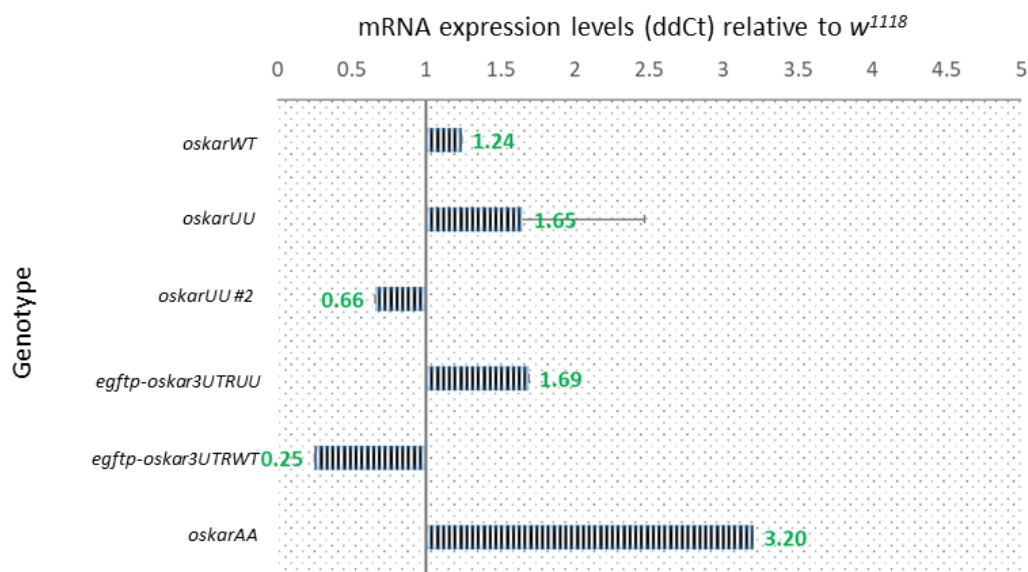


## Appendix I



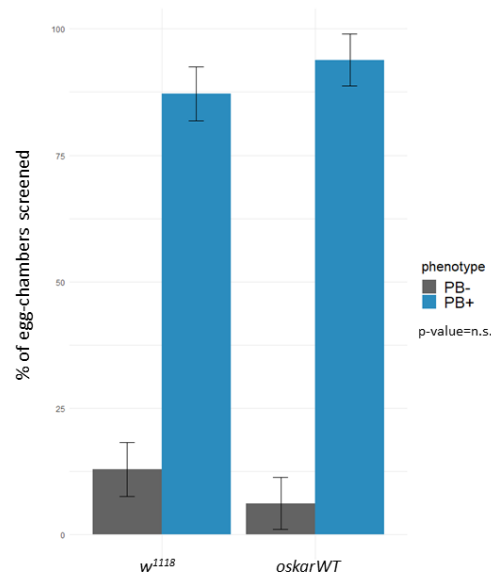
**Appendix I: A** Schematic representation of the 3'UTR of *oskar* mRNA with SL2a and SL2b. **B** Schematic representation of the SL2b (Jambor et al., 2014). The DD is highlighted in orange and the OES in green. **C** SL2b sequence in *oskar*<sup>WT</sup> and *oskar*<sup>UU</sup> and *oskar*<sup>AA</sup> mutants.

## Appendix II



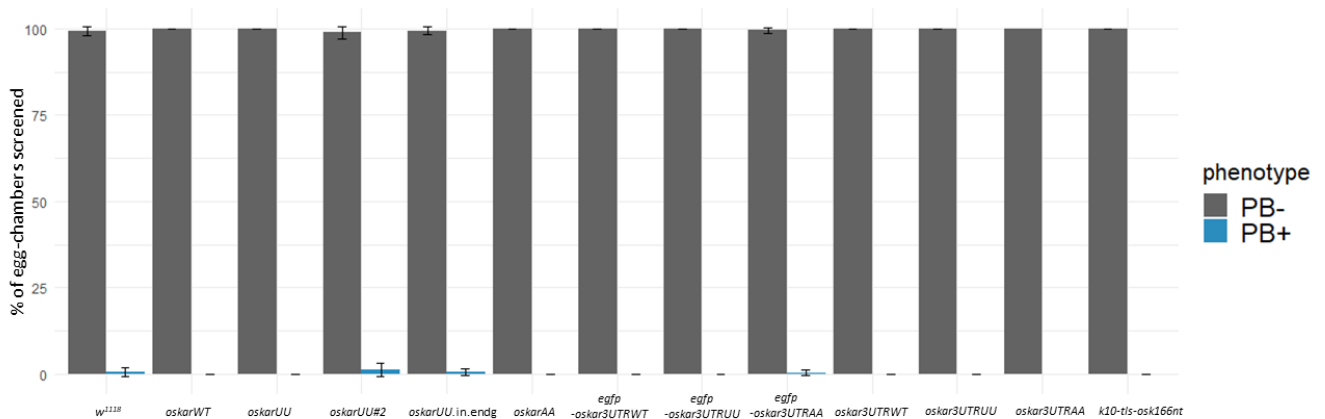
**Appendix II:** mRNA expression levels of P-element inserted transgenes in *oskar* null background (*oskar*<sup>A87</sup>/*oskar*<sup>attP,3P3-GFP</sup>). Name of each transgene is annotated alongside x-axis. Above each bar, levels of expression of each transgene relative to *w*<sup>1118</sup> are indicated. *w*<sup>1118</sup> ddCt=1.

## Appendix III



**Appendix III:** P-body formation in *oskarWT* transgenic flies is the same as in the wild-type flies (*w<sup>1118</sup>*). Graph showing the percentage of PB+ and PB- egg-chambers in *w<sup>1118</sup>* (N=247) and *oskarWT* (N=215). Stages 6 to 9 were scored. P-value of significance (t.test) is indicated below the legend of the graph. Transgenic *oskarWT* was expressed in *oskar* mRNA null background (*oskar<sup>attP,3P3-GFP/oskar<sup>A87</sup></sup>*).

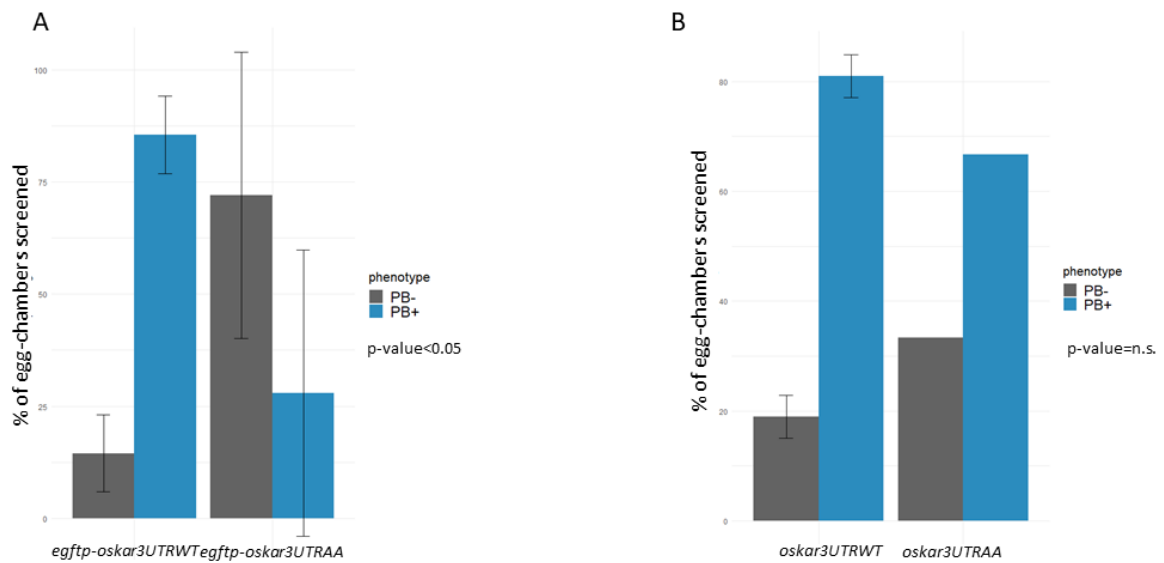
## Appendix IV



**Appendix IV:** Quantified P-body formation in all the fly lines in use under nutrient-rich conditions (0h starvation). Graph showing the percentage of PB+ and PB- egg-chambers in *w<sup>1118</sup>* (N=317), *oskarWT* (N=109), *oskarUU* (N=131), *oskarUU#2* (N=119), *oskarUU in endg.* (N=167), *oskarAA* (N=179), *egfp-oskar3UTRWT* (N=79), *egfp-oskar3UTRUU* (N=95), *egfp-oskar3UTRAA* (N=234), *oskar3UTRWT* (N=155), *oskar3UTRUU* (N=169), *oskar3UTRAA* (N=30), *k10tls-osk166nt* (N=129). Stages 6 to 9 were scored. All tested *oskar* transgenes except in *w<sup>1118</sup>* were expressed in an *oskar* mRNA null background (*oskar<sup>attP,3P3-GFP/oskar<sup>A87</sup></sup>* or *oskar<sup>A87/Df(3R)p-XT103</sup>*).

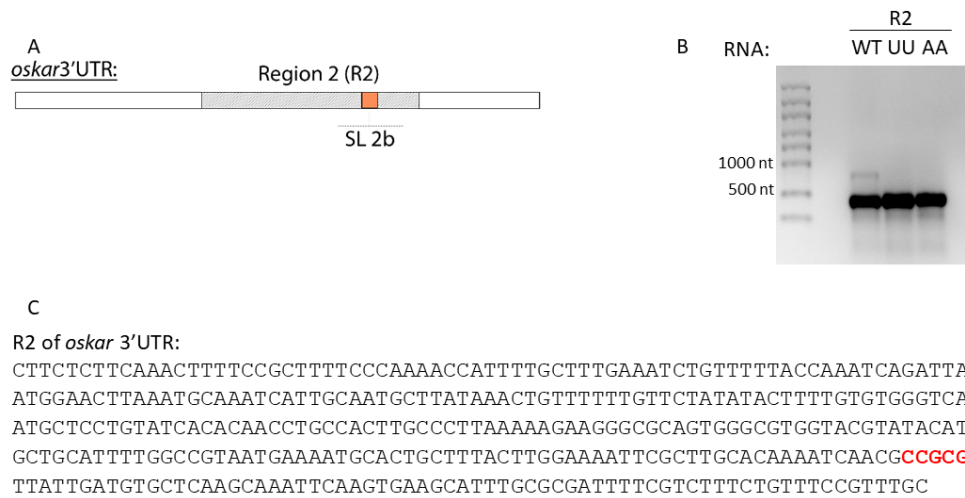


## Appendix V



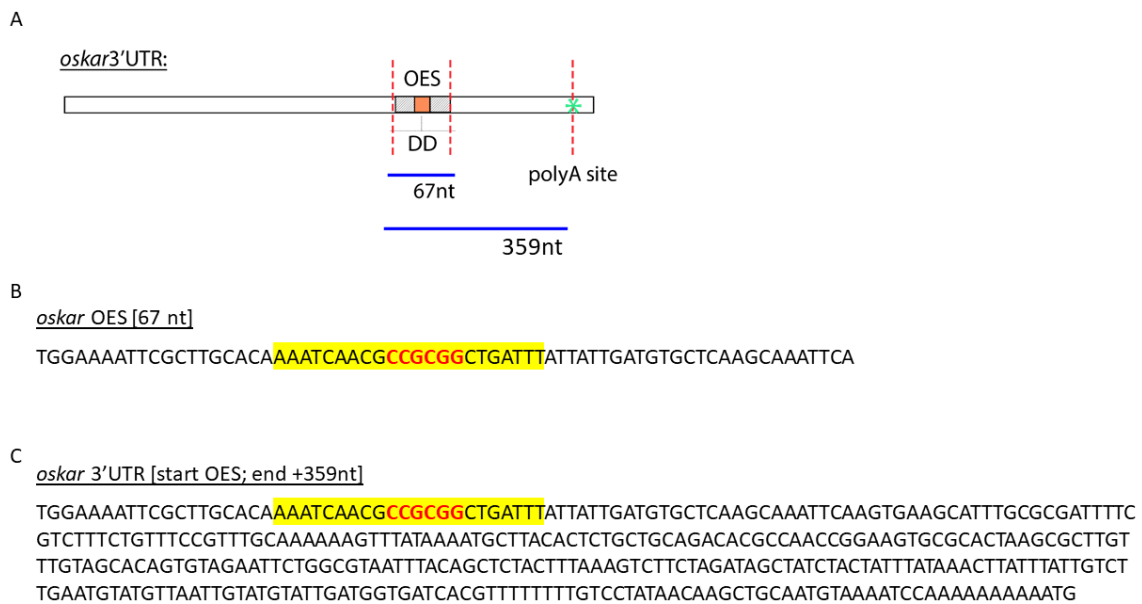
**Appendix V: A** Quantified P-body formation in *egfp-oskar3UTRAA* mutants compared to *egfp-oskar3UTRWT* after 6h under nutrient-poor conditions. Graph showing the percentage of PB+ and PB- egg-chambers in *egfp-oskar3UTRWT* (N=172) and *egfp-oskar3UTRAA* (N=264). Stages 6 to 9 were scored. P-value of significance (t.test) is indicated below the legend of the graph. All tested *oskar* transgenes except in *w<sup>1118</sup>* were expressed in an *oskar* mRNA null background (*oskar<sup>attP,3P3-GFP/oskar<sup>A87</sup></sup>*). **B** Quantified P-body formation in *oskar3UTRAA* mutants compared to *oskar3UTRWT* after 6h under nutrient-poor conditions. Graph showing the percentage of PB+ and PB- egg-chambers in *oskar3UTRWT* (N=269) and *oskar3UTRAA* (N=120). Stages 6 to 9 were scored. P-value of significance (t.test) is indicated below the legend of the graph. All tested *oskar* transgenes except in *w<sup>1118</sup>* were expressed in an *oskar* mRNA null background (*oskar<sup>A87</sup>/Df(3R)p-XT103*). Only one biological replicate was obtained for *oskar3UTRAA* mutant line. In order to get more conclusive results at least two more replicates need to be analyzed.

## Appendix VI



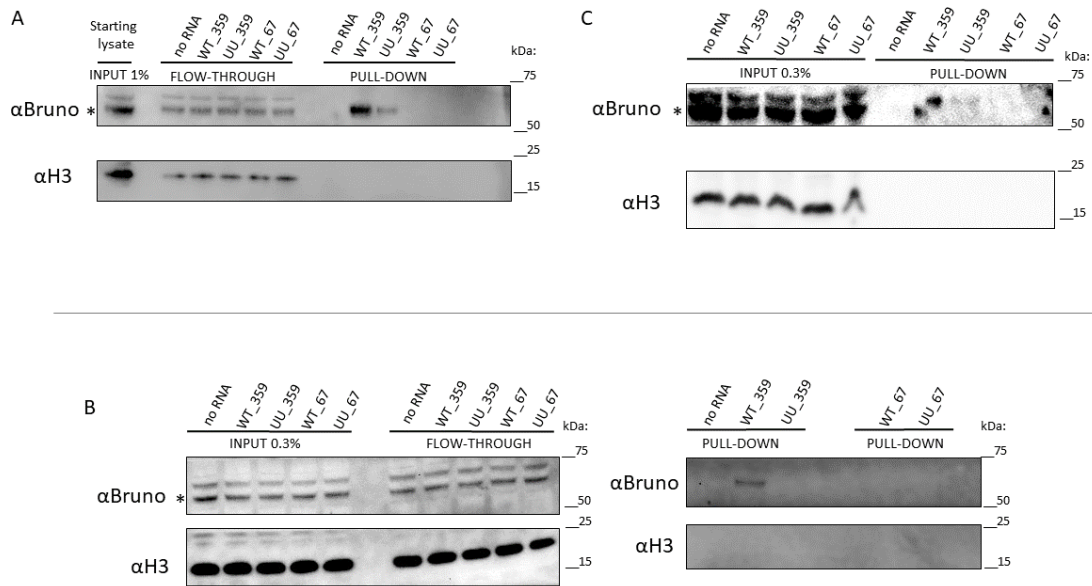
**Appendix VI** Sequence template for *in vitro* dimerization assay. **A** Schematic representation of the 3'UTR of *oskar* mRNA with highlighted region 2 (R2) in gray and SL2b in orange. **B** Quality control of *in vitro* transcribed R2 (WT, UU and AA fragments). RNA was loaded on denaturing formaldehyde based 1.5 % agarose gel (2.25g agarose, 109.5ml H<sub>2</sub>O, 15ml 10x MOPS, 25.5ml 37% formaldehyde, ultrapure grade) **C** Sequence of the R2 template (5'→3') with highlighted region of the dimerization domain loop in red (WT). Sequence in the UU mutant: TTGCGG. Sequence in the AA mutant: CCGCAA.

## Appendix VII



**Appendix VII** Sequence template for *in vitro* RNA affinity pull-down assay. **A** Schematic representation of the 3'UTR of *oskar* mRNA with highlighted OES in gray and the dimerization domain in orange. Fragments of the 3'UTR which were transcribed for the pull-downs are indicated with blue lines (67nt "short" and 359nt "long" fragment). PolyA site is indicated with green asterisk. **B** Sequence of the "short" template (5'→3') with highlighted region of the OES in yellow and the dimerization domain loop in red (WT). **C** Sequence of the "long" template (5'→3') with highlighted region of the OES in yellow and the dimerization domain loop in red (WT). Sequence in the UU mutant: TTGCGG.

## Appendix VIII



**Appendix VIII RNA affinity pull-down assay replicates. A** Replicate 1: Immunoblot showing Bruno in UU\_359 pull-down, compared to WT\_359. In addition to the no RNA control, WT\_67 and UU\_67, which lack Bruno binding sites were used further as negative controls. Input (1%) was loaded from starting lysate before splitting it to 5 independent pull-downs for each sample. Asterisk indicates specific Bruno bend. **B** Replicate 2: Immunoblots showing Bruno in UU\_359 pull-down, compared to WT\_359. In addition to the no RNA control, WT\_67 and UU\_67, which lack Bruno binding sites were used further as negative controls. Input (0.3%) and flow-through were run on separate gel. Asterisk indicates specific Bruno bend. **C** Replicate 3-a: Immunoblot showing Bruno in UU\_359 pull-down, compared to WT\_359. In addition to the no RNA control, WT\_67 and UU\_67, which lack Bruno binding sites were used further as negative controls. Asterisk indicates specific Bruno bend. Note that in the lane of WT\_359 pull-down membrane got broken, thus bend was split in two smaller ones. Replicate 3-b is shown in the results section (Figure 3.11 C). Replicates 3-a and 3-b are from the same pull-down (one biological replicate) but two different western blots.

## Appendix IX

Table 1:

Gene name	Comparison	Hit annotation	logFC	pvalue.limma	fdr.limma
ZN72D	WT_359 - beads_only	enriched hit	1.872005	6.15E-10	4.09E-07
<b>TBPH</b>	WT_359 - beads_only	enriched hit	5.106587	7.13E-10	4.09E-07
MLE	WT_359 - beads_only	enriched hit	2.408158	5.90E-08	2.26E-05
CG5641	WT_359 - beads_only	enriched hit	2.101827	8.45E-08	2.42E-05
NS4	WT_359 - beads_only	enriched hit	2.638336	4.47E-07	0.000102562
<b>CG9890</b>	WT_359 - beads_only	enriched hit	4.308055	6.81E-07	0.000130101
LSM	WT_359 - beads_only	enriched hit	1.679388	1.01E-06	0.000144738
KLP10A	WT_359 - beads_only	enriched hit	2.289367	2.39E-06	0.000304778
SYP	WT_359 - beads_only	enriched hit	1.125284	3.89E-06	0.000445666
<b>ARET</b>	WT_359 - beads_only	enriched hit	2.116714	5.06E-06	0.000483635

<b>YPS</b>	WT_359 - beads_only	enriched hit	1.367739	8.74E-06	0.000679632
SSL1	WT_359 - beads_only	enriched hit	1.692589	8.89E-06	0.000679632
CG10562	WT_359 - beads_only	enriched hit	1.050297	1.03E-05	0.00069591
CG1582	WT_359 - beads_only	enriched hit	1.133239	1.31E-05	0.000832281
DCR	WT_359 - beads_only	enriched hit	3.001506	1.49E-05	0.000896084
<b>BSF</b>	WT_359 - beads_only	enriched hit	1.446044	1.77E-05	0.000965904
CG10628	WT_359 - beads_only	enriched hit	2.323325	2.13E-05	0.00110861
SSX	WT_359 - beads_only	enriched hit	1.379536	2.26E-05	0.001125301
SEC5	WT_359 - beads_only	enriched hit	1.131385	3.77E-05	0.001610718
RRP4	WT_359 - beads_only	enriched hit	1.429884	4.69E-05	0.001734936
CKIIBETA	WT_359 - beads_only	enriched hit	1.158943	5.09E-05	0.00178719
MTR3	WT_359 - beads_only	enriched hit	1.375235	5.30E-05	0.00178719
NOP60B	WT_359 - beads_only	enriched hit	1.759056	6.77E-05	0.002157097
RUMP	WT_359 - beads_only	enriched hit	1.068972	7.96E-05	0.002341901
CSL4	WT_359 - beads_only	enriched hit	1.30472	8.19E-05	0.002348857
SXL	WT_359 - beads_only	enriched hit	2.561977	8.87E-05	0.002421925
<b>HRB27C</b>	WT_359 - beads_only	enriched hit	1.08904	9.43E-05	0.002429056
CG9684	WT_359 - beads_only	enriched hit	1.219828	0.000115572	0.002665249
128UP	WT_359 - beads_only	enriched hit	1.052686	0.00011772	0.002665249
LOQS	WT_359 - beads_only	enriched hit	3.109402	0.000138201	0.002990877
CG17141	WT_359 - beads_only	enriched hit	2.562819	0.000148919	0.003105642
CAF1	WT_359 - beads_only	enriched hit	1.311297	0.000204477	0.003782818
R2D2	WT_359 - beads_only	enriched hit	2.393485	0.000298609	0.004695736
LSM7	WT_359 - beads_only	enriched hit	1.386831	0.000301509	0.004695736
LSM3	WT_359 - beads_only	enriched hit	1.275302	0.000311139	0.004695736
RAN	WT_359 - beads_only	enriched hit	2.114593	0.000354227	0.005276603
CG4038	WT_359 - beads_only	enriched hit	1.271939	0.000509153	0.007121939
SQD	WT_359 - beads_only	enriched hit	1.204295	0.00107295	0.012557894
SNRNP	WT_359 - beads_only	enriched hit	1.034925	0.001128899	0.01294847
RRP46	WT_359 - beads_only	enriched hit	1.887489	0.001349521	0.014439295
CG3689	WT_359 - beads_only	enriched hit	1.22024	0.00140844	0.014817464
SRP54K	WT_359 - beads_only	enriched hit	1.276148	0.001796724	0.017685086
RRP47	WT_359 - beads_only	enriched hit	1.311096	0.001803971	0.017685086
CG5973	WT_359 - beads_only	enriched hit	2.062272	0.004510818	0.031937704
CAZ	WT_359 - beads_only	enriched hit	1.650197	0.004606362	0.0322855
CPSF73	WT_359 - beads_only	enriched hit	1.051962	0.004728827	0.0322855
EF1ALPHA48D	WT_359 - beads_only	enriched hit	1.085261	0.004977393	0.033582763
CPSF100	WT_359 - beads_only	enriched hit	1.111925	0.005502582	0.036482438
<b>GLO</b>	WT_359 - beads_only	enriched hit	1.424588	0.006416836	0.040000603
MED16	WT_359 - beads_only	enriched candidate	0.746798	1.56E-05	0.000896084
PASHA	WT_359 - beads_only	enriched candidate	0.921221	2.88E-05	0.001357206
LOST	WT_359 - beads_only	enriched candidate	0.707548	2.96E-05	0.001357206
<b>BICD</b>	WT_359 - beads_only	enriched candidate	0.590436	3.93E-05	0.001610718
LKB1	WT_359 - beads_only	enriched candidate	0.842304	6.40E-05	0.002097205
CG5642	WT_359 - beads_only	enriched candidate	0.854974	7.31E-05	0.002266588
CG3808	WT_359 - beads_only	enriched candidate	0.765203	7.70E-05	0.002323433

DIS3	WT_359 - beads_only	enriched candidate	0.690523	8.83E-05	0.002421925
RPB5	WT_359 - beads_only	enriched candidate	0.701592	9.43E-05	0.002429056
CG6745	WT_359 - beads_only	enriched candidate	0.823848	9.53E-05	0.002429056
PP2A	WT_359 - beads_only	enriched candidate	0.661206	0.000109323	0.002665249
ECD	WT_359 - beads_only	enriched candidate	0.643602	0.000118507	0.002665249
XPD	WT_359 - beads_only	enriched candidate	0.962621	0.000162875	0.003336031
PATR	WT_359 - beads_only	enriched candidate	0.625604	0.000166499	0.003350427
MED25	WT_359 - beads_only	enriched candidate	0.932579	0.000176661	0.003434409
KAP	WT_359 - beads_only	enriched candidate	0.60275	0.000191038	0.003592142
CDC27	WT_359 - beads_only	enriched candidate	0.7084	0.000237905	0.004331383
TRIP1	WT_359 - beads_only	enriched candidate	0.931637	0.000273863	0.004641372
NSUN2	WT_359 - beads_only	enriched candidate	0.881117	0.000280883	0.004641372
RPI1	WT_359 - beads_only	enriched candidate	0.595043	0.000282816	0.004641372
MAHE	WT_359 - beads_only	enriched candidate	0.749351	0.000299928	0.004695736
CG4849	WT_359 - beads_only	enriched candidate	0.730557	0.000554653	0.007664905
U2AF50	WT_359 - beads_only	enriched candidate	0.671073	0.000573478	0.00783071
<b>STAU</b>	WT_359 - beads_only	enriched candidate	0.600434	0.000670586	0.00884095
PIX	WT_359 - beads_only	enriched candidate	0.771854	0.000715395	0.009297537
CED	WT_359 - beads_only	enriched candidate	0.839099	0.000754254	0.009403582
UPF1	WT_359 - beads_only	enriched candidate	0.678285	0.000891416	0.010650569
SRP68	WT_359 - beads_only	enriched candidate	0.920858	0.001181286	0.013154707
SNR1	WT_359 - beads_only	enriched candidate	0.602621	0.001276997	0.013818066
NS1	WT_359 - beads_only	enriched candidate	0.86781	0.001359585	0.014439295
NS2	WT_359 - beads_only	enriched candidate	0.612849	0.001900513	0.018318393
CG9596	WT_359 - beads_only	enriched candidate	0.624044	0.00249302	0.022285443
CG16742	WT_359 - beads_only	enriched candidate	0.73609	0.002940804	0.024985941
EIF6	WT_359 - beads_only	enriched candidate	0.841817	0.003006481	0.025171045
CG12909	WT_359 - beads_only	enriched candidate	0.670284	0.003064458	0.02528729
CDK7	WT_359 - beads_only	enriched candidate	0.656292	0.003259669	0.026706004
CG6767	WT_359 - beads_only	enriched candidate	0.605126	0.003376473	0.027093933
U4	WT_359 - beads_only	enriched candidate	0.66385	0.003401505	0.027093933
IP259	WT_359 - beads_only	enriched candidate	0.816521	0.003761877	0.028958877
SYM	WT_359 - beads_only	enriched candidate	0.876817	0.003984714	0.029678357
CG8635	WT_359 - beads_only	enriched candidate	0.958277	0.004162466	0.030248498
SBF	WT_359 - beads_only	enriched candidate	0.728945	0.004939906	0.033527057
CG10418	WT_359 - beads_only	enriched candidate	0.981371	0.005587212	0.036649026
CG10341	WT_359 - beads_only	enriched candidate	0.73186	0.006225959	0.039454003
WASH	WT_359 - beads_only	enriched candidate	0.723856	0.006592717	0.040437683
CG10914	WT_359 - beads_only	enriched candidate	0.758946	0.009323716	0.053740212
CCDC53	WT_359 - beads_only	enriched candidate	0.730737	0.009796858	0.055354658
RYR	WT_359 - beads_only	enriched candidate	0.824686	0.010143171	0.055401035
CG10672	WT_359 - beads_only	enriched candidate	0.719604	0.010461625	0.056335607
RPN9	WT_359 - beads_only	enriched candidate	0.622991	0.012187308	0.06354019
NHP2	WT_359 - beads_only	enriched candidate	0.740314	0.012645513	0.065335149
CG5664	WT_359 - beads_only	enriched candidate	0.677677	0.016643048	0.080259964
DPH5	WT_359 - beads_only	enriched candidate	0.907489	0.023589025	0.10210042

NS3	WT_359 - beads_only	enriched candidate	0.886353	0.025349991	0.106507106
NEOS	WT_359 - beads_only	enriched candidate	0.749523	0.027362029	0.11248834
DPPIII	WT_359 - beads_only	enriched candidate	0.852627	0.029494977	0.116833168
EEF1DELTA	WT_359 - beads_only	enriched candidate	0.862745	0.046864031	0.160937256
SMG5	WT_359 - beads_only	enriched candidate	0.59383	0.048795932	0.16461451
EF1GAMMA	WT_359 - beads_only	enriched candidate	0.698986	0.055991218	0.177563681

**Appendix IX (table 1) Differential enrichment analysis of MS data; WT\_359 vs beads only (no RNA control):** List of enriched hits and enriched candidates is provided. Proteins were considered hits with a false discovery rate (fdr) smaller 5 % and a fold-change cut-off of 100 % and considered candidates with an fdr smaller 20 % and a fold-change cut-off of 50 %. Protein candidates which did not satisfy these conditions were not listed. No hit list is available upon request. Number of putative novel *oskar* interactors is highlighted in orange. The known *oskar* interactors and proteins found to be part of *oskar* mRNPs are highlighted in green.

## Appendix X

Table 2:

gene_name	comparison	hit_annotation	logFC	pvalue.limma	fdr.limma
<b>TBPH</b>	(WT_359 - beads_only) - (WT_67 - beads_only)	enriched hit	5.87764	5.46E-11	6.27E-08
ZN72D	(WT_359 - beads_only) - (WT_67 - beads_only)	enriched hit	2.014045	2.12E-10	1.22E-07
CG5641	(WT_359 - beads_only) - (WT_67 - beads_only)	enriched hit	2.37247	1.62E-08	6.19E-06
MLE	(WT_359 - beads_only) - (WT_67 - beads_only)	enriched hit	2.493258	3.68E-08	1.06E-05
SYP	(WT_359 - beads_only) - (WT_67 - beads_only)	enriched hit	1.188876	1.99E-06	0.000457
YPS	(WT_359 - beads_only) - (WT_67 - beads_only)	enriched hit	1.482576	3.36E-06	0.000642
KLP10A	(WT_359 - beads_only) - (WT_67 - beads_only)	enriched hit	2.196307	3.95E-06	0.000648
CG1582	(WT_359 - beads_only) - (WT_67 - beads_only)	enriched hit	1.176575	8.47E-06	0.000972
PASHA	(WT_359 - beads_only) - (WT_67 - beads_only)	enriched hit	1.000195	1.14E-05	0.001032
<b>BSF</b>	(WT_359 - beads_only) - (WT_67 - beads_only)	enriched hit	1.499622	1.17E-05	0.001032
<b>ARET</b>	(WT_359 - beads_only) - (WT_67 - beads_only)	enriched hit	1.946945	1.34E-05	0.001098
SSL1	(WT_359 - beads_only) - (WT_67 - beads_only)	enriched hit	1.596128	1.74E-05	0.00133
<b>GLO</b>	(WT_359 - beads_only) - (WT_67 - beads_only)	enriched hit	-2.73398	1.91E-05	0.001366
DCR	(WT_359 - beads_only) - (WT_67 - beads_only)	enriched hit	2.909264	2.12E-05	0.00143
SXL	(WT_359 - beads_only) - (WT_67 - beads_only)	enriched hit	2.909802	2.27E-05	0.001448
SSX	(WT_359 - beads_only) - (WT_67 - beads_only)	enriched hit	1.318545	3.71E-05	0.002237
<b>HRB27C</b>	(WT_359 - beads_only) - (WT_67 - beads_only)	enriched hit	1.16393	4.70E-05	0.002666
CG9684	(WT_359 - beads_only) - (WT_67 - beads_only)	enriched hit	1.325517	4.88E-05	0.002666
RUMP	(WT_359 - beads_only) - (WT_67 - beads_only)	enriched hit	1.036325	0.000109	0.004702
LOQS	(WT_359 - beads_only) - (WT_67 - beads_only)	enriched hit	3.167549	0.000115	0.004702
RRP4	(WT_359 - beads_only) - (WT_67 - beads_only)	enriched hit	1.273066	0.000155	0.005913
CSL4	(WT_359 - beads_only) - (WT_67 - beads_only)	enriched hit	1.143242	0.000301	0.010163
MTR3	(WT_359 - beads_only) - (WT_67 - beads_only)	enriched hit	1.108614	0.000443	0.013728
CG10628	(WT_359 - beads_only) - (WT_67 - beads_only)	enriched hit	1.633337	0.000709	0.019355
CG17141	(WT_359 - beads_only) - (WT_67 - beads_only)	enriched hit	2.099773	0.000929	0.023168

SNRNP	(WT_359 - beads_only) - (WT_67 - beads_only)	enriched hit	1.030336	0.001171	0.027413
CAF1	(WT_359 - beads_only) - (WT_67 - beads_only)	enriched hit	1.022311	0.001811	0.038475
R2D2	(WT_359 - beads_only) - (WT_67 - beads_only)	enriched hit	1.905947	0.002092	0.042094
<b>SQD</b>	(WT_359 - beads_only) - (WT_67 - beads_only)	enriched hit	1.098175	0.002239	0.043529
RRP47	(WT_359 - beads_only) - (WT_67 - beads_only)	enriched hit	1.250563	0.002591	0.049247
<b>BICD</b>	(WT_359 - beads_only) - (WT_67 - beads_only)	enriched candidate	0.706659	5.11E-06	0.000733
DIS3	(WT_359 - beads_only) - (WT_67 - beads_only)	enriched candidate	0.871034	6.81E-06	0.000868
LOST	(WT_359 - beads_only) - (WT_67 - beads_only)	enriched candidate	0.64455	7.99E-05	0.004164
CG6745	(WT_359 - beads_only) - (WT_67 - beads_only)	enriched candidate	0.818596	0.000102	0.004702
CG3808	(WT_359 - beads_only) - (WT_67 - beads_only)	enriched candidate	0.738189	0.000111	0.004702
MED16	(WT_359 - beads_only) - (WT_67 - beads_only)	enriched candidate	0.620442	0.000114	0.004702
CG9596	(WT_359 - beads_only) - (WT_67 - beads_only)	enriched candidate	0.808598	0.000276	0.009872
UPF1	(WT_359 - beads_only) - (WT_67 - beads_only)	enriched candidate	0.770651	0.000284	0.009872
CDC27	(WT_359 - beads_only) - (WT_67 - beads_only)	enriched candidate	0.684368	0.00033	0.010799
XPD	(WT_359 - beads_only) - (WT_67 - beads_only)	enriched candidate	0.868176	0.000433	0.013728
<b>STAU</b>	(WT_359 - beads_only) - (WT_67 - beads_only)	enriched candidate	0.622078	0.00049	0.014789
LKB1	(WT_359 - beads_only) - (WT_67 - beads_only)	enriched candidate	0.597652	0.001534	0.035186
MED25	(WT_359 - beads_only) - (WT_67 - beads_only)	enriched candidate	0.708683	0.001967	0.040287
SEC5	(WT_359 - beads_only) - (WT_67 - beads_only)	enriched candidate	0.705645	0.002822	0.05187
LSM	(WT_359 - beads_only) - (WT_67 - beads_only)	enriched candidate	0.718686	0.004603	0.070988
128UP	(WT_359 - beads_only) - (WT_67 - beads_only)	enriched candidate	0.660307	0.00583	0.080786
LSM7	(WT_359 - beads_only) - (WT_67 - beads_only)	enriched candidate	0.911343	0.008061	0.097323
CKIIBETA	(WT_359 - beads_only) - (WT_67 - beads_only)	enriched candidate	0.631928	0.008527	0.100835
SYM	(WT_359 - beads_only) - (WT_67 - beads_only)	enriched candidate	0.775743	0.008949	0.102229
CG3689	(WT_359 - beads_only) - (WT_67 - beads_only)	enriched candidate	0.934432	0.00933	0.102229
LSM3	(WT_359 - beads_only) - (WT_67 - beads_only)	enriched candidate	0.812407	0.009968	0.104806
CG10914	(WT_359 - beads_only) - (WT_67 - beads_only)	enriched candidate	0.749383	0.010071	0.104806
IP259	(WT_359 - beads_only) - (WT_67 - beads_only)	enriched candidate	0.701813	0.010158	0.104806
RPN9	(WT_359 - beads_only) - (WT_67 - beads_only)	enriched candidate	0.626008	0.011849	0.114507
NS4	(WT_359 - beads_only) - (WT_67 - beads_only)	enriched candidate	0.852892	0.017369	0.141704
CCDC53	(WT_359 - beads_only) - (WT_67 - beads_only)	enriched candidate	0.600785	0.028281	0.189641
PATR	(WT_359 - beads_only) - (WT_67 - beads_only)	enriched no hit	0.522269	0.000872	0.023168
RPI1	(WT_359 - beads_only) - (WT_67 - beads_only)	enriched no hit	0.513415	0.00105	0.025618
MAHE	(WT_359 - beads_only) - (WT_67 - beads_only)	enriched no hit	0.546149	0.00403	0.066661
RPB5	(WT_359 - beads_only) - (WT_67 - beads_only)	enriched no hit	0.446273	0.004573	0.070988
NS2	(WT_359 - beads_only) - (WT_67 - beads_only)	enriched no hit	0.530858	0.005389	0.080063
CG5642	(WT_359 - beads_only) - (WT_67 - beads_only)	enriched no hit	0.516193	0.005514	0.080063
ECD	(WT_359 - beads_only) - (WT_67 - beads_only)	enriched no hit	0.396356	0.006607	0.086119
CG10562	(WT_359 - beads_only) - (WT_67 - beads_only)	enriched no hit	0.508538	0.007278	0.092064
TRIP1	(WT_359 - beads_only) - (WT_67 - beads_only)	enriched no hit	0.575691	0.011028	0.111934
CED	(WT_359 - beads_only) - (WT_67 - beads_only)	enriched no hit	0.577756	0.011279	0.113478
KAP	(WT_359 - beads_only) - (WT_67 - beads_only)	enriched no hit	0.35223	0.012278	0.11543
CG16742	(WT_359 - beads_only) - (WT_67 - beads_only)	enriched no hit	0.578217	0.01408	0.126174
SNR1	(WT_359 - beads_only) - (WT_67 - beads_only)	enriched no hit	0.41541	0.016015	0.136556
U2AF50	(WT_359 - beads_only) - (WT_67 - beads_only)	enriched no hit	0.41009	0.018476	0.14615
NS1	(WT_359 - beads_only) - (WT_67 - beads_only)	enriched no hit	0.582038	0.019343	0.151963

CG4849	(WT_359 - beads_only) - (WT_67 - beads_only)	enriched no hit	0.414429	0.026477	0.184058
CG8635	(WT_359 - beads_only) - (WT_67 - beads_only)	enriched no hit	0.6741	0.031801	0.200416
RAN	(WT_359 - beads_only) - (WT_67 - beads_only)	enriched no hit	1.087005	0.033393	0.207036
CDK7	(WT_359 - beads_only) - (WT_67 - beads_only)	enriched no hit	0.436073	0.035287	0.213024
<b>CG9890</b>	(WT_359 - beads_only) - (WT_67 - beads_only)	enriched no hit	1.238337	0.03638	0.216209
EEF1DELTA	(WT_359 - beads_only) - (WT_67 - beads_only)	enriched no hit	-0.9127	0.036803	0.217224
CPSF100	(WT_359 - beads_only) - (WT_67 - beads_only)	enriched no hit	0.788318	0.03693	0.217224
EF1GAMMA	(WT_359 - beads_only) - (WT_67 - beads_only)	enriched no hit	-0.75621	0.040514	0.22234
CG12909	(WT_359 - beads_only) - (WT_67 - beads_only)	enriched no hit	0.42601	0.041344	0.224746
CG10418	(WT_359 - beads_only) - (WT_67 - beads_only)	enriched no hit	0.670309	0.043837	0.232984
PP2A	(WT_359 - beads_only) - (WT_67 - beads_only)	enriched no hit	0.275438	0.049065	0.250586
CG6767	(WT_359 - beads_only) - (WT_67 - beads_only)	enriched no hit	0.351088	0.062916	0.279955
NEOS	(WT_359 - beads_only) - (WT_67 - beads_only)	enriched no hit	0.591214	0.073385	0.296381
RRP46	(WT_359 - beads_only) - (WT_67 - beads_only)	enriched no hit	0.928943	0.074061	0.29702
NSUN2	(WT_359 - beads_only) - (WT_67 - beads_only)	enriched no hit	0.356341	0.078721	0.300008
EIF6	(WT_359 - beads_only) - (WT_67 - beads_only)	enriched no hit	0.426167	0.095345	0.329401
CPSF73	(WT_359 - beads_only) - (WT_67 - beads_only)	enriched no hit	0.559603	0.099705	0.341896
SBF	(WT_359 - beads_only) - (WT_67 - beads_only)	enriched no hit	0.366983	0.11978	0.367603
WASH	(WT_359 - beads_only) - (WT_67 - beads_only)	enriched no hit	0.362602	0.136879	0.389064
RYS	(WT_359 - beads_only) - (WT_67 - beads_only)	enriched no hit	0.422948	0.153858	0.408506
NOP60B	(WT_359 - beads_only) - (WT_67 - beads_only)	enriched no hit	0.490709	0.154315	0.408774
CG10672	(WT_359 - beads_only) - (WT_67 - beads_only)	enriched no hit	0.35145	0.175266	0.43893
SRP68	(WT_359 - beads_only) - (WT_67 - beads_only)	enriched no hit	0.301749	0.213975	0.479353
SMG5	(WT_359 - beads_only) - (WT_67 - beads_only)	enriched no hit	0.343207	0.235146	0.504135
SRP54K	(WT_359 - beads_only) - (WT_67 - beads_only)	enriched no hit	0.387816	0.27133	0.541243
U4	(WT_359 - beads_only) - (WT_67 - beads_only)	enriched no hit	0.194266	0.328447	0.594338
CPB	(WT_359 - beads_only) - (WT_67 - beads_only)	enriched no hit	-0.15412	0.337409	0.599501
DPH5	(WT_359 - beads_only) - (WT_67 - beads_only)	enriched no hit	0.318204	0.392601	0.640682
DPPIII	(WT_359 - beads_only) - (WT_67 - beads_only)	enriched no hit	0.310663	0.39604	0.644337
NHP2	(WT_359 - beads_only) - (WT_67 - beads_only)	enriched no hit	-0.17988	0.504013	0.737377
CG5664	(WT_359 - beads_only) - (WT_67 - beads_only)	enriched no hit	0.158219	0.540485	0.759852
EF1ALPHA48D	(WT_359 - beads_only) - (WT_67 - beads_only)	enriched no hit	-0.19744	0.561009	0.774035
CG10341	(WT_359 - beads_only) - (WT_67 - beads_only)	enriched no hit	-0.11518	0.626142	0.8255
CAZ	(WT_359 - beads_only) - (WT_67 - beads_only)	enriched no hit	-0.22806	0.654423	0.848414
CG4038	(WT_359 - beads_only) - (WT_67 - beads_only)	enriched no hit	-0.09525	0.748392	0.894178
NS3	(WT_359 - beads_only) - (WT_67 - beads_only)	enriched no hit	0.102443	0.778911	0.903907
PIX	(WT_359 - beads_only) - (WT_67 - beads_only)	enriched no hit	-0.02682	0.885976	0.955338
CG5973	(WT_359 - beads_only) - (WT_67 - beads_only)	enriched no hit	0.079659	0.899832	0.960569
CG25C	(WT_359 - beads_only) - (WT_67 - beads_only)	hit	-1.26289	0.001769	0.038285
BRP	(WT_359 - beads_only) - (WT_67 - beads_only)	candidate	-0.67196	0.000104	0.004702
D1	(WT_359 - beads_only) - (WT_67 - beads_only)	candidate	0.73193	0.00016	0.005913
CG13773	(WT_359 - beads_only) - (WT_67 - beads_only)	candidate	0.601571	0.001148	0.027413
PROSALPHA4	(WT_359 - beads_only) - (WT_67 - beads_only)	candidate	-0.67581	0.002163	0.042779
SNF	(WT_359 - beads_only) - (WT_67 - beads_only)	candidate	-0.64544	0.003114	0.055806
TRAL	(WT_359 - beads_only) - (WT_67 - beads_only)	candidate	0.860702	0.003953	0.066661
SSB	(WT_359 - beads_only) - (WT_67 - beads_only)	candidate	-0.59845	0.004213	0.067114



TFIIIEALPHA	(WT_359 - beads_only) - (WT_67 - beads_only)	candidate	1.224579	0.00581	0.080786
SPN	(WT_359 - beads_only) - (WT_67 - beads_only)	candidate	0.638334	0.007801	0.09519
MBD	(WT_359 - beads_only) - (WT_67 - beads_only)	candidate	0.629956	0.012452	0.116117
TSR	(WT_359 - beads_only) - (WT_67 - beads_only)	candidate	-0.61967	0.01403	0.126174
EFSEC	(WT_359 - beads_only) - (WT_67 - beads_only)	candidate	0.662731	0.017002	0.141316
RPS28B	(WT_359 - beads_only) - (WT_67 - beads_only)	candidate	-0.5851	0.017707	0.142027
CG4546	(WT_359 - beads_only) - (WT_67 - beads_only)	candidate	0.766992	0.0292	0.192483

**Appendix X (table 2) Differential enrichment analysis of MS data; WT\_359 vs WT\_67 with beads only (no RNA control) subtracted:** List of enriched hits and enriched candidates is provided. Proteins were considered hits with a false discovery rate (fdr) smaller 5 % and a fold-change cut-off of 100 % and considered candidates with an fdr smaller 20 % and a fold-change cut-off of 50 %. Protein candidates which did not satisfy these conditions were not listed (no hit list available upon request). Proteins that were not found as enriched in the individual conditions and shown to be hits or candidates after differential analysis between two conditions were considered as falls positives and grouped with no hits (in gray). Number of putative novel *oskar* interactors is highlighted in orange. The known *oskar* interactors and proteins found to be part of *oskar* mRNPs are highlighted in green.

## Appendix XI

Table 3:

Gene name	Comparison	Hit annotation	logFC	pvalue.limma	fdr.limma
<b>CG9890</b>	(UU_359- beads_only) - (WT_359 - beads_only)	enriched hit	-4.09025	1.31E-06	0.001502
MED16	(UU_359- beads_only) - (WT_359 - beads_only)	enriched candidate	-0.63765	8.63E-05	0.032981
<b>TBPH</b>	(UU_359- beads_only) - (WT_359 - beads_only)	enriched candidate	-1.72608	0.000311	0.089317
CAMKII	(UU_359- beads_only) - (WT_359 - beads_only)	enriched candidate	1.093899	0.000532	0.122055
<b>HRB27C</b>	(UU_359- beads_only) - (WT_359 - beads_only)	enriched candidate	-0.79669	0.00162	0.196441
MUC	(UU_359- beads_only) - (WT_359 - beads_only)	enriched candidate	1.005947	0.002184	0.196441
RRP4	(UU_359- beads_only) - (WT_359 - beads_only)	enriched candidate	-0.9075	0.002883	0.196441
MTR3	(UU_359- beads_only) - (WT_359 - beads_only)	enriched no hit	-0.85139	0.003752	0.215154
CG5642	(UU_359- beads_only) - (WT_359 - beads_only)	enriched no hit	-0.53506	0.004315	0.227341
RPB5	(UU_359- beads_only) - (WT_359 - beads_only)	enriched no hit	-0.4429	0.004818	0.235368
<b>FMR1</b>	(UU_359- beads_only) - (WT_359 - beads_only)	enriched no hit	0.554538	0.005595	0.238485
CG2247	(UU_359- beads_only) - (WT_359 - beads_only)	enriched no hit	0.625079	0.006061	0.241543
SYM	(UU_359- beads_only) - (WT_359 - beads_only)	enriched no hit	-0.81481	0.006552	0.242439
SSL1	(UU_359- beads_only) - (WT_359 - beads_only)	enriched no hit	-0.79696	0.008008	0.257287
<b>ARET</b>	(UU_359- beads_only) - (WT_359 - beads_only)	enriched no hit	-0.94977	0.008022	0.257287
TRIP1	(UU_359- beads_only) - (WT_359 - beads_only)	enriched no hit	-0.5954	0.008997	0.271566
LKB1	(UU_359- beads_only) - (WT_359 - beads_only)	enriched no hit	-0.46124	0.009494	0.273815
ECD	(UU_359- beads_only) - (WT_359 - beads_only)	enriched no hit	-0.37213	0.009821	0.273815
CPSF73	(UU_359- beads_only) - (WT_359 - beads_only)	enriched no hit	-0.939	0.009852	0.273815
LSM	(UU_359- beads_only) - (WT_359 - beads_only)	enriched no hit	-0.62691	0.011048	0.281743
MED25	(UU_359- beads_only) - (WT_359 - beads_only)	enriched no hit	-0.547	0.011465	0.282942

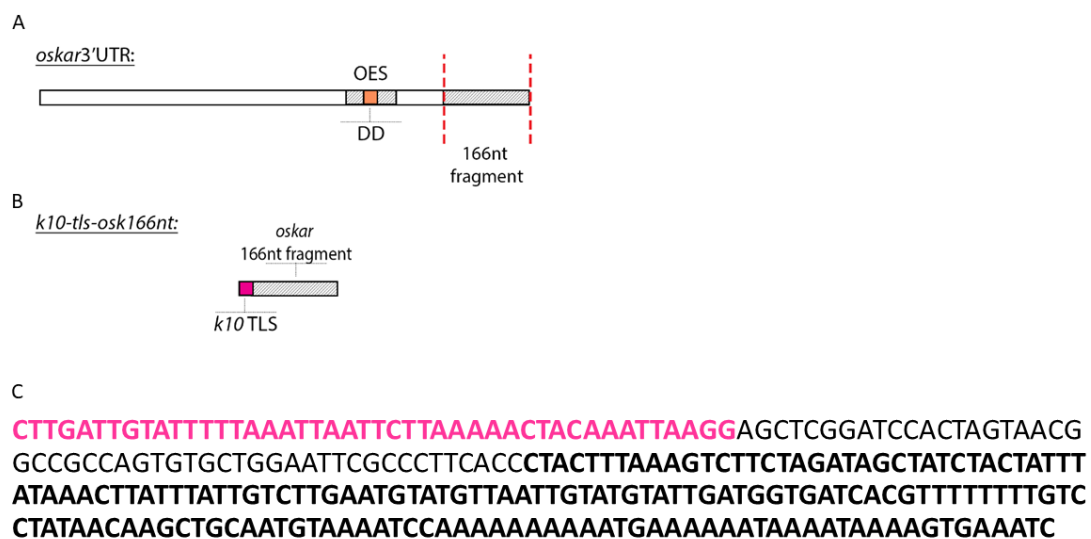
CG9925	(UU_359- beads_only) - (WT_359 - beads_only)	enriched no hit	0.553669	0.01367	0.308613
CAF1	(UU_359- beads_only) - (WT_359 - beads_only)	enriched no hit	-0.73318	0.01638	0.318713
MLE	(UU_359- beads_only) - (WT_359 - beads_only)	enriched no hit	-0.67461	0.016451	0.318713
<b>BICD</b>	(UU_359- beads_only) - (WT_359 - beads_only)	enriched no hit	-0.28023	0.01664	0.318713
RPN9	(UU_359- beads_only) - (WT_359 - beads_only)	enriched no hit	-0.58433	0.017447	0.318713
EIF6	(UU_359- beads_only) - (WT_359 - beads_only)	enriched no hit	-0.63732	0.017544	0.318713
CG3689	(UU_359- beads_only) - (WT_359 - beads_only)	enriched no hit	-0.82996	0.01838	0.318713
KAP	(UU_359- beads_only) - (WT_359 - beads_only)	enriched no hit	-0.32639	0.018741	0.318713
CSL4	(UU_359- beads_only) - (WT_359 - beads_only)	enriched no hit	-0.63848	0.020467	0.318713
CPSF100	(UU_359- beads_only) - (WT_359 - beads_only)	enriched no hit	-0.88376	0.021365	0.318713
PP2A	(UU_359- beads_only) - (WT_359 - beads_only)	enriched no hit	-0.32959	0.021528	0.318713
R2D2	(UU_359- beads_only) - (WT_359 - beads_only)	enriched no hit	-1.25702	0.027707	0.355462
CG16742	(UU_359- beads_only) - (WT_359 - beads_only)	enriched no hit	-0.50724	0.027892	0.355462
LSM3	(UU_359- beads_only) - (WT_359 - beads_only)	enriched no hit	-0.6515	0.032228	0.397484
SSX	(UU_359- beads_only) - (WT_359 - beads_only)	enriched no hit	0.541402	0.033419	0.398311
DPH5	(UU_359- beads_only) - (WT_359 - beads_only)	enriched no hit	-0.8413	0.033894	0.398311
SNRNP	(UU_359- beads_only) - (WT_359 - beads_only)	enriched no hit	-0.59707	0.036037	0.401514
DCR	(UU_359- beads_only) - (WT_359 - beads_only)	enriched no hit	-1.11578	0.036155	0.401514
CG4849	(UU_359- beads_only) - (WT_359 - beads_only)	enriched no hit	-0.3869	0.036489	0.401514
CG5664	(UU_359- beads_only) - (WT_359 - beads_only)	enriched no hit	-0.57649	0.036968	0.401514
LSM7	(UU_359- beads_only) - (WT_359 - beads_only)	enriched no hit	-0.65572	0.04467	0.430555
SEC5	(UU_359- beads_only) - (WT_359 - beads_only)	enriched no hit	-0.42388	0.04994	0.445568
CAZ	(UU_359- beads_only) - (WT_359 - beads_only)	enriched no hit	-1.0601	0.050226	0.445568
CG10562	(UU_359- beads_only) - (WT_359 - beads_only)	enriched no hit	-0.34838	0.051148	0.445568
WASH	(UU_359- beads_only) - (WT_359 - beads_only)	enriched no hit	-0.4872	0.051636	0.445568
CG10418	(UU_359- beads_only) - (WT_359 - beads_only)	enriched no hit	-0.64327	0.051925	0.445568
IP259	(UU_359- beads_only) - (WT_359 - beads_only)	enriched no hit	-0.50508	0.052054	0.445568
LA	(UU_359- beads_only) - (WT_359 - beads_only)	enriched no hit	0.264927	0.052745	0.448133
CG9684	(UU_359- beads_only) - (WT_359 - beads_only)	enriched no hit	0.485371	0.060068	0.464628
RPI1	(UU_359- beads_only) - (WT_359 - beads_only)	enriched no hit	-0.25917	0.060357	0.464628
U2AF50	(UU_359- beads_only) - (WT_359 - beads_only)	enriched no hit	0.314572	0.061231	0.467388
CDC27	(UU_359- beads_only) - (WT_359 - beads_only)	enriched no hit	-0.29725	0.064836	0.476708
SBR	(UU_359- beads_only) - (WT_359 - beads_only)	enriched no hit	0.303761	0.066228	0.483844
CG10341	(UU_359- beads_only) - (WT_359 - beads_only)	enriched no hit	-0.44526	0.07312	0.496265
SRP68	(UU_359- beads_only) - (WT_359 - beads_only)	enriched no hit	-0.4467	0.073585	0.496481
CCDC53	(UU_359- beads_only) - (WT_359 - beads_only)	enriched no hit	-0.47025	0.077228	0.512375
SNR1	(UU_359- beads_only) - (WT_359 - beads_only)	enriched no hit	-0.28297	0.085005	0.522471
<b>BSF</b>	(UU_359- beads_only) - (WT_359 - beads_only)	enriched no hit	0.437724	0.085094	0.522471
RRP47	(UU_359- beads_only) - (WT_359 - beads_only)	enriched no hit	-0.64138	0.085636	0.522471
CDK7	(UU_359- beads_only) - (WT_359 - beads_only)	enriched no hit	-0.34328	0.088936	0.531163
RRP46	(UU_359- beads_only) - (WT_359 - beads_only)	enriched no hit	-0.86542	0.093941	0.549748
XPD	(UU_359- beads_only) - (WT_359 - beads_only)	enriched no hit	-0.32209	0.119562	0.584804
U4	(UU_359- beads_only) - (WT_359 - beads_only)	enriched no hit	-0.31413	0.122806	0.584804
KLP10A	(UU_359- beads_only) - (WT_359 - beads_only)	enriched no hit	-0.51757	0.123584	0.584804
CKIIBETA	(UU_359- beads_only) - (WT_359 - beads_only)	enriched no hit	-0.34149	0.124237	0.584804
<b>YPS</b>	(UU_359- beads_only) - (WT_359 - beads_only)	enriched no hit	-0.34386	0.124404	0.584804

CG12909	(UU_359- beads_only) - (WT_359 - beads_only)	enriched no hit	-0.30962	0.126207	0.584804
SRP54K	(UU_359- beads_only) - (WT_359 - beads_only)	enriched no hit	-0.54681	0.127865	0.584804
NS2	(UU_359- beads_only) - (WT_359 - beads_only)	enriched no hit	-0.26129	0.132213	0.599398
DIS3	(UU_359- beads_only) - (WT_359 - beads_only)	enriched no hit	-0.20868	0.133955	0.604907
RYR	(UU_359- beads_only) - (WT_359 - beads_only)	enriched no hit	-0.43882	0.139949	0.605227
<b>STAU</b>	(UU_359- beads_only) - (WT_359 - beads_only)	enriched no hit	0.217787	0.145275	0.613519
ASPRS	(UU_359- beads_only) - (WT_359 - beads_only)	enriched no hit	0.235278	0.155992	0.629752
SBF	(UU_359- beads_only) - (WT_359 - beads_only)	enriched no hit	-0.33126	0.157309	0.629752
CG3808	(UU_359- beads_only) - (WT_359 - beads_only)	enriched no hit	-0.20331	0.178625	0.638648
CG10628	(UU_359- beads_only) - (WT_359 - beads_only)	enriched no hit	0.529897	0.192374	0.638648
LOQS	(UU_359- beads_only) - (WT_359 - beads_only)	enriched no hit	-0.82279	0.204518	0.640959
NEOS	(UU_359- beads_only) - (WT_359 - beads_only)	enriched no hit	-0.39411	0.219437	0.657166
MBD	(UU_359- beads_only) - (WT_359 - beads_only)	enriched no hit	0.271623	0.241649	0.692564
LOST	(UU_359- beads_only) - (WT_359 - beads_only)	enriched no hit	0.146576	0.247616	0.699546
CG12128	(UU_359- beads_only) - (WT_359 - beads_only)	enriched no hit	0.142171	0.26954	0.734352
MOD	(UU_359- beads_only) - (WT_359 - beads_only)	enriched no hit	0.14593	0.276996	0.741702
NSUN2	(UU_359- beads_only) - (WT_359 - beads_only)	enriched no hit	-0.21175	0.28057	0.741702
EEF1DELTA	(UU_359- beads_only) - (WT_359 - beads_only)	enriched no hit	-0.43931	0.288559	0.75222
SMG5	(UU_359- beads_only) - (WT_359 - beads_only)	enriched no hit	-0.28667	0.318062	0.791314
HBS1	(UU_359- beads_only) - (WT_359 - beads_only)	enriched no hit	0.389874	0.339687	0.806377
NOP60B	(UU_359- beads_only) - (WT_359 - beads_only)	enriched no hit	-0.32101	0.342376	0.806377
EF1ALPHA4 8D	(UU_359- beads_only) - (WT_359 - beads_only)	enriched no hit	0.317835	0.353521	0.810976
DPPIII	(UU_359- beads_only) - (WT_359 - beads_only)	enriched no hit	-0.33866	0.355903	0.814813
NS4	(UU_359- beads_only) - (WT_359 - beads_only)	enriched no hit	0.291026	0.377955	0.830152
CG17141	(UU_359- beads_only) - (WT_359 - beads_only)	enriched no hit	0.438299	0.408526	0.848876
NS3	(UU_359- beads_only) - (WT_359 - beads_only)	enriched no hit	0.272536	0.458623	0.874381
128UP	(UU_359- beads_only) - (WT_359 - beads_only)	enriched no hit	0.143407	0.498704	0.895896
CED	(UU_359- beads_only) - (WT_359 - beads_only)	enriched no hit	-0.13041	0.52642	0.897132
PATR	(UU_359- beads_only) - (WT_359 - beads_only)	enriched no hit	-0.08112	0.533564	0.897132
PIX	(UU_359- beads_only) - (WT_359 - beads_only)	enriched no hit	-0.11315	0.547471	0.897132
EF1GAMM A	(UU_359- beads_only) - (WT_359 - beads_only)	enriched no hit	-0.20679	0.550226	0.897132
CG1582	(UU_359- beads_only) - (WT_359 - beads_only)	enriched no hit	-0.10905	0.557012	0.897132
CG9596	(UU_359- beads_only) - (WT_359 - beads_only)	enriched no hit	-0.10332	0.560158	0.897132
LARK	(UU_359- beads_only) - (WT_359 - beads_only)	enriched no hit	0.086072	0.561599	0.897132
CG10672	(UU_359- beads_only) - (WT_359 - beads_only)	enriched no hit	-0.14574	0.564414	0.897132
ZN72D	(UU_359- beads_only) - (WT_359 - beads_only)	enriched no hit	0.080384	0.576777	0.898625
CG10914	(UU_359- beads_only) - (WT_359 - beads_only)	enriched no hit	0.145154	0.578975	0.898625
CG6767	(UU_359- beads_only) - (WT_359 - beads_only)	enriched no hit	-0.09241	0.605612	0.906175
GLO	(UU_359- beads_only) - (WT_359 - beads_only)	enriched no hit	-0.21576	0.640637	0.912303
CG8635	(UU_359- beads_only) - (WT_359 - beads_only)	enriched no hit	0.133628	0.64679	0.912303
NS1	(UU_359- beads_only) - (WT_359 - beads_only)	enriched no hit	-0.09534	0.675268	0.920966
SXL	(UU_359- beads_only) - (WT_359 - beads_only)	enriched no hit	0.201945	0.68588	0.925535
CG4038	(UU_359- beads_only) - (WT_359 - beads_only)	enriched no hit	-0.08879	0.764905	0.960949
CG6745	(UU_359- beads_only) - (WT_359 - beads_only)	enriched no hit	-0.04691	0.771451	0.965263
RUMP	(UU_359- beads_only) - (WT_359 - beads_only)	enriched no hit	-0.03369	0.869892	0.991071
MAHE	(UU_359- beads_only) - (WT_359 - beads_only)	enriched no hit	0.025705	0.876152	0.991071

SQD	(UU_359- beads_only) - (WT_359 - beads_only)	enriched no hit	-0.04447	0.884493	0.993635
NHP2	(UU_359- beads_only) - (WT_359 - beads_only)	enriched no hit	-0.03759	0.888168	0.993635
UPF1	(UU_359- beads_only) - (WT_359 - beads_only)	enriched no hit	-0.02076	0.902016	0.993635
PASHA	(UU_359- beads_only) - (WT_359 - beads_only)	enriched no hit	-0.01906	0.905815	0.993635
CG5973	(UU_359- beads_only) - (WT_359 - beads_only)	enriched no hit	0.073157	0.907967	0.993635
CG5641	(UU_359- beads_only) - (WT_359 - beads_only)	enriched no hit	-0.02547	0.911363	0.993635
RAN	(UU_359- beads_only) - (WT_359 - beads_only)	enriched no hit	0.023358	0.960667	0.993635
SYP	(UU_359- beads_only) - (WT_359 - beads_only)	enriched no hit	0.008077	0.961033	0.993635
FIP1	(UU_359- beads_only) - (WT_359 - beads_only)	candidate	-0.60152	0.001272	0.196441
CG11876	(UU_359- beads_only) - (WT_359 - beads_only)	candidate	0.585766	0.003028	0.196441

**Appendix XI (table 3) Differential enrichment analysis of MS data; UU\_359 vs WT\_359 with beads only (no RNA control) subtracted:** List of enriched hits and enriched candidates is provided. Proteins were considered hits with a false discovery rate (fdr) smaller 5 % and a fold-change cut-off of 100 % and considered candidates with an fdr smaller 20 % and a fold-change cut-off of 50 %. Protein candidates which did not satisfy these conditions were not listed (no hit list available upon request). Proteins that were not found as enriched in the individual conditions and shown to be hits or candidates after differential analysis between two conditions were considered as falls positives and grouped with no hits (in gray). Number of putative novel *oskar* interactors is highlighted in orange. The known *oskar* interactors and proteins found to be part of *oskar* mRNPs are highlighted in green.

## Appendix XII



**Appendix XII A** Schematic representation of the *oskar* 3'UTR. Dimerization domain (DD) is highlighted in orange. Oogenesis-rescuing 166 nucleotide (nt) fragment is marked with red dashed lines. **B** Scheme of the *k10-tls-osk166nt* construct. **C** Sequence of the *k10-tls-osk166nt* construct (5'→3') with highlighted region of the *K10* TLS in pink and *oskar* 166 nucleotide 3'UTR distal fragment in bold black.

## Appendix XIII

In the course of this work, I resequenced the transgenes previously made in the lab and integrated in the next fly lines: HJ4, HJ5, HJ33.1, HJ33.2 and HJ34.3 (Jambor, 2008; Jambor et al., 2011). Fly lines HJ5, HJ33.1 and HJ33.2 were previously annotated to contain AA nucleotide substitution in the DD loop, whilst HJ4 and HJ34.3 were annotated to contain UU nucleotide substitution in the DD loop. Sequencing revealed that the transgenes were wrongly annotated and that the lines containing UU mutation are actually HJ5, HJ33.1 and HJ33.2 and lines containing AA mutation are HJ4 and HJ34.3. Therefore, I assigned the proper identity and corrected annotation of each fly line and each plasmid in use (see 2.1.6 Plasmids and 2.1.9 Fly lines). For the sequence of the *oskar* DD loop of the WT and the mutants (UU or AA) see Appendix I.

